Structural geology and history of the Buck Mountain fault and adjacent intra-range faults, Teton Range, Wyoming
by Daniel Joseph Smith

A thesis submitted in partial fulfillment of the requirements for the degree of Master of Science in Earth Sciences
Montana State University

Abstract:
The Teton Range in northwestern Wyoming lies on the western margin of Laramide basement-involved deformation in the Rocky Mountain foreland. The study area is located in the central Teton Range and includes the high peaks of the range (the Cathedral Group) and several basement-involved deformation zones. The purpose of this study is to: 1) determine the geometry, kinematics and age of the Buck Mountain, Stewart and Static faults in the central Teton Range, and 2) to characterize post-Archean basement deformation in the Teton Range by examining mesoscopic and microscopic fabrics and alteration mineralogies in the study area.

The north-striking Buck Mountain and northeast-striking Stewart faults exhibit brittle deformation including closespaced, unstable fractures and cataclasites. Slickenlines and drag folds indicate reverse dip-slip on the Buck Mountain fault. Both faults are interpreted to be Laramide on the basis of their basement-involved, contractional nature and brittle deformation.

Static fault strikes northeast, dips steeply southeast and can be divided into two segments: 1) a southwest segment characterized by mylonitic rocks and exhibiting oriented chlorite, relict hornblende crystals, and rotated quartzo-feldspathic porphyroblasts (interpreted to be a Proterozoic phyllonite zone); and 2) a northeast segment that was reactivated by the Buck Mountain fault and exhibits brecciation and cataclasites.

The Laramide Buck Mountain and Stewart fault zones are overprinted by the greenschist-facies assemblage chlorite + sericite + epidote + calcite. These minerals exhibit post-kinematic textures. Palinspastic restoration across the Buck Mountain fault indicates that temperatures in the fault zone during the Laramide orogeny were about 9O°-100°C and pressure around 1 kilobar. It is suggested that late-stage, convective thermal fluids supplied the fault zone with the necessary heat and fluid to produce greenschist-facies assemblages while retaining the brittle nature of the zones.

Structural measurements indicate existence of an Archean discontinuity (the Static Peak discontinuity) where north-striking Archean foliation to the north changes strike to northeast south of Static Peak. Phanerozoic structures are concordant with Proterozoic ductile deformation zones and Archean fabrics indicating that Precambrian basement fabrics controlled the orientations of Phanerozoic structures.

STRUCTURAL GEOLOGY AND HISTORY OF THE BUCK MOUNTAIN FAULT AND ADJACENT INTRA-RANGE FAULTS, TETON RANGE, WYOMING

by

Daniel Joseph Smith

A thesis submitted in partial fulfillment
of the requirements for the degree

of

Master of Science

in

Earth Sciences

MONTANA STATE UNIVERSITY
Bozeman, Montana

January, 1991

APPROVAL

of a thesis submitted by

Daniel Joseph Smith

This thesis has been read by each member of the thesis committee and has been found to be satisfactory regarding content, English usage, format, citations, bibliographic style, and consistency, and is ready for submission to the College of Graduate Studies.

January 3, 1991
Date

David R. Cuyper
Chairperson, Graduate Committee

Approved for the Major Department

3 Jan 1991
Date

Head, Major Department

Approved for the College of Graduate Studies

January 3, 1991
Date

Henry L Parsons
Graduate Dean

STATEMENT OF PERMISSION TO USE

In presenting this thesis in partial fulfillment of the requirements for a master's degree at Montana State University, I agree that the Library shall make it available to borrowers under rules of the Library. Brief quotations from this thesis are allowable without special permission, provided that accurate acknowledgement of source is made.

Permission for extensive quotation from or reproduction of this thesis may be granted by my major professor, or in his/her absence, by the Dean of Libraries when, in the opinion of either, the proposed use of the material is for scholarly purposes. Any copying or use of the material in this thesis for financial gain shall not be allowed without my written permission.

Signature Daniel J. Smith

Date 1/3/91

ACKNOWLEDGEMENTS

Tiger! Tiger! burning bright
In the forests of the night,
What immortal hand or eye
Could frame thy fearful symmetry?
William Blake

First, I would like to thank Dr. David R. Lageson for suggesting the topic for this thesis and for his insights into the dynamics of Laramide deformation. I would also like to thank Dr. David W. Mogk, Dr. Michael Smith and Dr. James G. Schmitt for their thorough reviews of the manuscript.

There is not enough space to thank everyone whose support for which I am most grateful. A few require special mention...I wish to thank Julie and Molly for their love and companionship; my Graduate Student colleagues for accompanying me on this odyssey; Doug (Pierre) Killerud for reminding me we shall never grow old; my brother Mark for watching over me; and especially Douglas Barrie for believing in and encouraging me over the years.

Funding for this project was provided by the Geological Society of America, American Association of Petroleum Geologists, and through a Graduate Teaching Assistantship at Montana State University.

Lastly, I would like to thank my parents who have supported every path I have taken that ultimately led here.

TABLE OF CONTENTS

TABLE OF CONTENTS - Continued

LIST OF TABLES

LIST OF FIGURES

LIST OF FIGURES - Continued

LIST OF FIGURES - Continued

ABSTRACT

The Teton Range in northwestern Wyoming lies on the western margin of Laramide basement-involved deformation in the Rocky Mountain foreland. The study area is located in the central Teton Range and includes the high peaks of the range (the Cathedral Group) and several basement-involved deformation zones. The purpose of this study is to: 1) determine the geometry, kinematics and age of the Buck Mountain, Stewart and Static faults in the central Teton Range, and 2) to characterize post-Archean basement deformation in the Teton Range by examining mesoscopic and microscopic fabrics and alteration mineralogies in the study area.

The north-striking Buck Mountain and northeast-striking Stewart faults exhibit brittle deformation including close-spaced, unstable fractures and cataclasites. Slickenlines and drag folds indicate reverse dip-slip on the Buck Mountain fault. Both faults are interpreted to be Laramide on the basis of their basement-involved, contractional nature and brittle deformation.

Static fault strikes northeast, dips steeply southeast and can be divided into two segments: 1) a southwest segment characterized by mylonitic rocks and exhibiting oriented chlorite, relict hornblende crystals, and rotated quartzo-feldspathic porphyroblasts (interpreted to be a Proterozoic phyllonite zone); and 2) a northeast segment that was reactivated by the Buck Mountain fault and exhibits brecciation and cataclasites.

The Laramide Buck Mountain and Stewart fault zones are overprinted by the greenschist-facies assemblage chlorite + sericite + epidote + calcite. These minerals exhibit post-kinematic textures. Palinspastic restoration across the Buck Mountain fault indicates that temperatures in the fault zone during the Laramide orogeny were about 90°-100°C and pressure around 1 kilobar. It is suggested that late-stage, convective thermal fluids supplied the fault zone with the necessary heat and fluid to produce greenschist-facies assemblages while retaining the brittle nature of the zones.

Structural measurements indicate existence of an Archean discontinuity (the Static Peak discontinuity) where north-striking Archean foliation to the north changes strike to northeast south of Static Peak. Phanerozoic structures are concordant with Proterozoic ductile deformation zones and Archean fabrics indicating that Precambrian basement fabrics controlled the orientations of Phanerozoic structures.

INTRODUCTION

Purpose of Investigation

The term "Laramide deformation" refers to predominantly compressional, crystalline basement-involved deformation that occurred in the Rocky Mountain foreland province of the western United States during Late Cretaceous to early Tertiary time (Love and Reed, 1971). Many diverse interpretations of structural styles and deformation-enhanced metamorphism representing Laramide deformation have been suggested. These interpretations include purely brittle deformation of a homogeneous basement (e.g., Mitra and Frost, 1981; Matthews, 1986; Mitra, 1990), folding and/or reactivation of preexisting basement fabrics, and greenschist-grade metamorphism associated with Laramide structures (e.g. Wagner, 1957; Hoppin, 1970; Schmidt and Garihan, 1983; Woodward, 1986; Miller, 1987), and brittle to ductile transition in Laramide deformation zones (e.g. Mitra, 1978; Mitra, 1984). Mitra and Frost (1981) have suggested that there are three generations of basement deformation zones in the Wind River Range corresponding to development in the: 1) early Precambrian; 2) late Precambrian; and 3) Laramide. Their work can be used as a

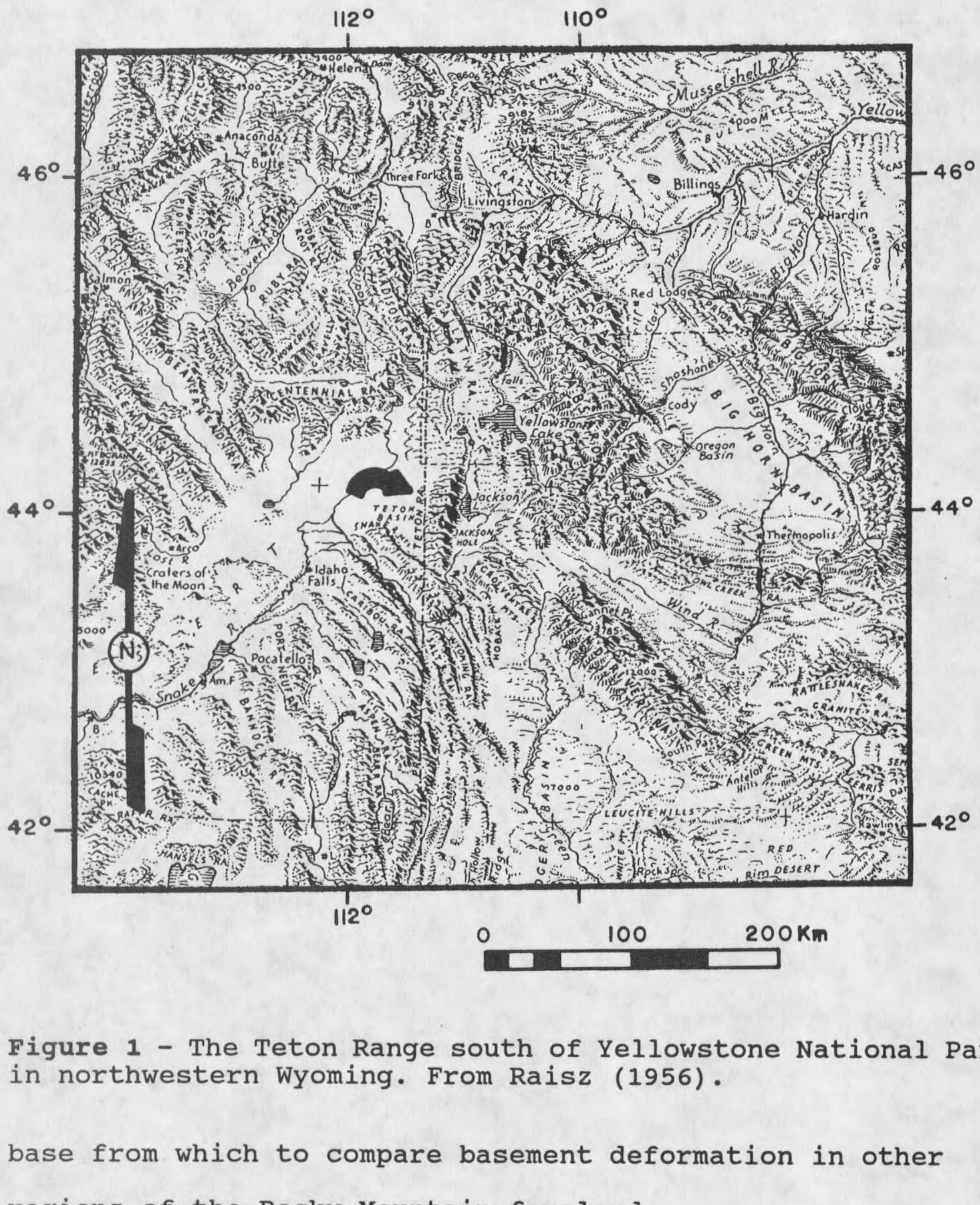

Figure 1 - The Teton Range south of Yellowstone National Park in northwestern Wyoming. From Raisz (1956).

base from which to compare basement deformation in other regions of the Rocky Mountain foreland.

The Teton Range (Figure 1) lies on the western-most margin of Laramide (basement-involved) deformation in the Wyoming foreland. The highest peaks in the Teton Range, the Cathedral Group, are clustered in the central part of the range. They are bounded on the west and south by the Buck Mountain reverse fault (Love, 1968), on the southeast by the Static and Stewart faults (Bradley, 1956), and on the east by the Teton normal fault (Figure 2).

It has been assumed that the Buck Mountain fault in the central Teton Range is a Late Cretaceous to Early Eocene, Laramide-style reverse fault on which the high peaks of the Teton Range were uplifted (Love, 1968; Love and Reed, 1971; Love and others, 1973). In addition, Bradley (1956) mapped the Static and Stewart faults in the central Teton Range as high-angle Precambrian reverse faults that were reactivated during the Laramide orogeny. However, no definitive evidence has been presented to support these contentions. Furthermore, the mechanical response of Archean "basement" rocks and metamorphism occurring as a result of the Laramide orogeny have not been well documented in this area.

The purpose of this study is to: 1) characterize the geometry, kinematics, and ages of the Buck Mountain, Static, and Stewart faults, and determine their structural relationship; and 2) further the understanding of Laramide basement deformation by comparing the criteria presented by Mitra and Frost (1981) for differentiating early Precambrian, late Precambrian, and Laramide deformation zones in the Wind River Range with characteristics of deformation in the study area.

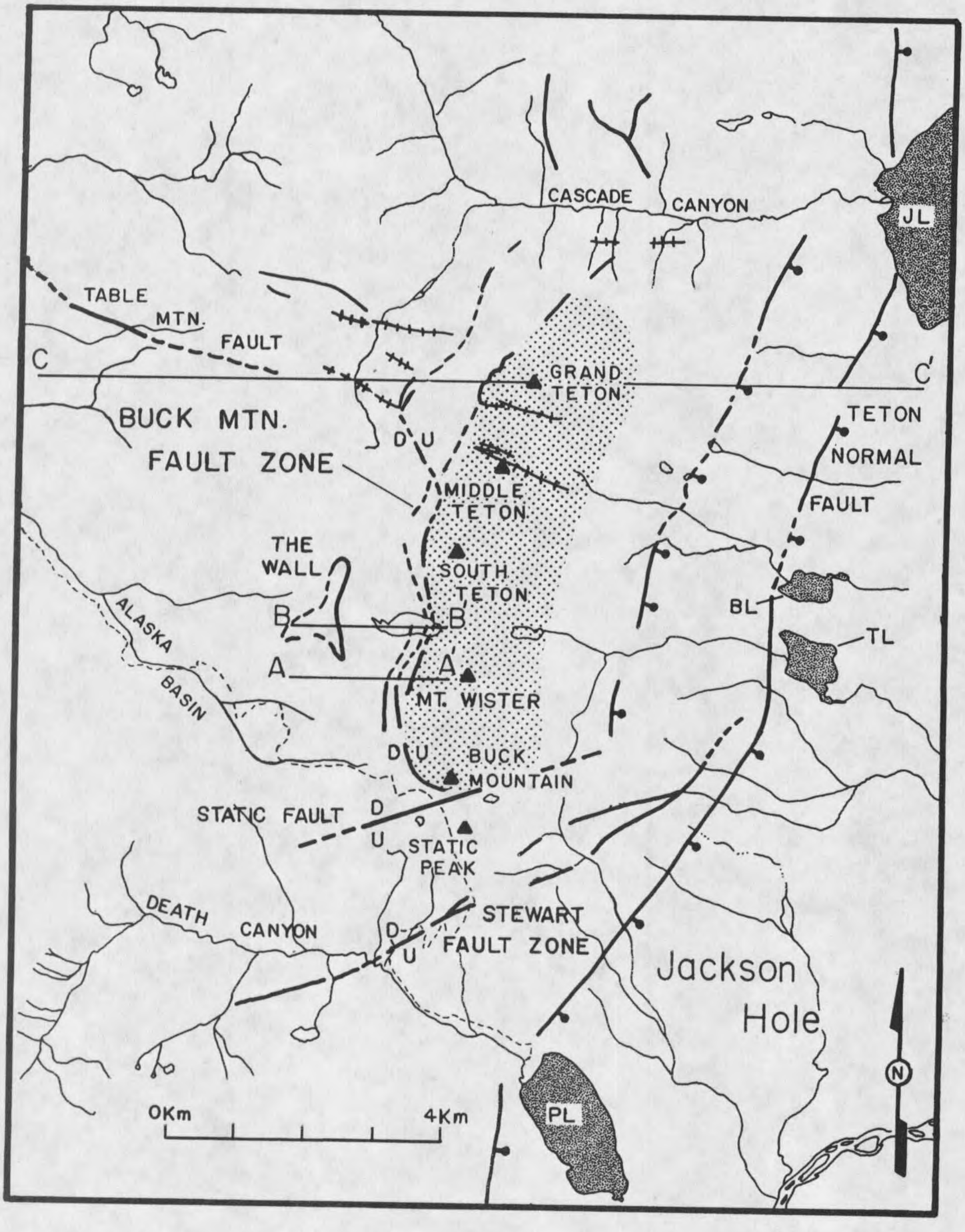

Figure 2 - Structure index map of study area. PL = Phelps Lake, JL = Jenny Lake, TL = Taggart Lake, and BL = Bradley Lake. Dot pattern = the Cathedral Group. Structure is from Bradley (1956), Reed (1973), Smith and others (1990), and mapping done in this thesis.

Questions addressed in this study are: 1) What are the geometries of the Buck Mountain, Static, and Stewart faults, and the Cathedral Group block as a whole? 2) What is the sense of movement on these faults, i.e., has movement been dip-slip or oblique-slip? 3) What are the controls on faulting; did pre-existing zones of weakness control fault geometry? 4) What are the ages of the Buck Mountain, Static and Stewart faults? 5) What mineralogic assemblages and deformational textures characterize the faults, and how do they compare with the findings of Mitra and Frost (1981) in the Wind River Range?

Study Area

The Teton Range is a north-trending, basement-cored, Miocene to Holocene uplift located in northwestern Wyoming (Figure 3). The Range is approximately 60 kilometers long by 15-25 kilometers wide and is bounded on the east by a range-front normal fault that dips 35 degrees east (Behrendt and others, 1968) and has a throw of approximately 10 kilometers (Love and Reed, 1971; Doser and Smith, 1983).

The study area for this investigation is centered on the Cathedral Group in the central Teton Range, which contains the highest peaks in the range (Figures 2 and 4). Included in the Cathedral Group are the Grand Teton (4,197m), Middle Teton (3,903m), South Teton (3,814m), Buck Mountain (3,639m), and a number of less prominent peaks; all

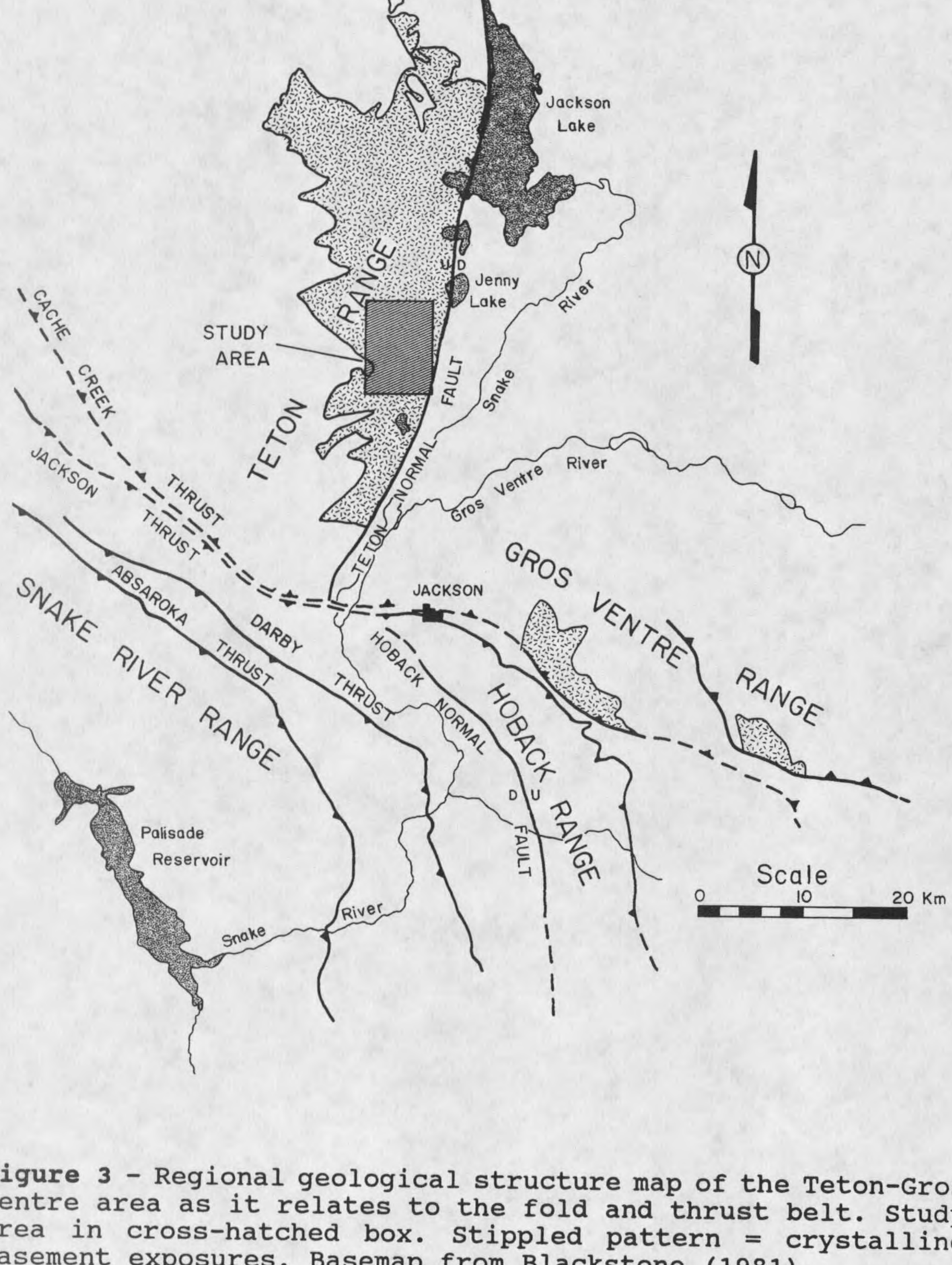

Figure 3 - Regional geological structure map of the Teton-Gros Ventre area as it relates to the fold and thrust belt. Study area in cross-hatched box. Stippled pattern = crystalline basement exposures. Basemap from Blackstone (1981).

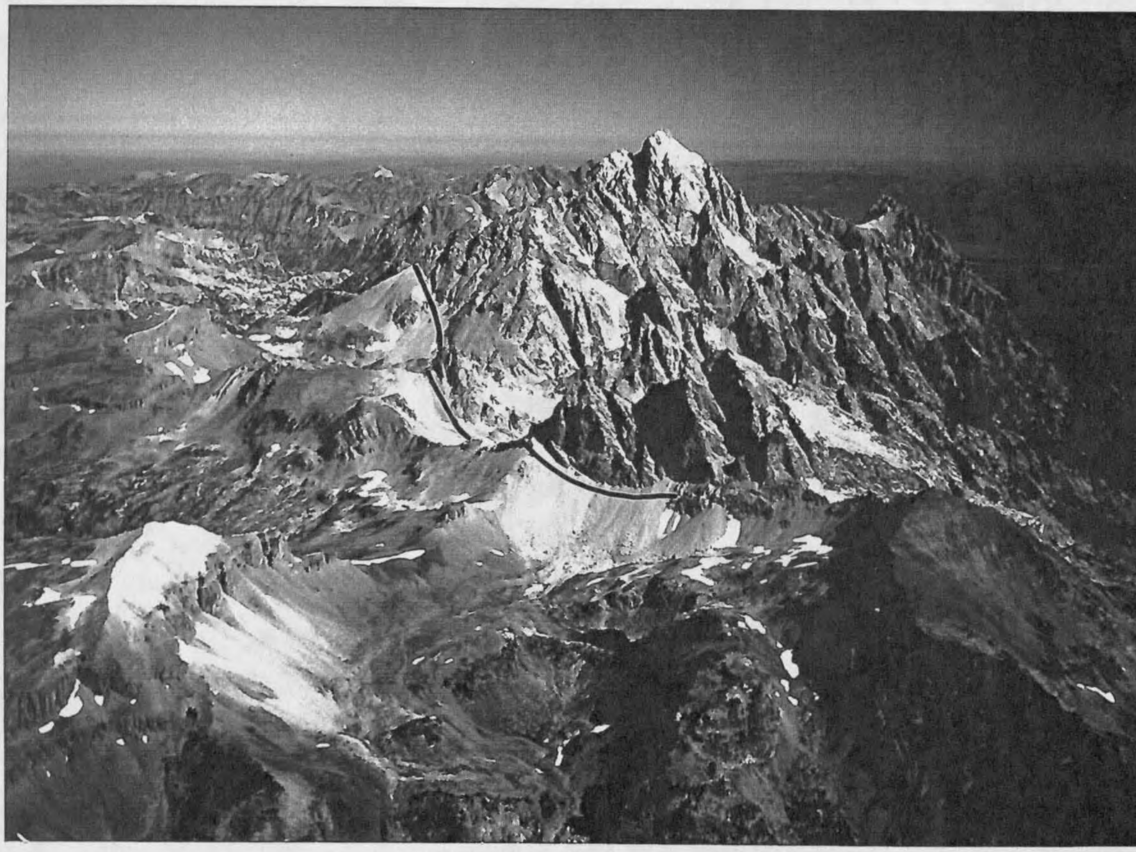

Figure 4 - Aerial photograph looking northeast of the west flank of the middle Teton Range. Note breccia zones cutting the western flanks of the high peaks of the Cathedral Group.

of these mountains are within the boundaries of Grand Teton National Park. These high peaks are bounded on the south by Death Canyon and the Static and Stewart faults, and on the north by Cascade Canyon (Figure 2). Both Death Canyon and Cascade Canyon are deeply cut glacial valleys. The Cathedral Group is bounded on the west by a high-angle, north-trending, east-dipping reverse fault known as the Buck Mountain fault, and on the east by the Teton normal fault

(Love, 1968) (Figure 2). The Buck Mountain fault juxtaposes Precambrian gneiss and intrusive rocks on the east against gently westward-dipping, Paleozoic sedimentary rocks to the west. This fault extends from approximately the area of Mount Moran southward to Buck Mountain where it curves to the east around the south flank of Buck Mountain. At that location, the fault intersects the northeast-striking Static fault (Bradley, 1956) (Figure 2). The Stewart fault, also mapped by Bradley (1956), lies south of the Static fault.

Access to the Buck Mountain fault is from the Death Canyon and Static Peak Divide trails. From Whitegrass Ranger Station follow the Death Canyon trail approximately 3.4 kilometers to the National Park patrol cabin. There, the Static Peak Divide trail branches off to the north and continues for 9.6 kilometers to the divide. Elevation change from the patrol cabin to Static Peak Divide is 1,200 meters. The total distance from Whitegrass Ranger Station to Static Peak Divide is approximately 13 kilometers (Figure 2).

An alternative access route begins on the west flank of the Teton Range in the Targhee National Forest Teton Campground. From there, follow the Alaska Basin trail east approximately 15 kilometers to Buck Mountain. Elevation change is approximately 1,000 meters (Figure 2).

Avalanche Canyon, Garnet Canyon and Cascade Canyon provide other alternate access routes to the Buck Mountain fault. However, precipitous down-climbs and greater travel length make these approaches less efficient.

Regional Overview

The Teton Range is uniquely located at the juncture of four major tectonic provinces including the: 1) basement-involved Laramide foreland, 2) Wyoming salient of the Sevier fold and thrust belt, 3) Neogene to Recent Basin and Range province, and 4) Yellowstone Plateau and Snake River Plain within the intermountain seismic belt (Doser and Smith, 1983; Anders and others, 1989) (Figure 5).

Laramide foreland: The Teton Range is located at the western-most margin of the Laramide Rocky Mountain foreland province, that region of basement-involved uplifts and basins bounded by the undeformed craton to the east and the decollement-style fold and thrust belt to the west (Brown, 1984). The present-day Teton and Gros Ventre Ranges have evolved from the late Cretaceous-early Tertiary, northwest-trending ancestral Teton-Gros Ventre uplift, which rose along the northeast-dipping Cache Creek thrust fault (Love and Reed, 1971; Love, 1973; Love, 1977). At the northwest end of the Gros Ventre Range, the Neogene to Recent Teton normal fault trends nearly perpendicular to the older Teton-Gros Ventre uplift (Figure 3). The Cache Creek thrust fault, may serve as a sole or basement "decollement" for the Teton

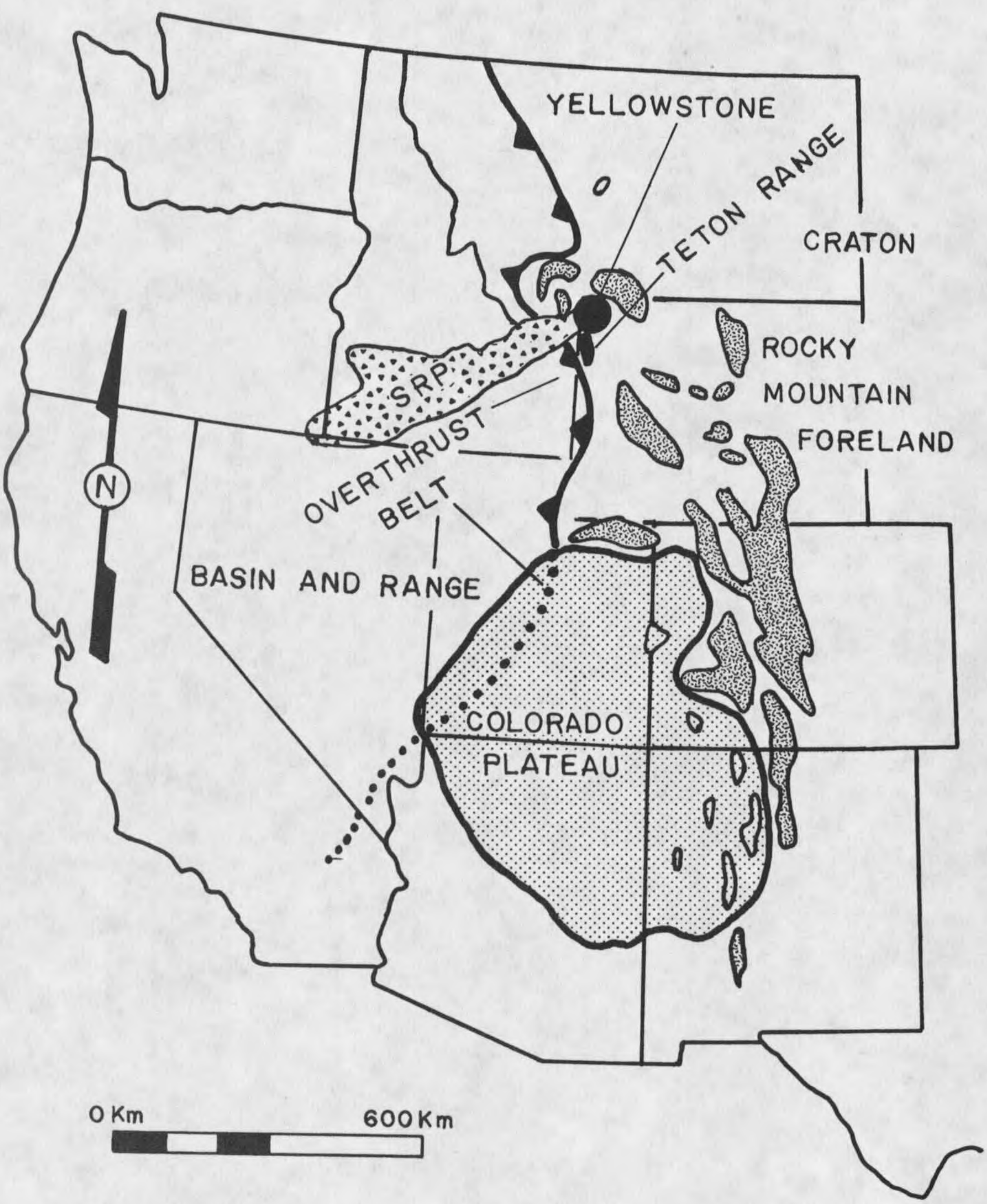

Figure 5 - Teton Range in the context of the major structural provinces of western North America. SRP = Snake River Plain. Triangle pattern = volcanics; mottled pattern = basement uplifts; dot pattern = area of Colorado Plateau. Base map from Burchfiel (1981).

normal fault and other smaller associated normal faults (Reese, unpublished; Lageson, 1987; Lageson, 1990, in press) (Figure 6).

Sevier fold and thrust belt: The Teton Range lies on the eastern-most margin of the thin-skinned, Sevier fold and thrust belt (Late Jurassic to early Paleogene) (Armstrong and Oriel, 1965). The eastern extent of Sevier-style deformation closely coincides with the eastern boundary of the Paleozoic-Mesozoic miogeocline (Suppe, 1985). Also, the Laramide Cache Creek thrust overlaps the thin-skinned Jackson thrust at Teton Pass (Figure 3) (Royse, Warner and Reese, 1975; Vasko, 1982; Zeller, 1982; Dunn, 1983).

Basin and Range province: Late Cenozoic extensional deformation has been recognized as far east as western Wyoming and as far north as northwest Montana (Zoback and Zoback, 1980). The Teton Range lies on the eastern-most margin of the Basin and Range tectonic province in Wyoming (Lageson, 1990) (Figure 5). It has been shown by several investigators that late Cenozoic extensional structures have overprinted late Mesozoic-early Tertiary Sevier structures (e.g. Royse and others, 1975; Allmendinger and others, 1983; Sales, 1983; Smith and Bruhn, 1984; Olson and Schmitt, 1987), but fewer examples exist where Basin and Range structures have overprinted Laramide foreland structures (Reese, unpublished; Sales, 1983; Royse, 1983; Lageson and Zim, 1985; Zim and Lageson, 1985; Lageson, 1990, in press).

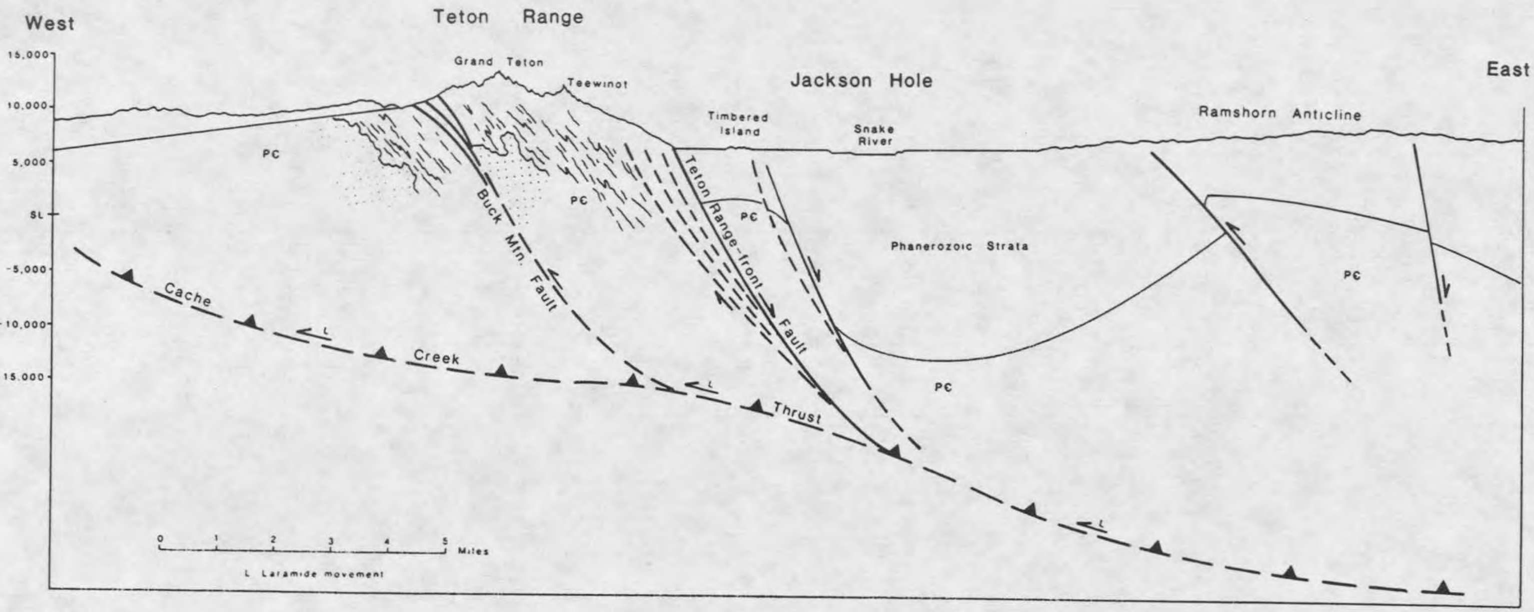

Figure 6 - East-west cross-section through the Buck Mountain fault. The Laramide Cache Creek reverse fault may act as a sole for the Teton normal fault. From Lageson (1987), modified from Love (1968).

The Teton normal fault may merge into the Cache Creek fault as a late Cenozoic overprint on the Laramide ancestral Teton-Gros Ventre uplift (Love and Reed, 1971; Lageson, 1990, in press).

Yellowstone hotspot and Snake River Plain: Over the past 15 m.y. the North American tectonic plate has migrated southwestward over the Yellowstone "hotspot" at a rate of approximately 3.5cm/yr (Anders and others, 1989; Smith, 1990). However, the first-order tectonic origins of this "hotspot," if indeed it is a hotspot, are as yet unknown. The volcanic scar left by this migration is known as the Snake River Plain and extends from south-central Idaho to the present location of the hotspot at Yellowstone National Park, north of the Teton Range (Figure 5). Latest Quaternary movement on the Teton normal fault of 1.7-2.2 mm/yr may be in response to decreased lithospheric strength due to the rising mantle plume beneath the Yellowstone Plateau (Anders and others, 1989).

Additionally, the Precambrian rocks of the Teton Range are part of a terrain known as the Wyoming Province (Engel, 1963; Reed and Zartman, 1973; Houston, 1990). The Wyoming Province consists of basement rocks which have metamorphic and plutonic ages greater than 2.5 b.y. and includes most of the basement uplifts in Wyoming and south-central Montana (Reed and Zartman, 1973).

Methods of Investigation

The following field and laboratory methods were used during the course of this investigation:

Mapping

1) Air photo interpretation: air photos were used to determine if geomorphologic features in the vicinity of the Cathedral Group, such as stream drainages and lineaments, coincide with structural features in the area. Air photos used for this investigation are United States Department of Agriculture vertical photographs (code number TAR16043; roll number 0275; exposures 34-38; scale 1:66,300). The flightline extends from south of Buck Mountain northward over the Cathedral Group to Cascade Canyon. Low altitude oblique air photos of the Buck Mountain and associated faults were also examined to help characterize structural relationships in the study area.

2) Field mapping: mapping consisted of detailed field checking of Reed's (1973) Geologic Map of the Precambrian Rocks of the Teton Range (1:62,500). Macroscopic features such as fault and diabase dike trends, as well as Precambrian and Phanerozoic outcrops, were field checked using the USGS Grand Teton and Mount Moran 1:24,000 quadrangle maps, and a revised map of the field area was

drafted. Three-point problems (method of Rowland, 1986) were used to determine the dip of the Buck Mountain fault surface. Reed's (1973) <u>Geologic Map of the Precambrian Rocks of the Teton Range</u> (1:62,500), and field maps compiled in this investigation (1:24,000) were used for this purpose.

3) <u>Modeling</u>: Cross-sections through the Buck Mountain fault, including retrodeformation (method of Erslev, 1986) to the time of Laramide deformation, were prepared to represent the subsurface and subaerial configuration of the Buck Mountain fault and the Cathedral Group block, and to characterize the environment of deformation at the stated times.

<u>Mesoscopic</u>

1) <u>Geometry</u>: strike and dip of metamorphic foliation and compositional layering, and trend and plunge of folds were plotted on lower-hemisphere, equal-area stereographic (Schmidt net) projections. These data assisted in establishing basement geometry, and subsurface projections. Additionally, Archean and post-Archean fold geometries were differentiated and used to help characterize different deformation events.

2) <u>Kinematics</u>: fault zone slickenlines were measured to determine the rake of net slip on faults. In addition, drag folds were studied on the Buck Mountain and Static faults to constrain the most recent sense of movement on the faults.

3) Field observations: fault characteristics such as fault zone width, cataclasis, and weathering were studied to help characterize the geometry and deformational styles of the Buck Mountain, Static, and Stewart faults. Also, mesoscopic rock textures in deformation zones were studied in detail as a prelude to thin section analysis.

Microscopic and Other Techniques

1) Thin section study: thin sections from deformation zones, country rock and intrusive bodies in the study area were examined to characterize: 1) primary mineral assemblages; 2) deformation textures; 3) alteration mineralogies; and 4) grade of metamorphism.

2) X-Ray Diffraction: x-ray diffraction analysis of fault gouge from the Buck Mountain, Stewart and Static faults was conducted to help characterize the sub-microscopic alteration mineralogy along the faults. Powdered smearslides of gouge were examined using a Phillips Instrument X-Ray diffractometer at Montana State University and using (two theta) copper radiation determinative tables.

Previous Investigations

The Precambrian rocks of the Teton Range were first described by members of the Hayden Survey of 1872 (Bradley, 1873; St. John, 1879). The Buck Mountain fault was first recognized by Fryxell in 1929 (Edmund, 1956), and later mapped by Horberg and Fryxell (1942). Horberg and Fryxell

(1942) recorded a general N-S strike and steep east dip of "crystalline foliates" in the Precambrian rocks of the range. Other early workers recognized "Laramide" (basement-involved) deformation in and around the Teton Range (Fryxell and others, 1941; Horberg and others, 1949; Horberg and others, 1955; Edmund, 1956; Love, 1956).

Bradley (1956) conducted a study of the Precambrian complex of Grand Teton National Park, focusing on the Buck Mountain area for detailed field work. He presented a preliminary structure map of the Buck Mountain area, recognizing several northeast-trending, southeast-dipping fault zones, as well as the north-trending Buck Mountain fault (Figure 7). At that time, he described the Static and Stewart faults. Bradley (1956) also described all the major metamorphic and intrusive rock types in the Buck Mountain area using hand sample descriptions. His descriptions include: 1) gneiss and schist composed of plagioclase, biotite, hornblende, quartz and orthoclase; 2) augen gneiss of numerous varieties including "quartz-orthoclase, hornblende-plagioclase, schist-ball, and feldspar-magnetite augen" (Bradley, 1956; p.35); 3) leopard diorite (pods of rock consisting of half hornblende and half plagioclase); 4) granite, later identified as quartz monzonite by Reed (1973); 5) pegmatite, aplite, and quartz dikes and veins; 6) diorite dikes; and 7) epidote veins (Bradley, 1956).

Reed (1963) began a study of the Precambrian crystalline complex of the northern Teton Range that was followed by in-depth investigations and mapping (Behrendt and others, 1968; Reed, 1973; Reed and Zartman, 1973; Miller and others, 1986). Behrendt and others (1968), utilizing seismic refraction, gravity, and aeromagnetic data, showed that the Teton normal fault was not high-angle, as previously thought, but averaged around 35 degrees east dip. Recently, Smith and others (1990) have indicated that dips near the surface of the Teton normal fault range from 45° to 60°.

Love (1968) theorized that the Teton Range was formed in two stages (Behrendt et al, 1968, p.E10);

> During late Cretaceous and early Tertiary times it was the northwestern part of a broad northwest trending fold continuous with the Gros Ventre Range. Later in Cenozoic time this uplift was thrust southwest. Then the overriding block was broken by a series of faults, the largest of which is the Teton fault. The area of downfaulted blocks became the southern part of Jackson Hole, and thereby separated the uplift into two very different segments. The Teton Range continued to rise, whereas the Gros Ventre Range did not.

Giletti and Gast (1961) made the earliest isotopic age determinations in the Teton Range using the Rb-Sr method. Their findings were somewhat ambiguous, but suggested that rocks in the Teton Range were older than 2,300 m.y. (see Chapter 3). Later, Reed and Zartman (1973) conducted Rb-Sr and K-Ar studies on gneisses and granitoid rocks, as well as diabase dikes, throughout the range. Their determinations

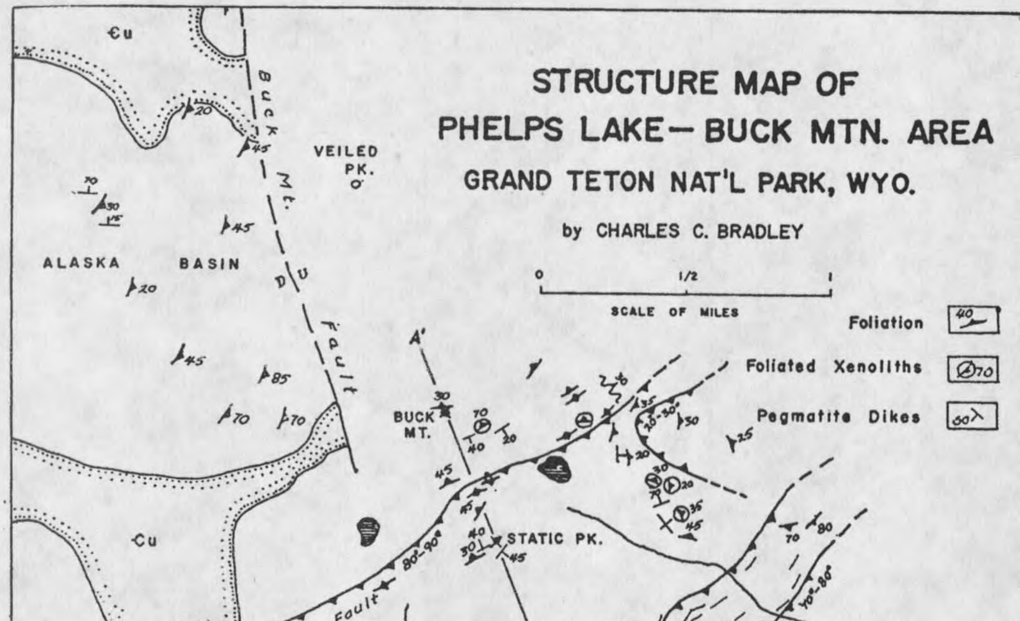

Figure 7 - Bradley's (1956) structure map of the Buck Mountain area. Note the nearly 90 degree intersection of the north-trending Buck Mountain fault with the ENE-trending Stewart and Static faults.

suggested that a regional high-grade metamorphism occurred in the Teton Range at approximately 2,875 m.y., and that extensive granitoid material was intruded into the Archean gneiss at approximately 2,495 m.y. Diabase dikes were intruded sometime during the Proterozoic (see Chapter 3). Roberts and Burbank (1988) provided preliminary results of fission-track studies of apatite in basement rocks of the Teton Range indicating two stages of uplift, one beginning in "late Cretaceous" and another in "Plio-Pleistocene" time (Chapter 3).

Love and Reed (1971) synthesized the geologic knowledge of the Teton Range in their landmark book Creation of the Teton Landscape. They described the Buck Mountain fault as a reverse fault associated with the ancestral Teton-Gros Ventre uplift of the "Laramide Revolution." The age of the fault was placed at either 50 to 55 million years ago, or "during a later episode of movement" (Love and Reed, 1971; p.91).

More recently, other workers have related the Buck Mountain fault and the Teton normal fault to other regional structures such as the Cache Creek thrust and the Gros Ventre Range. Reese (unpublished) depicted the Teton normal fault and numerous other faults to the east soling into the Cache Creek thrust. Sales (1983) makes a case for "collapse" of the Teton normal fault into the sole of the Cache Creek thrust. Royse (1983) proposed that the Teton-Gros Ventre uplift has extended 5 kilometers through a series of north-trending, westward-tilted blocks. Lageson (1987) modified Love's (1968) cross-section interpretation of the Teton Range to show the Buck Mountain fault and the Teton normal fault soling into the Cache Creek thrust. He also suggested the possibility of reactivation of north-trending basement shear zones by the Teton normal fault. Smith and Lageson (1989) provided evidence for the Laramide origin of the Buck Mountain fault. Furthermore, Lageson (1990) suggested that the series of north-striking faults on the southern margin of the Teton Range, including the Teton normal fault, are Cenozoic westward-tilted normal faults that reactivate or sole into the Laramide Cache Creek thrust fault.

MAPPING

Air Photo Analysis

Analysis of vertical air photos of the study area revealed numerous mappable lineaments including fault traces, erosional scars and canyons (Figure 8). Three generalized trends are prominent: east-west, north-south, and northeast-southwest.

East-west trends are represented by Cascade Canyon north of the Cathedral Group and Table Mountain fault west of the Grand Teton (Reed, 1973). The Table Mountain fault is parallel to diabase dikes within, and drainages on the east side of, the Cathedral Group (Figure 2). Glacier-cut drainages in the study area also trend generally east-west, with tributaries oriented north-south.

North-south trends are represented by the Teton normal fault (Teton range front), the Buck Mountain fault, and several distinct lineaments reflecting erosional depressions east of the Cathedral Group (Figure 8). The Teton normal fault strikes approximately N 15 E north of Static Peak and abruptly changes to N 30 E south of there (Lageson, 1990) (Figure 8). The Buck Mountain fault exhibits a more north-south, anastomosing orientation on the west side of the Cathedral Group. Splays of the fault coincide with two,

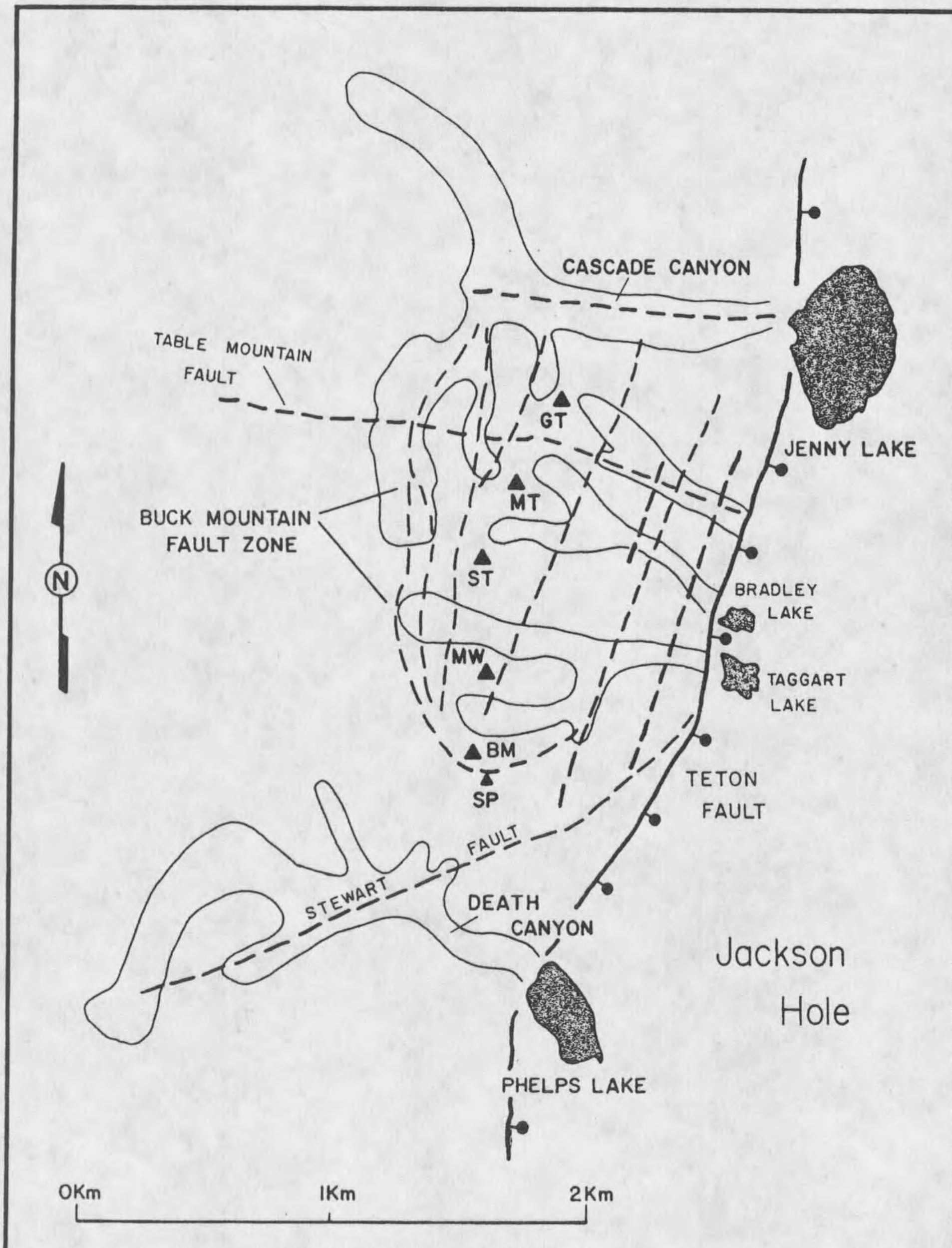

Figure 8 - Air photo interpretation of lineaments in the central Teton Range, Wyoming. Canyons are outlined with solid lines. Dashed lines represent erosional lineaments. GT = Grand Teton, MT = Middle Teton, ST = South Teton, MW = Mount Wister, BM = Buck Mountain, SP = Static Peak, mottled pattern = water. Ball and bar on downthrown side of Teton fault. Teton fault structure from Smith and others (1990).

nearly parallel, south forks of Cascade Canyon (Figure 8). West of the Teton normal fault and east of the Cathedral Group, several distinct erosional lineaments parallel the strike of the fault (Figure 8).

The only northeast-southwest lineament recognized on aerial photographs coincides with the Stewart fault. The fault can be traced from the Teton normal fault southwest to the headwaters of Death Canyon (Figure 8) where a southwest-trending tributary of Death Canyon appears to be controlled by the Stewart fault.

Field Mapping

Faults

Two general fault orientations are found in the study area, north-south and northeast (Figure 9). Also, the Table Mountain fault strikes west-northwest, parallel to the diabase dikes, west of the Grand Teton (Figure 9).

The Buck Mountain fault strikes north from Buck Mountain to an area somewhere north of Cascade Canyon. At its southern termination the Buck Mountain fault curves to the east around Buck Mountain.

The Teton normal fault also strikes generally north-south along the eastern base of the Teton range. South of the field area, beginning east of Static Peak, the Teton normal fault doglegs to the west, changing strike from N 15 E to N 30 E (Lageson, 1990, in press) (Figure 3).

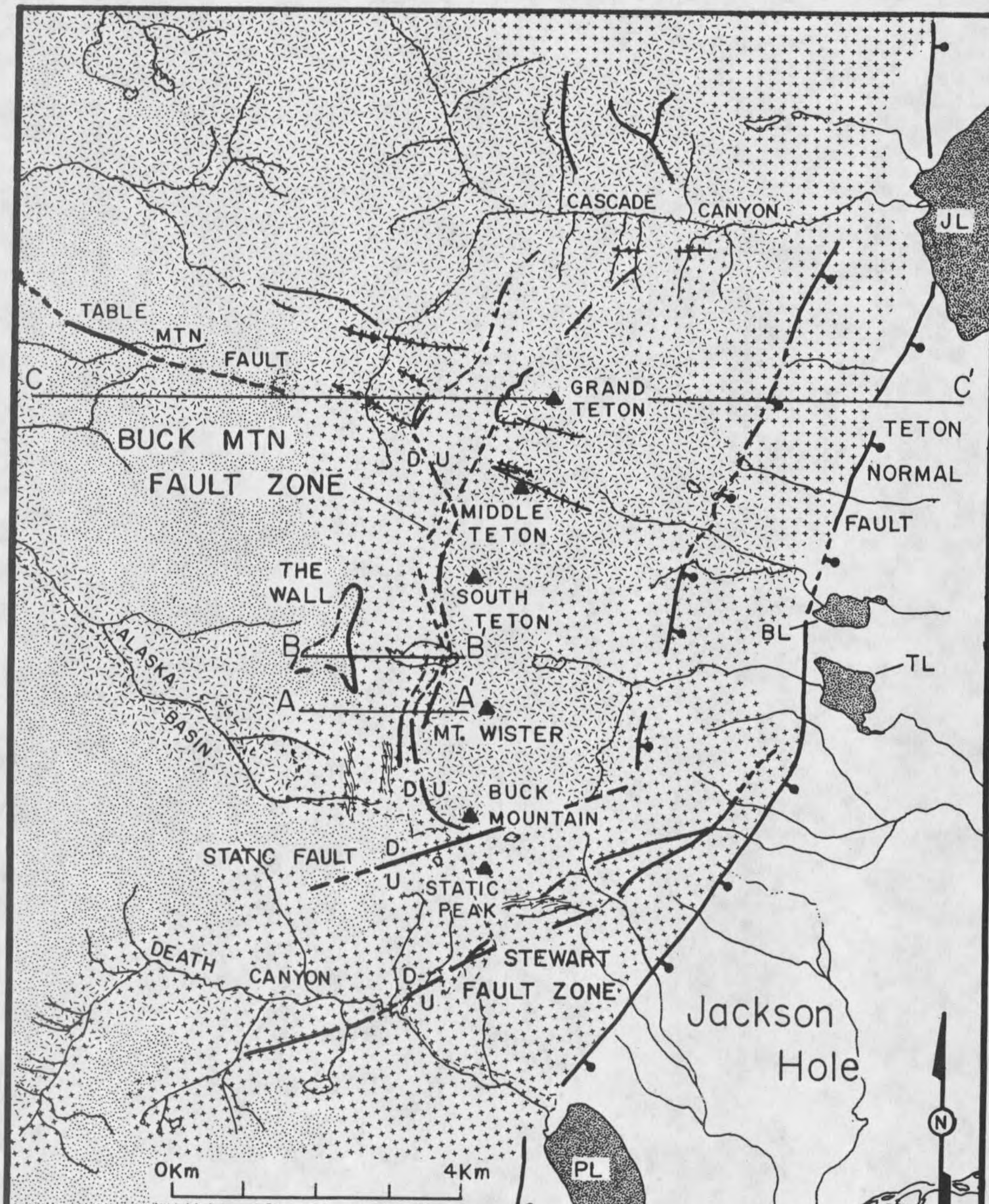

Figure 9 - Geologic map of the study area. Legend on following page. Geology from Bradley (1956), Reed (1973) and mapping conducted in this study.

LEGEND

Quaternary undifferentiated

Paleozoic undifferentiated

Mount Owen Quartz Monzonite - The Mount Owen Quartz Monzonite, in places, incorporates large xenoliths of Precambrian basement and is extensively criss-crossed with pegmatite dikes.

Archean layered gneiss and schist

- Ductile shear zone of probable Proterozoic age

JL - Jenny Lake

PL - Phelps Lake

BL - Bradley Lake

TL - Taggart Lake

- Diabase Dike

U D - High-angle reverse fault: U = up, D = down

- Normal Fault: ball and bar on downthrown side

Static fault strikes approximately N 75 E; it emerges from beneath the Paleozoic section southwest of Buck Mountain, converges with the Buck Mountain fault on the pass between Buck and Static peaks, and disappears in the south fork of Avalanche canyon (Figure 9).

Stewart fault trends approximately N 55 E and can be traced from the headwaters of Death Canyon northeast to Avalanche Canyon (Figure 9).

Additionally, several Precambrian shear zones are recognized in the area. One green-colored ductile shear zone coincides with the trace of the Static fault (Figure 9). Another narrow (5-10 meters), east-west striking, ductile shear zone was mapped for 500 meters southeast of Static Peak (Figure 9). In Alaska Basin, several north-striking zones represent both recrystallized mylonites and green-colored ductile shear zones similar to the one along Static fault (Chapter 3) (Figure 9).

Buck Mountain Fault. The Buck Mountain fault cuts across the western flanks of the Grand, Middle and South Tetons, Veiled Peak (Figure 10) and Buck Mountain, placing Precambrian basement on the east against Paleozoic sedimentary rocks to the west (Figure 9). It is a zone of variable deformation, including areas of extreme brecciation characterized by orange to yellow coloring (Figure 10). Directly west of Buck Mountain, the fault exhibits a single continuous breccia zone approximately 30-90 meters wide.

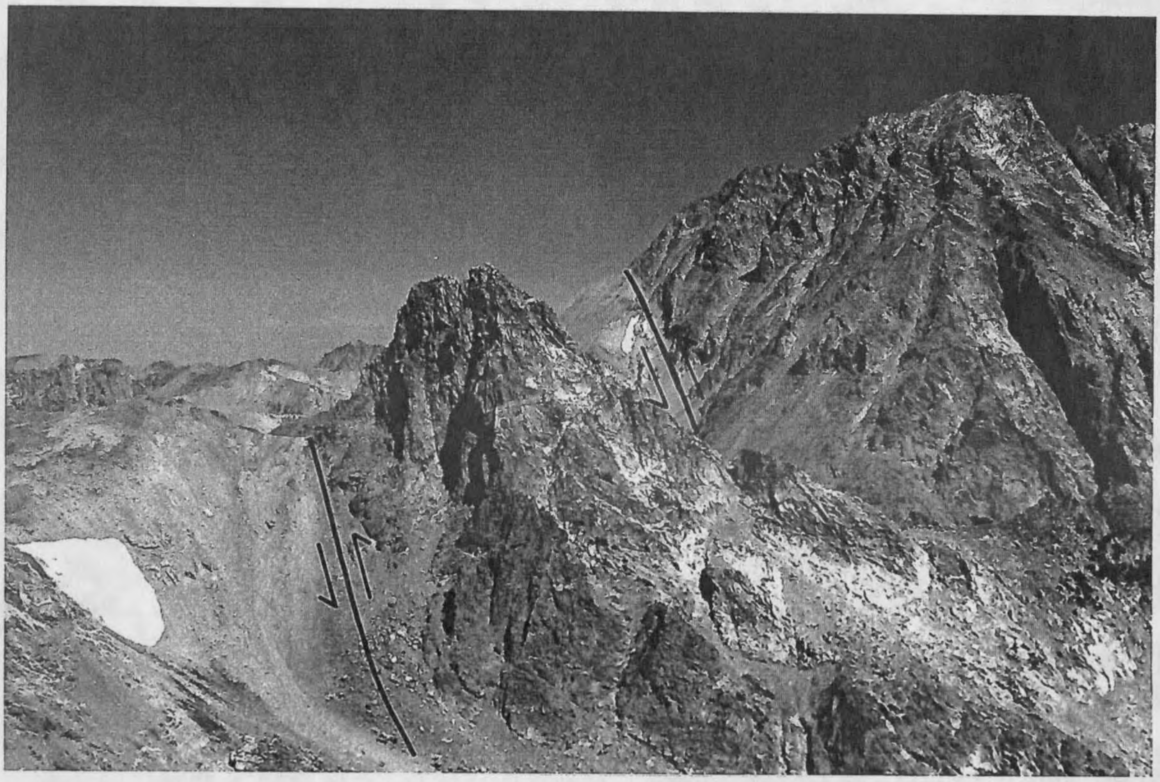

Figure 10 - Photo looking north: intense deformation of the Buck Mountain fault west of Veiled Peak (in the foreground), and the Middle Teton north of there.

Farther north, the fault splits into an anastomosing array as wide as 500 meters, with mildly deformed slices or macrolithons of gneiss and schist between the fault splays (Figure 11). On the margins of the fault, brittle deformation is observed in the form of jointing and fracturing of gneiss and pegmatite veins on a scale of meters to tens of meters. Closer to the fault, fracturing is on a centimeter to tens of centimeters scale. A topographic depression coincides with the trace of the fault west of the Cathedral Group due to erosion of the brecciated fault zone material. At its southern termination, the Buck Mountain fault curves to the east around Buck Mountain and intersects Static fault at the Buck Mountain-Static Peak divide (Figure 9). At that location, the fault zone is highly pulverized and rich in very fine-grained, non-directional (non-foliated), chloritic cataclasite (Groshong, 1988), with larger (millimeter to centimeter scale) angular fragments of potassium feldspar suspended in the fine-grained matrix.

Visual inspection suggests that the Buck Mountain fault dips at a high-angle, at least at shallow depths (Figure 4). In map view, the Buck Mountain fault has a sinuous trend due to the extremely high relief between mountains and deep canyons over which the trace of the fault is superimposed, thus permitting application of the three-point method to determine angle of dip (Rowland, 1986). The solutions of three-point problems from four locations along the trace of the Buck Mountain fault are as follows:

I. Veiled Peak - 57° East

II. South Teton - 68° East

III. Buck Mountain - 59° East

IV. Cascade Canyon - 42° East

Based on these measurements, the average dip of the Buck Mountain fault along its leading edge is 57 degrees east. The angle of dip is greater where the fault lies adjacent to the high peaks and seems to diminish northward where the fault cuts across Cascade Canyon. It is unclear, however, whether the change in dip is due to a change in

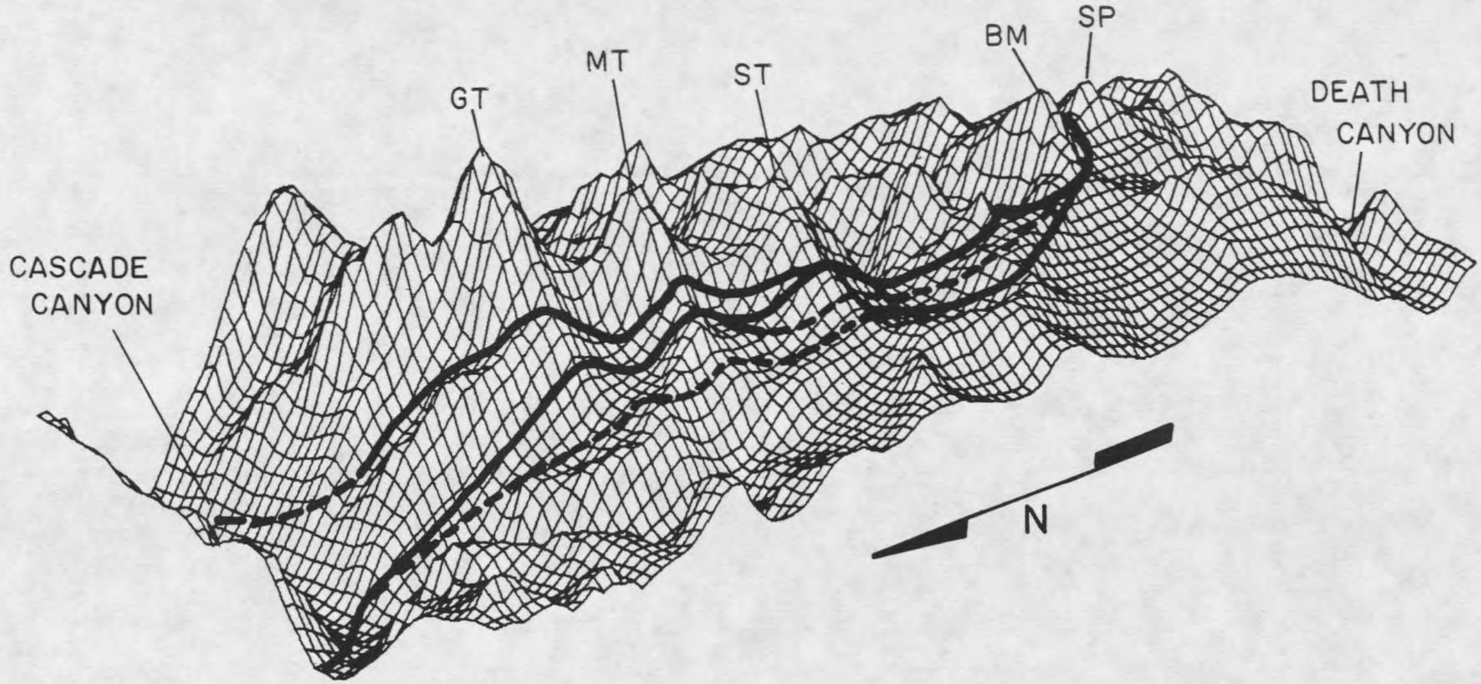

Figure 11 - The Buck Mountain fault zone on the west flank of the Cathedral Group of the middle Teton Range. GT = Grand Teton, MT = Middle Teton, ST = South Teton, BM = Buck Mountain, SP = Static Peak. 3-D model generated from digitized X-Y-Z coordinates with the Golden Software Surfer program.

fault angle, later rotation of the fault, differential uplift, or to inaccurate mapping across the Quaternary deposits of Cascade Canyon. Evidence provided later in the text supports the differential uplift concept.

Static Fault. West of Static Peak in a glacially scoured basin draining the southwest flank of Buck Mountain, a 10-50 meter wide, anastomosing, ductile deformation zone coincides with the Static fault (Bradley, 1956) (Figure 9). The Static fault can be divided into two linear zones. The northeast segment coincides with the Buck Mountain fault zone where the two faults converge at the Buck Mountain - Static Peak divide. This segment exhibits extreme cataclasis and gouge resulting in a non-oriented cataclasite. The southwest segment extends southwest from Buck - Static divide into the footwall of the Buck Mountain fault (Figure 9), and is characterized by a green, strongly foliated chloritic shear zone, locally interlayered with brecciated, red, magnetite and quartz-rich zones, that cross-cuts all basement rocks. Static fault strikes N 75 E and extends from the Buck Mountain-Static Peak Divide southwest to the west side of the aforementioned basin (approximately 1.5 kilometers), where it is unconformably overlain by Paleozoic sedimentary rocks (Figure 9). Unlike the cataclasite on Buck-Static divide, this material exhibits a strong preferred orientation of biotite and chlorite and has a phyllitic sheen.

Bradley (1956) mapped Static fault as a high-angle reverse fault. This can be demonstrated on the east face of Static Peak, where the Static fault dips approximately 50° southeast (Figure 12). Static Peak is the sheared-out limb of a large antiform that is cut by the Static fault (Figure 13 A and B). Drag folds (using the definition of Suppe, 1985, p.342) in the hanging wall of Static fault indicate a reverse sense of movement (Bradley, 1956) (Figures 13A and 13B).

Due to access problems, the east face of Static Peak could not be sampled directly. However, red and green weathering can be observed around the folded layers. The red color is interpreted as iron-oxide staining and the green as chloritization, and both may be products of hydrothermal alteration (Chapter 4).

Stewart Fault. Another distinct fault trace, the Stewart fault, exists roughly 1,000 meters southeast of Static fault. The fault strikes approximately N 55 E and dips steeply to the southeast (Bradley, 1956). The Stewart fault can be traced from the headwaters of Death Canyon northeast to the Teton normal fault (Figure 9). The Stewart fault zone is approximately 100 to 200 meters wide and is easily recognized on aerial photographs and on the ground by its bright, orange-yellow and green coloring and highly brecciated nature. As with the Buck Mountain fault,

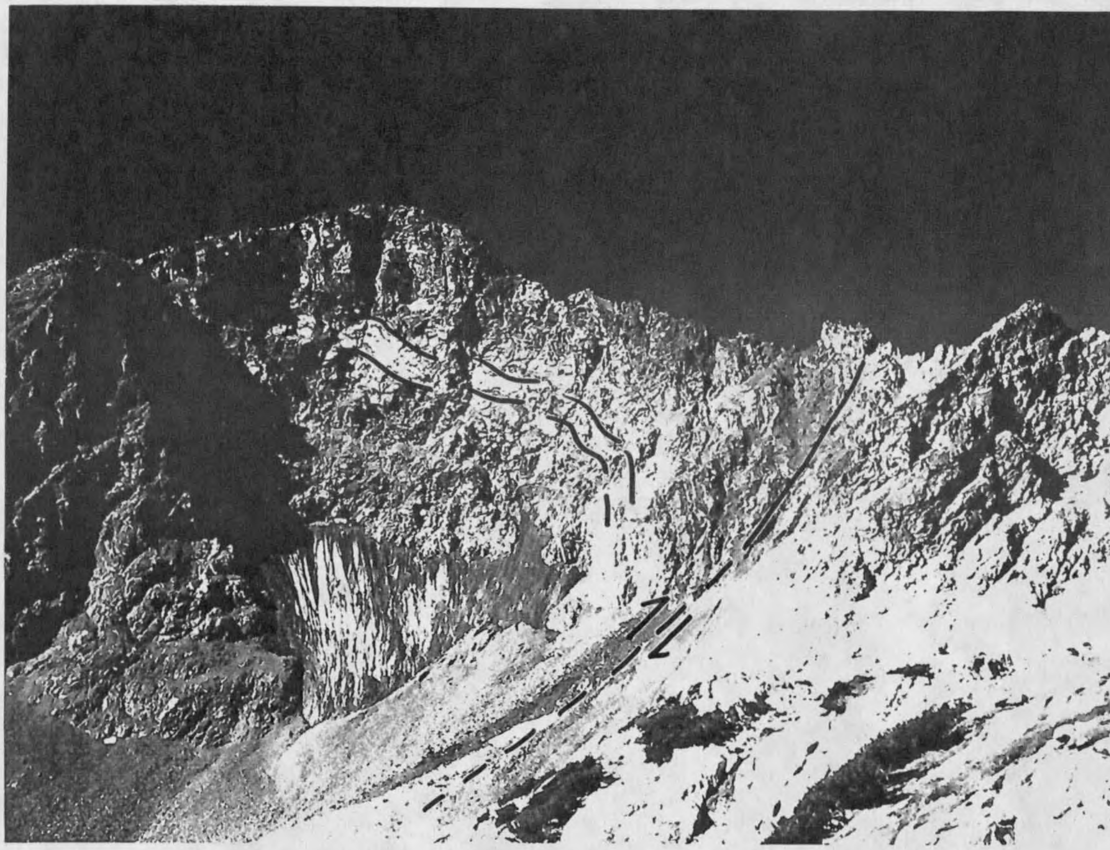

Figure 12 - East face of Static Peak. Note the overturned drag folds in the hanging wall of Static fault.

deformation increases from nearly undeformed country rock to a zone of iron-oxide stained, chloritic breccia (chapter 4). Closely-spaced (centimeter scale), unstable fractures (Mitra and Frost, 1981) in typical layered gneiss of the area are common close to the maximum zone of deformation.

General lithologies

The literature provides several alternative interpretations for the distribution of Precambrian lithologies in the Teton Range as related to the study area. Horberg and Fryxell (1942) recognized the complex

A

B

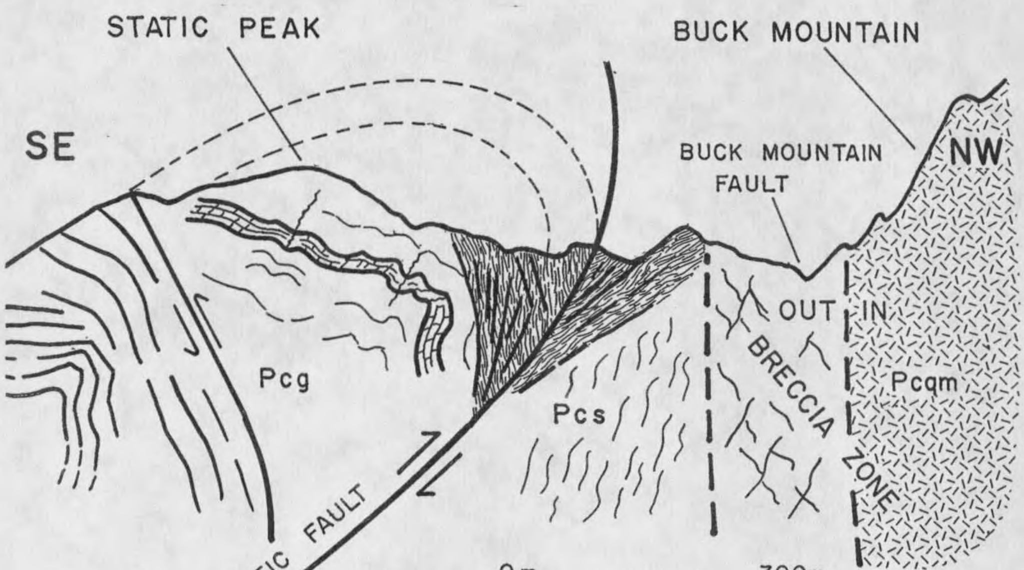

Figure 13 - A: Oblique aerial view of the east face of Static Peak and Buck Mountain. Notice the black color of Static Peak (hornblende gneiss and amphibolite).B: Structure on the east face of Static Peak. Hatchured pattern (Pcqm) = Precambrian quartz-monzonite and pegmatite; Pcs = Precambrian ductile shear zone; Pcg = Precambrian gneiss and schist; dense line pattern at top of Static fault = breccia and gouge.

relationship of granitoid intrusives with gneisses and schists (Figure 14). Bradley (1956) suggested that the high peaks (the Cathedral Group) consist of a "well-knit" matrix of granite and xenoliths, and that this may be responsible for the weathering resistance of the Cathedral Group. Reed (1963, 1973), and Reed and Zartman (1973) produced maps of the Teton Range differentiating Precambrian rocks. Reed (1973) showed Mount Owen Quartz Monzonite in the Cathedral Group north of the South Teton (scale of 1:62,500); he mapped the South Teton and Buck Mountain as layered gneiss and migmatite (Figure 14). Mapping by this author at 1:24,000 in the vicinity of the Cathedral Group refines Reed's (1973) interpretation (Figure 9). In the following discussion, I present descriptions of relations between mapped units:

Layered Gneiss and Schist. Layered gneiss and schist (Chapter 3) are the oldest rocks in the study area, as they are crosscut by all other rocks. They are exposed predominantly along the Teton Range front east of the high peaks of the Cathedral Group, in the Death Canyon area south of Static fault, and just west of the Buck Mountain fault in the footwall block (Figure 9). In Alaska Basin, layered gneiss is located only in the upper reaches of the basin, directly adjacent to the fault trace. Reed (1973) mapped Mount Owen Quartz Monzonite in the lower basin (Figure 9).

Figure 14 - Precambrian lithologies are extremely complex in the Teton Range. Here, leopard diorite pods (Bradley, 1956) may be migmatitic (Reed, 1973). Later intrusive granitoids cross-cut the Archean rocks. Hammer for scale in center of photograph.

<u>**Granitoids**</u>. Major intrusive quartz monzonite stocks and granitoid dikes and pegmatites are found south of Cascade Canyon, predominantly in the hanging wall of the Buck Mountain fault (Figure 9). Pegmatites cross-cut the quartz monzonite and are themselves cross-cut by quartz monzonite, indicating they occurred at approximately the same time (Figure 15). In the Cathedral Group, the granitoid material incorporates xenoliths of country rock (Precambrian layered gneiss and schist) in a matrix (Figure 16) resulting in formation of a coherent, block where penetrative fabric has

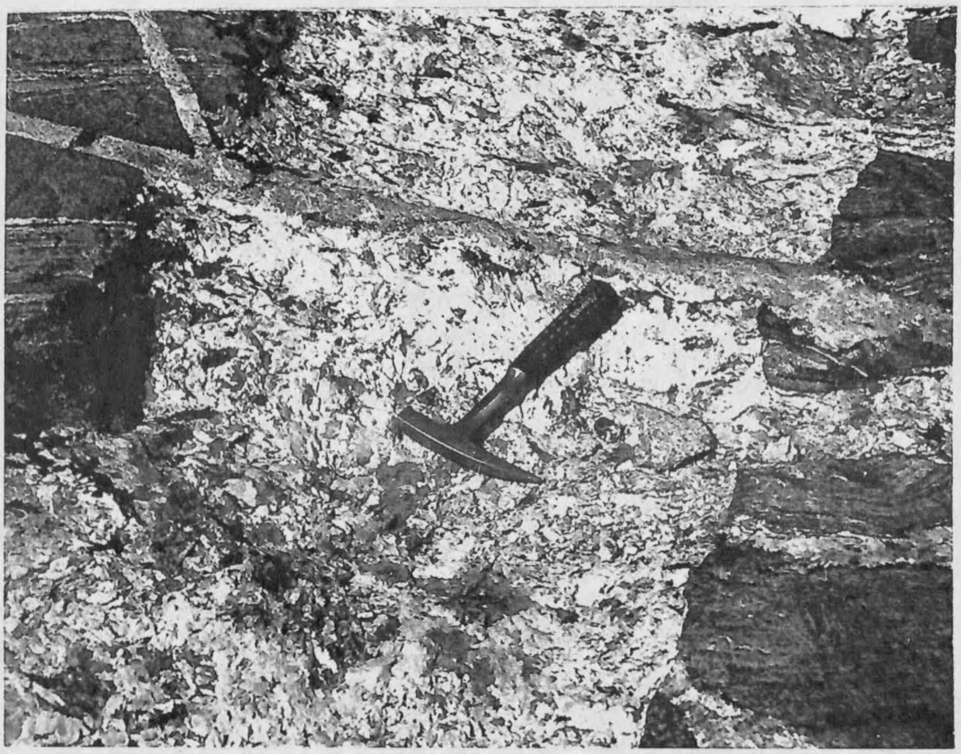

Figure 15 - A one meter wide, coarse-grained pegmatite dike cross-cuts Archean gneiss near the Middle Teton. Above the rock hammer, a medium-grained quartz monzonite dike cross-cuts the gneiss and the pegmatite.

been destroyed, herein recognized as the Cathedral Group block. The granitoids cross-cut all basement rocks in the area. Granitoid and pegmatite dikes are found in the footwall block, adjacent to the Buck Mountain fault, albeit in a strikingly lower concentration. All granitoid rocks are cut by the Buck Mountain fault (Figure 9).

Diabase dikes. Several near-vertical black diabase dikes strike east-west to N 70 W in the northern part of the study area and cut all other Precambrian rock types (Figure 9). One dike bisects the Middle Teton at the head of Garnet

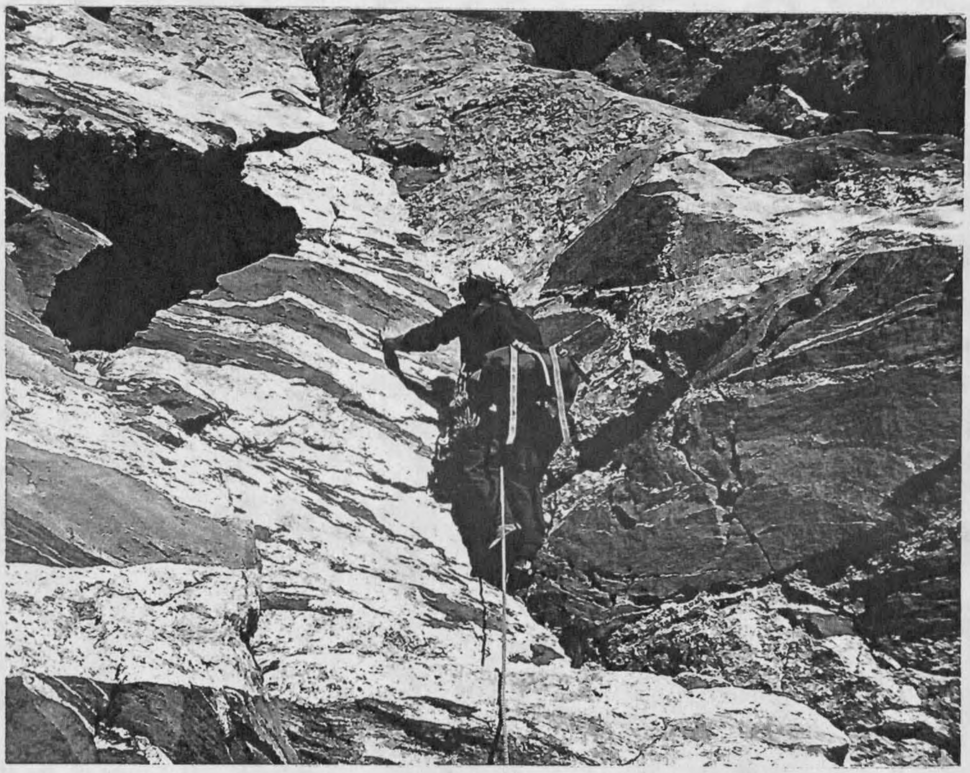

Figure 16 - A climber on the Middle Teton is met with a spectacular collage of coarse crystalline pegmatites and quartz monzonite encasing xenoliths of Archean gneiss and schist. Regional penetrative fabric is destroyed.

Canyon. Another cuts the south flank of the Grand Teton and is itself cut by the Buck Mountain fault in the South Fork of Cascade Canyon (Figure 9); both are 10 to 20 meters wide. North of the field area, a 30 to 45 meter wide diabase dike bisects the east face of Mount Moran and was mapped for 16 kilometers (Figure 26) (Reed and Zartman, 1973).

<u>Paleozoic strata</u>. West of the Cathedral Group block and the Buck Mountain fault, Paleozoic strata dip gently to the west (Figures 9 and 17). Middle Cambrian Flathead Sandstone (Love and Reed, 1971) is the basal unit of the Phanerozoic

Figure 17 - Photograph, looking southwest, of Paleozoic strata dipping gently to the west on the west flank of the central Teton Range. The strata rest nonconformably on the Precambrian basement.

succession, resting nonconformably on the Precambrian basement.

PRECAMBRIAN LITHOLOGY AND DEFORMATION

The previous chapter described the spatial relationship of the layered gneiss and schist, granitoids, and diabase dikes in the study area. In this chapter, mesoscopic rock descriptions and deformational fabrics will be detailed, metamorphic grade of the Archean gneiss and schist will be discussed, and the most current age-dating studies of Precambrian rocks from the Teton Range will be presented.

Mesoscopic Descriptions

Layered Gneiss and Schist

Rock Descriptions. The oldest Precambrian lithology in the central Teton Range is strongly foliated, compositionally layered, gneiss and schist (Reed, 1963; Behrendt and others, 1968; Reed, 1973; Reed and Zartman, 1973). Compositional layers extend along strike for meters to hundreds of meters and range in thickness from millimeters to tens of meters. The heterogeneous layered gneiss and schist consists of biotite gneiss, biotite-hornblende gneiss, quartz-plagioclase gneiss, hornblende gneiss, and amphibolite (Table 1), interlayered with mica schist and amphibole schist. A magnetite and quartz-rich

Table 1 - Modal rock compositions from the Teton Range. Average modes in volume percent of 50 random grains counted.

MINERALS	Biotite gneiss	Qtz-Plag gneiss	Amphibole gneiss	Amphibolite	Quartz Monzonite
Quartz	40.9	36.2	16.3	7.8	35.8
K-Feld-spar	3.9	7.6	-----	-----	27.3
Plagio-clase	35.8	47.6	37.1	21.2	29.6
Biotite	16.2	2.4	5.8	.3	3.0
Horn-blende	-----	-----	33.2	70.5	-----
Muscovite	.7	2.8	-----	-----	3.3
Chlorite	1.6	-----	2.6	.2	.8
Garnet	.9	.6	1.3	trace	-----
Epidote	1.4	2.6	1.5	.4	trace
Leucoxene	trace	trace	.7	.1	-----
Sphene	trace	trace	.7	.1	-----
Magnetite	trace	trace	1.1	.1	-----
Ilmenite	trace	trace	1.1	.1	-----

From Reed (1968)

formation occurs locally, and irregular masses of metagabbro and ultra-mafic rocks are scattered throughout the area (Bradley, 1956; Reed, 1963; Behrendt and others, 1968; Reed, 1973; Reed and Zartman, 1973). Some gneissic layers are discontinuous and/or exhibit pinch and swell structure or boudinage. Reed and Zartman (1973) suggest that the considerable lateral extent of similar layers indicates a supracrustal protolith for the gneisses, either metasedimentary or volcanic / volcaniclastic.

Much of the layered gneiss is buff to gray, fine to medium-grained, biotite gneiss and dark gray to black, fine to medium-grained, biotite-hornblende gneiss. Interlayered with the biotite and biotite-hornblende gneiss are: 1) light-gray to white, medium to coarse-grained, quartzo-feldspathic gneiss with garnet porphyroblasts up to several centimeters in diameter; 2) dark green to black, fine to medium-grained, amphibolite; 3) lenses of black and white, coarse-grained diorite (leopard diorite; Bradley, 1956) (Figure 14); 4) conspicuous, highly schistose layers of black, medium-grained, biotite schist and white mica schist; 5) green to black, fine to coarse-grained, proto-mylonite and phyllonite zones; and 6) light gray to white; medium to coarse-grained, aplitic granitoid in close proximity to the leopard diorite pods; these pods exhibit some foliation and are interpreted to be migmatitic (Reed and Zartman, 1973)

Deformational Fabrics. Deformational fabrics in the layered gneiss and schist are detailed below.

1) At least two generations of regional planar foliation are observable in the study area. An early metamorphic foliation (S_1) is folded into isoclines whose axial planes are sub-parallel with a later fabric (S_2) (Figure 18). Primary bedding (S_0) may have been a precursor to the heterogeneous compositional layering in the Archean rocks of the Teton Range; however, none of the original structures are preserved. S_2 foliation is characterized by strong parallel arrangement of biotite and white mica in schistose layers giving a planar fissility to the rocks.

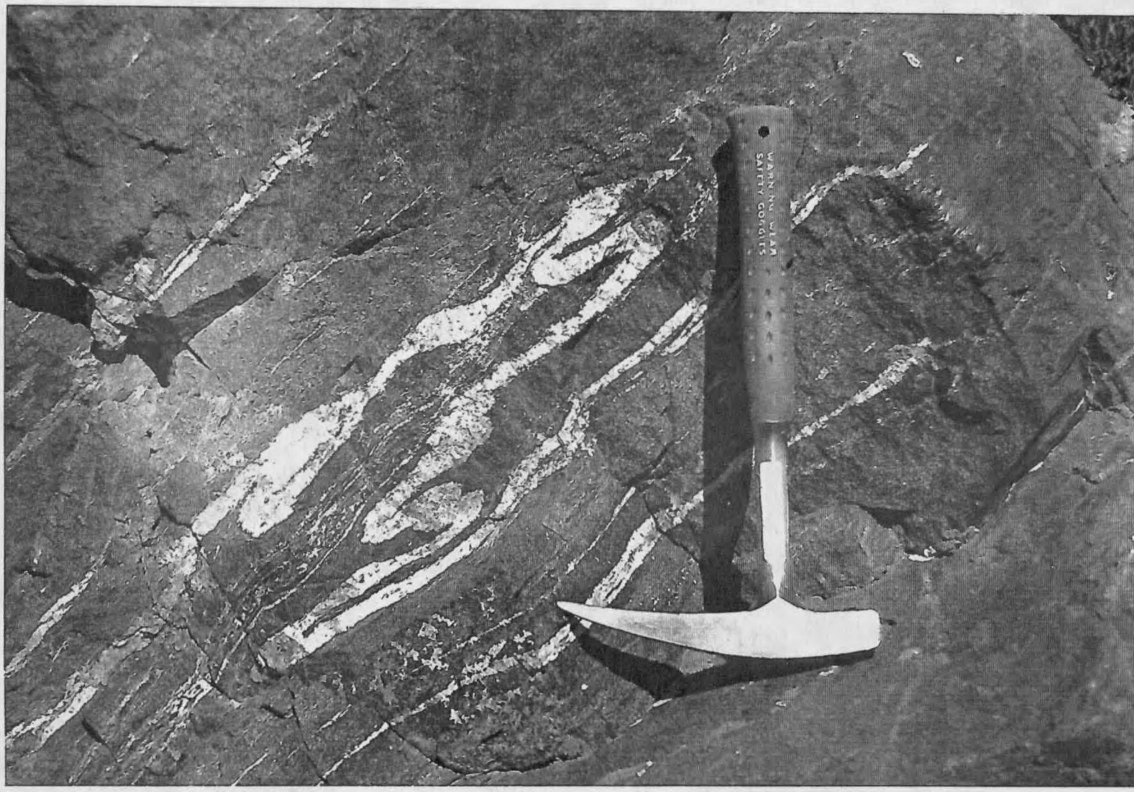

Figure 18 - Isoclinal F_1 folds in the Archean gneiss of the Teton Range. Axial planes of the isoclines are parallel to S_2 regional foliation.

Amphibole and biotite grains are aligned and alternate with coarse-grained quartzo-feldspathic layers in gneissic banding. Quartz and feldspar grains are elongate and aligned parallel to foliation and layering (Figure 19A). The heterogeneous layering and foliation of gneiss and schist create regional planar anisotropies in the basement rock.

2) Several laterally discontinuous (meters to tens of meters) ductile deformation zones were observed penetrating the Archean gneiss and schist in Alaska Basin and in the Static Peak area. The mylonitic foliation, interpreted as S_3, is concordant with S_2 metamorphic foliation in the

A

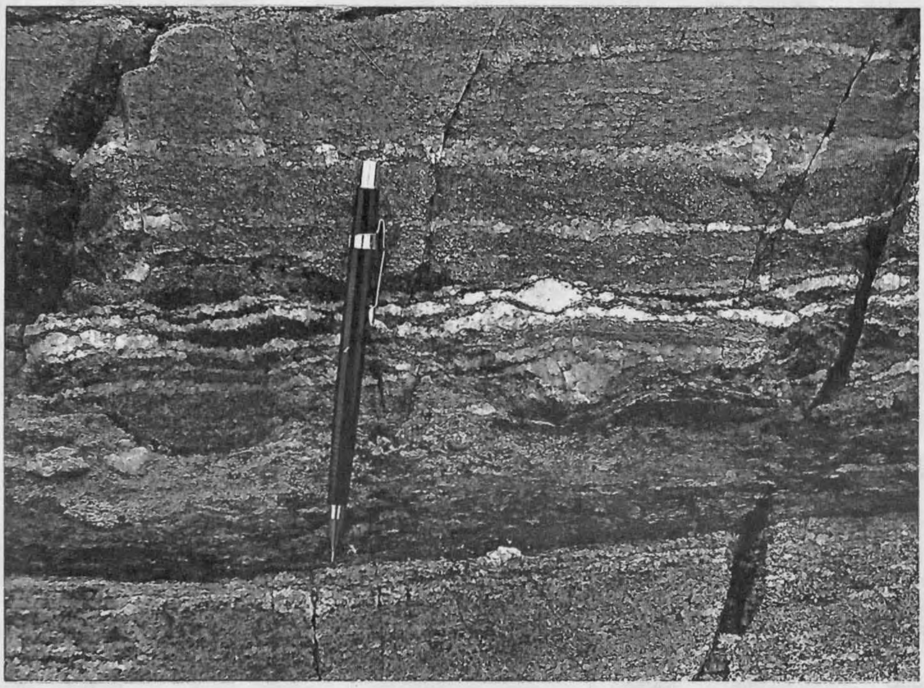

B

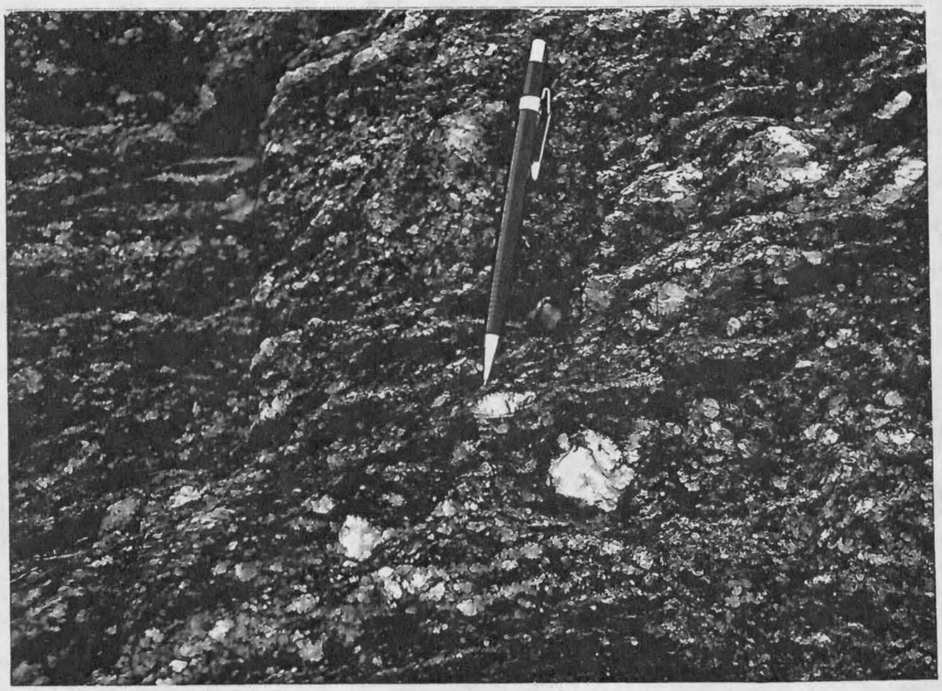

Figure 19 - A: Stretching of quartzo-feldspathic porphyroblasts is evident in the layered gneiss of Alaska Basin. B: Proto-mylonite in Alaska Basin. Observed deformation includes stretching, rotation, recrystallization and incipient foliation.

layered gneiss and schist. Miller and others (1986) also recognized concordant mylonite zones in the northern Teton Range.

Black, proto-mylonite layers exhibit stretching of quartz and feldspar grains, rotated porphyroclasts and incipient distorted foliations that penetrate the country rock (Figure 19B). These zones are 1-10 meters wide and are associated with amphibolites and biotite gneiss.

Green, chloritic mylonites penetrating the Archean gneiss and schist may be coeval with the black, proto-mylonites (Chapter 4). The green mylonites exhibit extensive chloritization and/or preferred orientation of chlorite, biotite and amphiboles, and have a phyllitic sheen. Rotated quartzo-feldspathic porphyroclasts are observed within the ductile zones. Hyndman (1985) defines a phyllonite as a phyllite-like rock produced from a coarser-grained, commonly higher-grade rock by extreme deformation and mineralogical changes. The green mylonitic rocks in these zones are interpreted to be phyllonites.

South of Buck Mountain, the Static fault coincides with a 10-50 meter wide, anastomosing phyllonite zone (Figure 9). This zone is sub-parallel to the strike of regional axial-planar foliation and proto-mylonitization, but cuts the antiformal structure at a high angle. Because of this cross-cutting relationship, the phyllonites are interpreted to be younger than the layered gneiss. In Alaska Basin, the phyllonite zones are 1-3 meters wide and conform to the S_2 orientation of the layered gneiss and schist. Evidence for a Proterozoic age for the mylonites is found in the northern Teton Range where mylonite zones cross-cut the 2,495 m.y. old Mount Owen Quartz Monzonite (Miller and others, 1986) (see Age Relationships; p.55).

3) In Alaska Basin, many pegmatites that are concordant with compositional layering are highly fractured and exhibit close-spaced (centimeter scale) unstable fractures. Other pegmatite veins cross-cut the layered gneiss and schist obliquely and are generally not deformed. The non-penetrative deformation of concordant pegmatites is evidently a Laramide fabric, as indicated by the cross-cutting relationship of the pegmatites to Archean gneiss and the brittle nature of deformation.

Precambrian Folding. At least two and possibly three generations of ductile folding are observed in the layered gneiss and schist. The earliest folds, designated F_1, are represented by isoclinal, passive-flow folds (Reed and Zartman, 1973) which deform S_1 foliation (Figure 18). Wavelengths range from centimeter to meter scale. Axial planes of the isoclinal folds are parallel to regional S_2 foliation.

Evidence also exists for broad, open F_2 folding of the F_1 isoclines with diverse axial trends (Reed and Zartman,

A

B

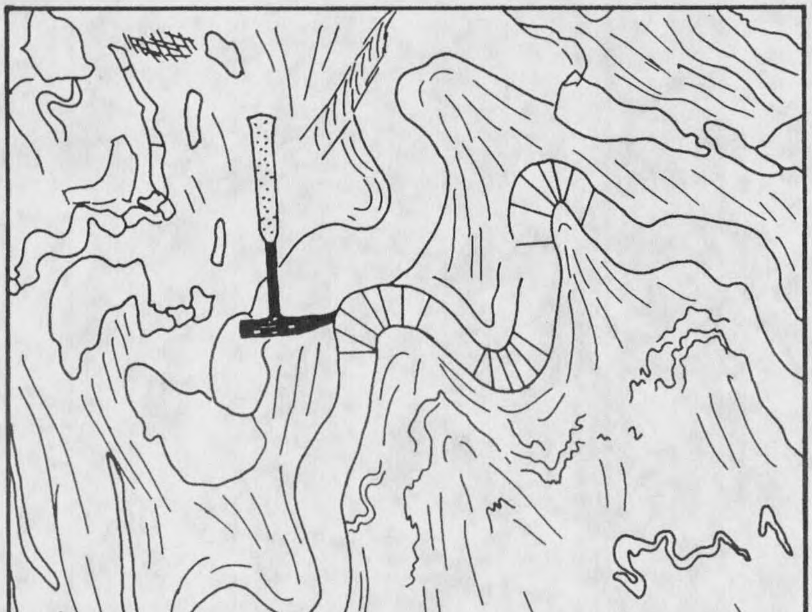

Figure 20 - A: F_3 folds located west of Static Peak and south of Buck Mountain. B: Ramsay's (1987) dip isogon method of fold classification places these folds somewhere between parallel and similar folds.

Figure 21 - Air photo of Buck Mountain - Static Peak area looking north. The hummocky area just below Buck Mountain in the right center of the photo exhibits extensive F_3 folding.

1973). Both F_1 and F_2 folds are preserved in highly recrystallized, high-grade gneiss.

The third generation of Precambrian folding, designated F_3, exhibits relatively tight, curved to angular folds that deform S_2 regional foliation and F_1 isoclines (Figure 20A). Individual competent layers maintain near-constant layer thickness; however, flow has occurred in less competent layers creating thickened, schistose hinge zones (Figure 20A). Folds exhibiting these characteristics formed by a flexural-flow mechanism (Donath and Parker, 1964). Wavelengths of the folds range from centimeter to tens of meters scale. These folds are recognized in abundance in the area south of Buck Mountain near Static Peak (Figure 21).

Ramsay's (1987) dip isogon method of fold classification was applied to the F_3 folds in the Static Peak area. Figures 20A and 20B show a tightly folded area where layers of quartzo-feldspathic gneiss have acted as competent beams interlayered with a less-competent schistose material. The folded competent layers fit into Class 1-C of Ramsay's classification: weakly convergent dip isogons. These folds are classed somewhere between parallel and similar folds (Ramsay, 1987). Dahlstrom (1970) classifies this type of fold as pseudo-similar. The east face of Static Peak also exhibits F_3 folds (Figure 12).

The distinguishing characteristics of the three generations of folding are: 1) F_1 folds are isoclinal, passive-flow folds (Donath and Parker, 1964) that are preserved in highly recrystallized, high-grade gneiss; 2) F_2 folds are broad, open folds with diverse axial trends that only mildly deform the S_2 foliation and F_1 axial planes (Reed and Zartman, 1973); and 3) F_3 folds are relatively tight, flexural-flow folds (Donath and Parker, 1964) that apparently formed during a lower-grade deformation. Thickened hinge zones exhibit schistose to mylonitic texture. These folds are recognized only in the vicinity of Static Peak where regional foliation strikes change from N-S to NE (Figure 21) (Bradley, 1956).

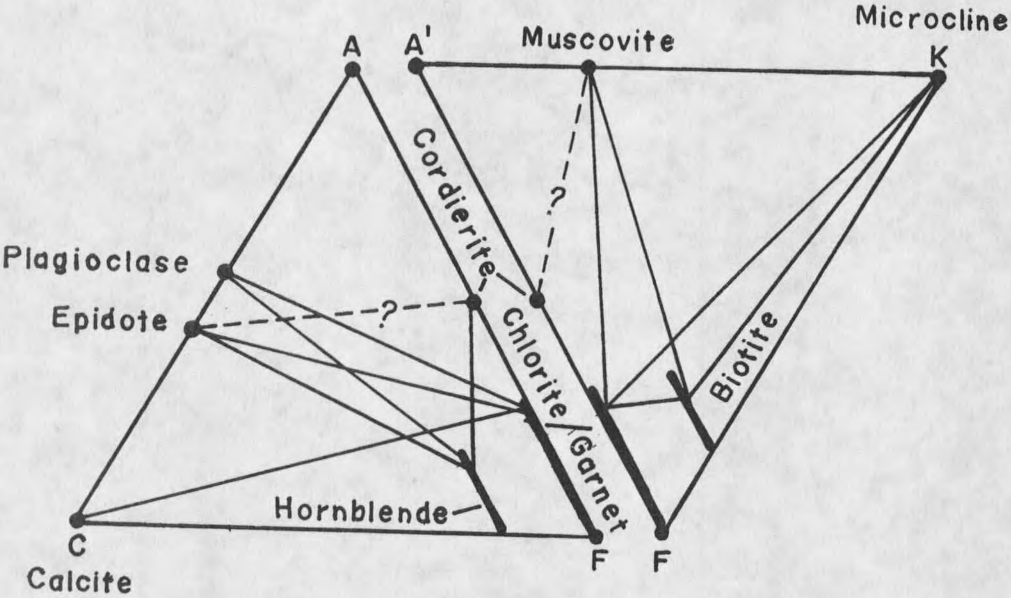

Figure 22 - ACF-A'KF diagram of assemblages in the study area. Regressive greenschist assemblages overprint amphibolite-grade rocks. Diagramatic only.

Metamorphic Grade. The primary fabric in rocks of the Teton Range is amphibolite-grade, as indicated by the assemblages "quartz + oligoclase or andesine + biotite +/- garnet +/- K-feldspar in the biotite gneisses and quartz + andesine or labradorite + hornblende +/- biotite +/- garnet in the amphibolite gneisses and amphibolites" (Reed and Zartman, 1973; p.563). However, the metamorphic alteration assemblage chlorite + epidote + sericite + albite + calcite overprints those amphibolite grade minerals (Figure 22) (see Chapter 4). Reed and Zartman (1973) interpreted alteration phases in the Teton Range as retrograde metamorphism. Figure 22 diagramatically illustrates the overlapping of

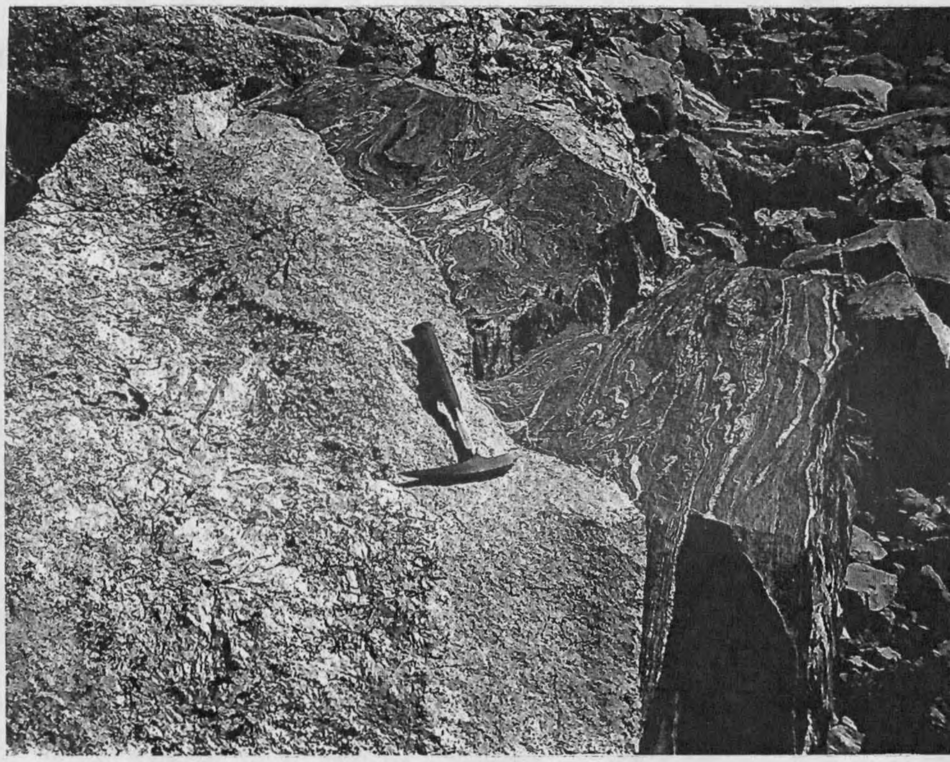

Figure 23 - Contacts between Archean gneiss, quartz monzonite and pegmatite in the vicinity of Buck Mountain. Note the sharp contact between the Archean gneiss and the quartz monzonite.

greenschist-facies alteration on amphibolite-grade assemblages. Furthermore, Reed and Zartman (1973) recognized cordierite in metamorphic rocks of the northern Teton Range, however, cordierite was not observed in rocks from my field area. Therefore, the tie lines for cordierite are dashed in Figure 22.

Intrusive Granitoids

The high peaks of the Cathedral Group consist of fine to medium-grained, light gray to pink quartz monzonite stocks (Table 1) and a network of coarse to very coarse-grained muscovite and biotite pegmatites (Figure 23)

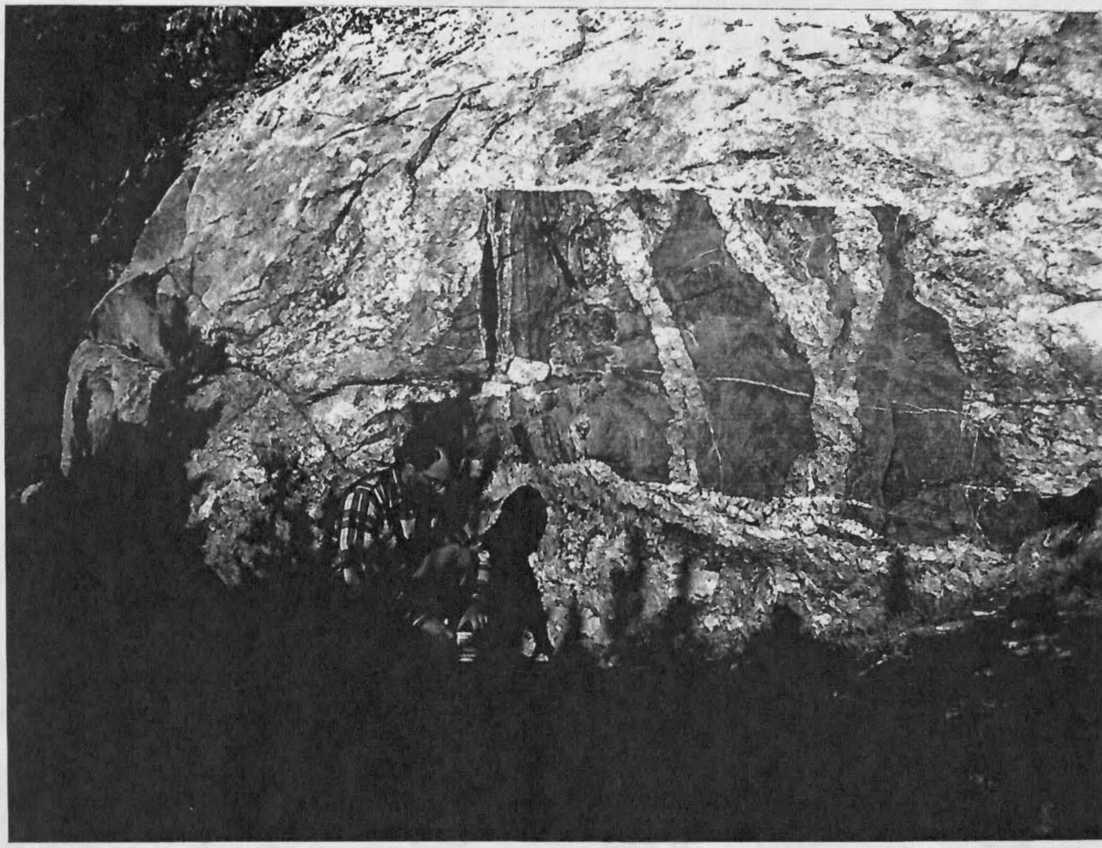

Figure 24 - Two meter wide xenolith of Archean gneiss encased in granitoid material near the Middle Teton.

(Behrendt and others, 1968; Reed and Zartman, 1973). Most of the large quartz-monzonite bodies exhibit hypidiomorphic granular texture. However, where the granitoid intrusives have incorporated large xenoliths of country rock (layered gneiss) into the matrix (Figure 24), some flow foliation (i.e., preferred orientation of biotite) is seen in the granitoid material around the xenoliths. The flow-foliation is generally discordant with foliation in the xenoliths. Contacts between granitoid intrusives and country rock are

Figure 25 - Coarse-grained pegmatite cross-cutting Archean gneiss in Alaska Basin. Some pegmatites conform to S_2 foliation layers, while others cross-cut the layers.

sharp (Figures 16 and 23). Pegmatite veins comprise a large portion of the granitoid material, in some places as much as a quarter or more. They cut the quartz-monzonite and are themselves cut by the quartz-monzonite, suggesting an overlapping timing sequence (Figure 15). The coarse-grained pegmatites (Figure 25) exhibit irregular masses of gray to glassy quartz, subhedral crystals of white plagioclase and gray to pink potassium feldspar, and radiating to tabular masses of muscovite up to tens of centimeters long. Garnets, from millimeter to tens of centimeters in diameter, are found in some pegmatite veins.

The granitoids exhibit alteration including chloritization of biotite and sericitization of plagioclase (Chapter 4). This indicates that a greenschist metamorphic event occurred sometime after crystallization of the quartz monzonite. A more thorough elemental analysis is needed to determine if the alteration event in the layered gneiss and schist is coeval with the alteration described above.

Layered gneiss on the margin of the Cathedral Group is laced with anastomosing, discordant quartz monzonite and pegmatite dikes (Figure 25). These become less abundant away from the intrusive bodies of the Cathedral Group.

Diabase

The dike rocks are dark-green to black, fine to medium-grained diabase consisting mostly of plagioclase and amphibole. They exhibit subophitic to ophitic texture and tend to have chilled margins (1-3 centimeters) at their contacts with the country rock. Some samples are mildly magnetic based on attraction of a hand magnet. The dike south of the Grand Teton is brecciated on its southern margin and is also displaced by faulting in the south fork of Cascade canyon (Figure 9). Reed and Zartman (1973) state that chemical analyses of the diabase rocks indicate they are "typical" tholeiitic basalts.

Some alteration has occurred in the diabase rocks; plagioclase grains are sericitization, and amphiboles exhibit alteration to chlorite and epidote. In addition, occasional transgranular epidote fractures cross-cut the diabase rocks. Thus, it is possible a greenschist overprint exists in the diabase as it does in all other Precambrian rocks in the study area.

Age Relationships

The intent of this discussion is to provide a broad overview of the various age-dating studies that have been conducted on rocks from the Teton Range (Giletti and Gast, 1961; Behrendt and others, 1968; Reed and Zartman, 1973; Roberts and Burbank, 1988), and, from the results of those studies, to compile a chronology of tectonic events.

Most recently, Roberts and Burbank (1988) used fission-track dating of apatite in basement rocks to determine the pattern and timing of uplift within the Teton Range. Their preliminary results suggest that at least two discrete episodes of uplift occurred, one beginning in "late Cretaceous" and the other in "Plio-Pleistocene" time. They also found that their northern-most samples (north-central Teton Range) exhibit "considerably" younger ages than their southern samples (southern and south-central Teton Range). They consider two possibilities to explain this dichotomy: 1) that differential uplift has occurred in the Teton Range "with greater post-Oligocene rates to the north," and 2) that partial annealing occurred in the north part of the range due to the proximity to the geothermal anomaly of

Yellowstone. The second theory seems unlikely for the following reason; the North American plate has been moving over the Yellowstone "hotspot" at a rate of approximately 3.5cm/yr since the Mesozoic (Engebretson and others, 1985; Anders and others, 1989). As recently as 5 million years ago, the Yellowstone hotspot would have been located over 100 kilometers southwest of the northern Teton Range in the vicinity of the Blackfoot River of southeastern Idaho, most likely having no effect on rocks in the Teton Range. However, simple burial of the basement to 3 or 4 kilometers (see Chapter 6), assuming an average crustal geothermal gradient of 30°C/km (Strahler, 1985; p.168), would have provided the necessary 100°C temperature to anneal fission tracks in apatite (Skinner and Porter, 1987; p.191), thus resetting the radiometric clock.

Reed and Zartman (1973) used the Rb-Sr method to analyze whole rock samples, as well as mineral separates, from layered gneiss and granitoid intrusives of the Teton Range. They used the K-Ar method to analyze whole rock samples and mineral separates from the diabase dike on Mount Moran and adjacent wall rocks.

Reed and Zartman (1973) estimated that rocks in both the northern and southern Teton Range have undergone the same episode of high-grade regional metamorphism and deformation. Because of this, they calculated a single composite Rb-Sr isochron for whole-rock samples of several widely separated gneissic lithologies, yielding an age of 2,875 +/- 150 m.y. They concluded that, because of the extensive recrystallization of all rocks during high-grade regional metamorphism, the isochron age is the approximate age of the metamorphism. They derived similar K-Ar ages ranging from 2,600 +/- 90 m.y. to 2,800 +/- 80 m.y. from hornblende in the layered gneiss adjacent to the diabase dike on Mount Moran.

Whole-rock samples of Mount Owen Quartz Monzonite from the vicinity of the Cathedral Group define a Rb-Sr isochron indicating an age of 2,495 +/- 75 m.y. Reed and Zartman (1973) interpret the isochron age as being "close to the age of emplacement" of the Mount Owen Quartz Monzonite.

In addition, Reed and Zartman (1973) studied the Rb-Sr systematics of the major mineral phases in the Mount Owen Quartz Monzonite in order to determine the effect of later events on the mineral ages. They found that various mineral phases in the quartz monzonite vary with respect to the whole-rock isochron, suggesting that redistribution of rubidium and strontium occurred following initial crystallization of the Mount Owen Quartz Monzonite. Using the Rb-Sr method, they determined that: 1) plagioclase and microcline from the Mount Owen Quartz Monzonite are 1,800 m.y. old; 2) muscovite from two samples of Mount Owen Quartz Monzonite exhibits two different ages, one corresponding to the whole-rock isochron (2,495 +/- 75 m.y.) and one

Table 2 - Rb-Sr age Determinations (Giletti and Gast, 1961):

Locality	Mineral	Age (m.y.)
Pegmatite cutting Brighteyed gneiss, Death Canyon, Teton Range	Muscovite Microcline	2660 1990
Brighteyed gneiss, Teton Range	Biotite	1360
Pegmatite east of Jackson, Wyo.	Biotite	1760

From Giletti and Gast, 1961.

corresponding to the feldspar isochron (1,800 m.y.); and 3) apparent biotite ages from two samples of Mount Owen Quartz Monzonite are 1,440 m.y. and 1,550 m.y. Giletti and Gast (1961), using the Rb-Sr method, dated microcline from a pegmatite in Death Canyon at 1990 m.y. (Table 2).

The diabase dike and surrounding gneiss of Mount Moran were dated using the K-Ar method (Reed and Zartman, 1973). Three biotite samples collected from the wall-rock at 1.5, 12, and 30 meters from the dike margin exhibit analytically similar ages of 1,450 +/- 90 m.y., 1,320 +/- 50 m.y., and 1,350 +/- 50 m.y., respectively. These ages correspond with the 1360 m.y. age derived by Giletti and Gast (1961) (Rb-Sr method) for biotite from the layered gneiss of Death Canyon on the southern boundary of the study area.

A K-Ar whole-rock analysis of the chilled dike margin revealed an apparent age of 775 +/- 8 m.y., whereas plagioclase separates from the center of the dike were dated by the K-Ar method at both 396 +/- 6 m.y. and 583 +/- 8 m.y.

On the summit of Mount Moran the diabase dike is nonconformably overlain by Cambrian Flathead Sandstone (Figure 26), constraining the gross age of the dike to Precambrian. Thus, the 396 +/- 6 m.y. K-Ar age derived from one of the plagioclase samples of Reed and Zartman (1973) is not geologically possible. The 583 +/- 8 m.y. and 775 +/- 50 m.y. K-Ar ages for the dike are geologically possible, however they conflict with the consistent K-Ar ages for biotite in the adjacent gneiss. The Hanson and Gast (1967) model of dike dynamics suggests that a 33m thick dike with an initial temperature of 1,100 °C will heat the wall-rock 1.5m away to a maximum temperature of about 700 °C and will keep it above 300 °C (the estimated minimum temperature needed for complete loss of Ar from biotite) for more than 100 years (Reed and Zartman, 1973). If we accept the 775 +/- 50 m.y. or 583 +/- 8 m.y. ages for the dike, the biotite closest to the dike should reflect a substantial decrease in apparent age. As stated above, the apparent K-Ar age of biotite directly adjacent to the dike on Mount Moran is 1,450 +/- 90m.y., analytically indistinguishable from the ages of biotite at 12m and 30m from the dike (Reed and Zartman, 1973). This anomaly has not been resolved, however Reed and Zartman (1973) suggest that the dike was emplaced during or before the time recorded by the K-Ar ages for biotite in the wall-rock. This interpretation places the minimum age of the dike at

Figure 26 - A 30 to 50 meter wide diabase dike bisects Mount Moran north of the study area. The sedimentary remnant on top of Mount Moran lying unconformably over the dike is Cambrian Flathead Sandstone.

1,450 +/- 90 m.y. (the oldest apparent K-Ar age of biotite in the wall rocks). The maximum age of diabase dikes in the field area would have to be less than the age of the Mount Owen Quartz Monzonite (2,495 +/- 75 m.y.) since the dikes cut the quartz monzonite on the southern margin of the Grand Teton and on the Middle Teton. Furthermore, the extremely sharp contacts between diabase dikes and adjacent rock suggests the dikes were intruded into "cold" wall rocks. Intrusion of the diabase dikes, then, probably occurred sometime after crystallization of the granitoid rocks of the Teton Range.

Considering the radiometric and fission-track studies discussed above, the following thermal chronology can be suggested for the field area:

1) 2,875 +/- 150 m.y. - regional high-grade metamorphism of all rocks in the Teton Range (Reed and Zartman, 1973; Rb-Sr whole rock);

2) 2,495 +/- 75 m.y. - intrusion of the Mount Owen Quartz Monzonite and possible formation of proto-mylonite and phyllonite zones (Reed and Zartman, 1973; Rb-Sr whole rock);

3) 1,800 m.y. - 1990 m.y. - possible thermal event that altered plagioclase and microcline in the Mount Owen Quartz Monzonite at 1800 m.y. (Reed and Zartman, 1973; Rb-Sr method) and microcline in a pegmatite of Death Canyon at 1990 m.y. (Giletti and Gast, 1961; Rb-Sr method). Formation of the mylonites may have occurred at that time (Miller and others, 1986).

4) intrusion of the diabase dikes sometime between 2,495 +/- 75 m.y. (Reed and Zartman, 1973; Rb-Sr whole rock) (the age of the Mount Owen Quartz Monzonite) and 1,450 +/- 90 m.y. (Reed and Zartman, 1973; K-Ar method) (the age of biotite in wall-rock adjacent to the dike on Mount Moran);

5) 1300 m.y. to 1500 m.y. - a thermal event, possibly associated with intrusion of the diabase dikes, that altered biotite near the dike on Mount Moran at 1,450 m.y. +/- 90 m.y. (Reed and Zartman, 1973; K-Ar method) and in layered

gneiss of Death Canyon at 1,360 m.y. (Giletti and Gast, 1961; Rb-Sr method);

6) "late Cretaceous" - uplift of the Ancestral Teton-Gros Ventre Range (Roberts and Burbank, 1988; apatite fission track);

7) "Plio-Pleistocene" - later uplift of the Teton Range in Plio-Pleistocene time (Roberts and Burbank, 1988; apatite fission track).

MICRO-STRUCTURES AND DEFORMATION-ENHANCED METAMORPHISM

There has been considerable debate and confusion over the characterization of brittle and ductile deformation fabrics (Higgins, 1971; Bell and Ethridge, 1973; Groshong, 1988). In order to allay confusion concerning the brittle vs. ductile nature of deformation textures in the Teton Range, the following definitions will be used in the ensuing discussion:

1) cataclasite - "a cohesive rock formed mainly by brittle fracturing and usually showing evidence of grain rotations and grain-size reduction" (Groshong, 1988, p.1342);

2) mylonite - "a rock formed mainly by crystal-plastic deformation mechanisms [that] shows evidence of internal rotation and grain-size reduction. <u>Cataclasite or mylonite may be foliated or unfoliated, although, on the thin-section scale, many cataclasites are unfoliated and most mylonites are foliated</u>" (Groshong, 1988, p.1342);

3) breccia - "composed of angular or rounded fragments formed in the fault zone and consists of more than 30% fragments large enough to be seen by the naked eye" (Groshong, 1988, p.1342);

4) gouge - "a paste-like rock material formed in the fault zone in which less than 30% of the fragments are large enough to be seen by the naked eye" (Groshong, 1988, p.1342);

5) unstable fractures - "fractures that propagate spontaneously across grains and grain boundaries. They are observed as continuous fractures cutting across grains of different compositions and orientations" (Mitra, 1984, p.52);

6) stable fractures - "stable fractures die out within individual grains, or are stopped at grain-boundaries where the stresses at the fracture tip are dissipated by plastic deformation in adjacent grains" (Mitra, 1984, p.53).

Thin Section Study

Thirty-eight thin sections from a variety of locations along the Buck Mountain, Static and Stewart faults were examined for micro-structures and deformation-enhanced metamorphism. They were divided into five zones according to major lithologies and proximity to the fault zones:
1) Archean country rock: layered gneiss and schist that is cut by mylonite zones, intrusive granitoids and by the Buck Mountain, Static and Stewart faults; 2) Mylonite zones: Proterozoic ductile deformation zones that cross-cut the Archean layered gneiss and schist (Chapters 3 and 4); 3) quartz monzonite and pegmatite: intrusive quartz

monzonite and pegmatite predominantly from the hanging wall of the Buck Mountain fault; 4) marginal fault zone: brittley deformed rocks on the margin of the Buck Mountain and Stewart faults; 5) breccia and gouge zone: highly cataclastic areas including the most intense deformation along the Buck Mountain and Stewart faults.

Archean Country Rock

The layered gneiss and schist consists primarily of medium-grained gray biotite gneiss, black biotite-hornblende gneiss, biotite schist and white mica schist. As seen in thin section, biotite and muscovite exhibit strong preferred orientations in gneisses and schists creating microscopic planar anisotropies (Figure 27A). Heterogeneity is also quite obvious at the mesoscopic scale, represented by S_2 foliation planes of schistosity and gneissic banding. Most of the country rocks exhibit ductile deformation such as bending of albite twins and undulous extinction of quartz and feldspar. Stable fracturing is predominant in the country rock away from the fault zones; however, occasional unstable fractures (Figure 27B) and thin cataclasite veins cross-cut these rocks. Brittle deformation increases with proximity to the faults.

Regressive metamorphic features are found throughout the amphibolite-grade country rocks. Petrographic observation indicates that alteration tends to increase with

A

B

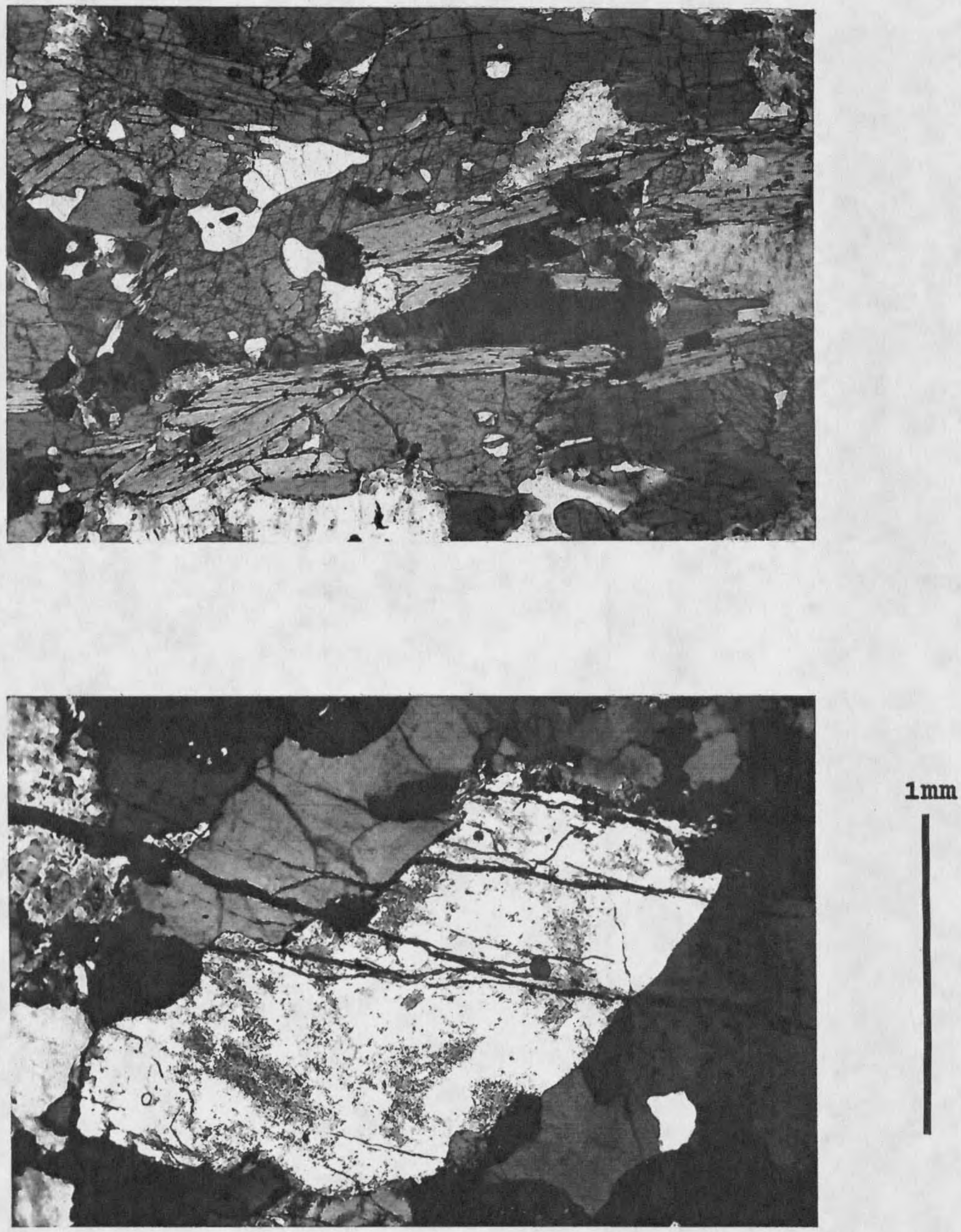

Figure 27 - A: Strongly oriented biotite grains in typical hornblende-biotite gneiss from the Static Peak area. B: Both unstable and stable fractures deform this quartzo-feldspathic gneiss from Alaska Basin. Hematite fills the unstable fractures.

proximity to deformation zones. Plagioclase feldspars exhibit minor to extensive sericitization and host various concentrations of microcrystalline epidote (Figure 28A). Amphiboles range from mildly to highly altered by chlorite and epidote, and some exhibit epidote rims. Two stages of chlorite growth (designated chlorite-1 and chlorite-2) are observed in one sample of country rock collected near the Stewart fault southeast of Static Peak (Figure 28B). Chlorite with silver-blue birefringence replaces the ragged ends of biotite grains, conforming to the tabular biotite habit. The biotite is interpreted to be primary because of its subhedral, habit and size. Patches of plumose or small radiating clusters of chlorite with anomalous purple and brown birefringence grow in voids between feldspar and biotite grains. Grain boundaries along the voids are sharp indicating that the plumose chlorite has not reacted with adjacent grains (Figure 28B). Chlorite replacing the primary biotite is interpreted to be chlorite-1, whereas, the void-filling, plumose chlorite is interpreted to be chlorite-2, because it does not penetrate the biotite and feldspar grains.

Giletti and Gast (1961) and Reed and Zartman (1973) find evidence for thermal events affecting the Precambrian basement of the Teton Range between 2,495 and 1360 million years ago (Chapter 3). A combination of these events, or possibly alteration associated with Laramide deformation,

A

B

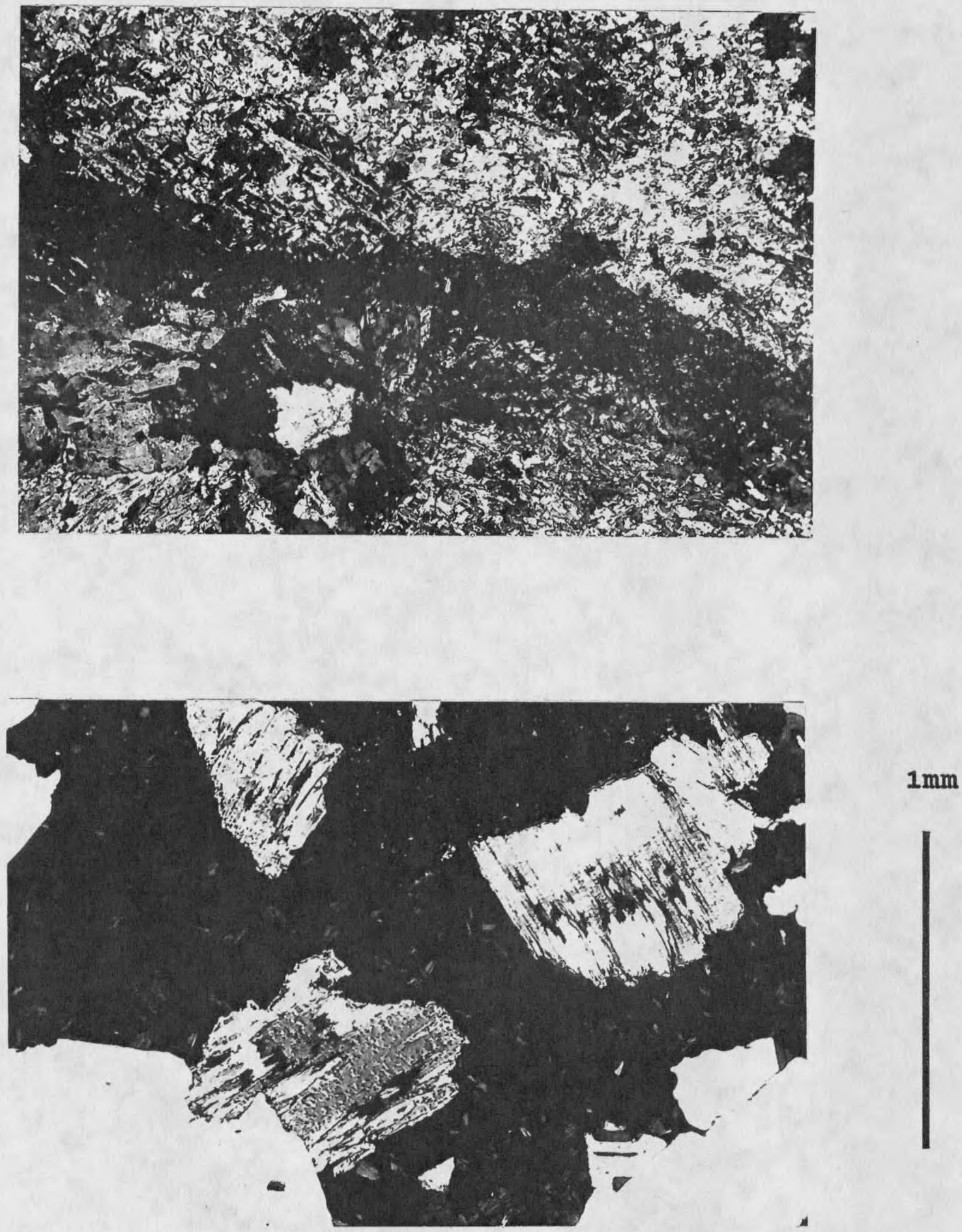

Figure 28 - A: Plagioclase highly altered to sericite and micro-crystalline epidote. A late-stage epidote vein angles across the center of the photograph. B: Feathery tips on the biotite crystals represents chlorite-1. Plumose chlorite (chlorite-2) fills voids.

could be responsible for the stages of chlorite growth described above. However, the timing of crystallization or determination of relative age differences of chlorite are beyond the scope of this thesis.

Another distinct, less abundant chlorite, chlorite-3, is recognized in thin cataclasite veins in the country rock. Small, tabular, non-oriented crystals grow within transgranular cataclasite veins. Random orientation and tabular growth indicate this chlorite is a product of post-kinematic Laramide alteration. The abundance of chlorite-3 in the Buck Mountain fault zone will be discussed later in the chapter.

<u>Mylonite Zones</u>

Proterozoic mylonite and phyllonite zones (Chapter 3) penetrate the Archean layered gneiss and schist in the footwall of the Buck Mountain fault. Phyllonites from the southwest segment of Static fault (Figure 9) exhibit a highly schistose texture with relict amphiboles retaining their shapes. Large (centimeter scale) porphyroclasts are rotated in the schistose material. Remnant hornblende and relatively large primary muscovite grains are highly fragmented with ragged edges (Figure 29A). The retrograde assemblage chlorite + epidote + sericite is strongly overprinted on the pre-existing amphibolite-grade rock. Chlorite exhibits preferred orientation and grows as elongate, fibrous crystals (Figure 29B). Chlorite has

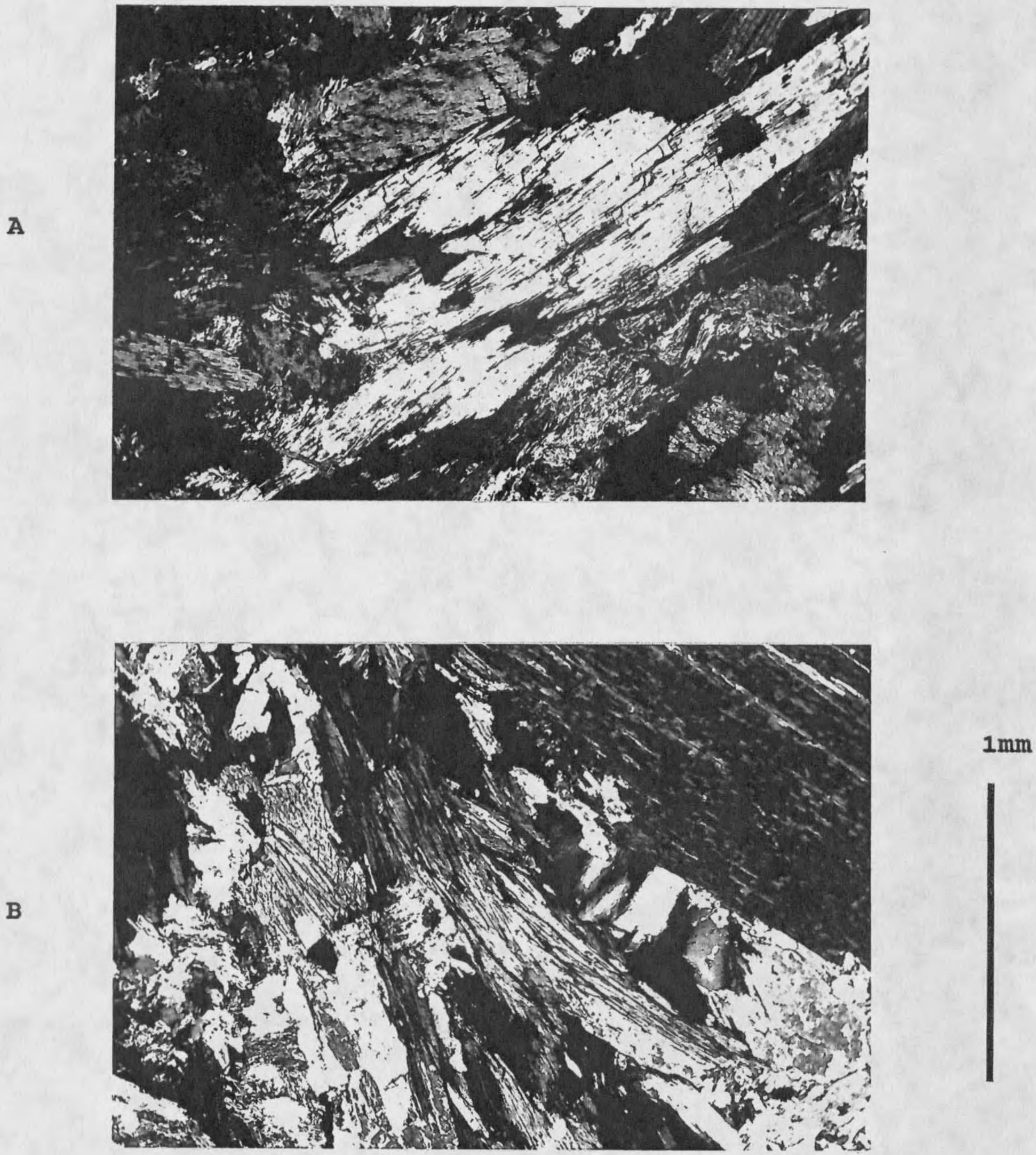

Figure 29 - A: Fragmented amphibole from Static fault. Chlorite grows along fracture and grain boundaries. B: Strongly oriented chlorite is the predominant post-amphibolite phase of this Static fault rock.

altered both hornblende and biotite from an earlier amphibolite-grade rock. Bending of chlorite occurs around some larger grains indicating syntectonic growth. Epidote generally grows as void-filling subhedral to euhedral crystals around anhedral opaque minerals. However, it also is found to form rims on hornblende in several cases. A few transgranular, quartz-filled fractures were observed cross-cutting all greenschist alteration in Static fault rocks. No calcite was observed in the southwest segment of the fault, except in brecciated iron and quartz-rich zones discussed below.

Several brecciated, maroon-orange-colored, iron-rich zones occur within the Static fault. In these zones, medium-grained, rounded to polygonal quartz grains are observed in cataclasite veins cross-cutting large quartz crystals with undulous extinction. The quartz grains show evidence of pressure solution and recrystallization. Iron-rich, opaque minerals have been granulated and incorporated into the cataclasites. The larger quartz grains and opaque minerals are matrix-supported. Numerous calcite-filled transgranular fractures cross-cut the entire formation.

Green, ductile deformation zones in Alaska Basin are similar to Static fault in that extreme chloritization is observed. However, the chlorite found in these zones has a different habit. One zone exhibits nearly complete alteration to plumose, radiating chlorite. Another zone in

Alaska Basin is extensively chloritized, again in the plumose habit, and exhibits relict feldspar grains speckled with new chlorite laths.

Quartz Monzonite and Pegmatite

Granitoid samples collected from intrusive bodies in the central Cathedral Group block generally exhibit hypidiomorphic texture. Some isolated samples display possible minor orientation of biotite grains, conceivably from flow foliation. However, these samples were not oriented, so it is uncertain whether the orientation of biotite is conformable with vein walls or other contacts. A combination of stable and unstable fractures indicates deformation at the brittle-ductile transition (Figure 30A) (Mitra, 1984). Alteration, considered by other investigators to be retrograde (Miller and others, 1986), has been observed in these plutonic rocks. Some biotite grains are partially altered to chlorite. Small blebs of subhedral epidote are also associated with biotite (Figure 30B). Plagioclase feldspars exhibit minor sericitization.

On the margins of the Cathedral Group block, close to the Buck Mountain fault, quartz-monzonite bodies exhibit incipient cataclasis. Samples collected from adjacent to the fault display hematite-filled, unstable fractures. (Paterson, 1978; Mitra, 1984). Some albite twins are slightly offset. Very thin (micron scale) cataclasite veins are occasionally observed in this zone, exhibiting grain-

A

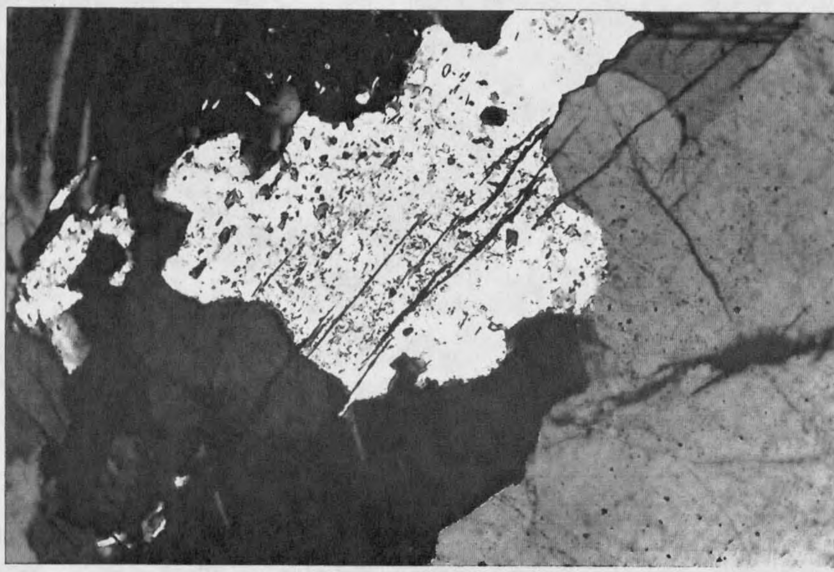

B

1mm

Figure 30 - A: Stable and unstable fractures in the quartz monzonite intrusives of the Cathedral Group block. B: Subhedral epidote bleb in the center of photo is associated with biotite in quartz monzonite from the Cathedral Group block.

size reduction, but no rotation of grains. Also, a few thin, quartz-filled, transgranular veins are observed. Retrograde mineralization is more extensive near the margins of the intrusive bodies. The assemblage chlorite + epidote + sericite overprints the granitoid rocks near the Buck Mountain fault. Plagioclase is extensively sericitized. Microcrystalline epidote grows along grain boundaries, and small subhedral laths of chlorite are consistently associated with opaques.

Marginal Fault Zone

Samples of layered gneiss and granitoids collected in areas marginal to the Buck Mountain fault display close-spaced fractures and orange-yellow iron-oxide coloration. Unstable fractures penetrate through grains and across grain boundaries (Figure 31). The fracture lengths range from millimeter to meter scale, while rock between the fractures remains relatively undeformed. Quartz and/or iron-oxide fill some fractures, and some comminution or mortar structure (Hyndman, 1985) is observed along grain boundaries.

Generally, alteration of country rock increases with proximity to the fault zones. Rocks marginal to the Buck Mountain and Stewart faults are extensively altered. Some plagioclase grains are almost completely altered to sericite or minute laths of white mica (Figure 28A). Hornblende is fragmented and hosts microcrystalline epidote and small randomly oriented laths of chlorite. Thin, post-

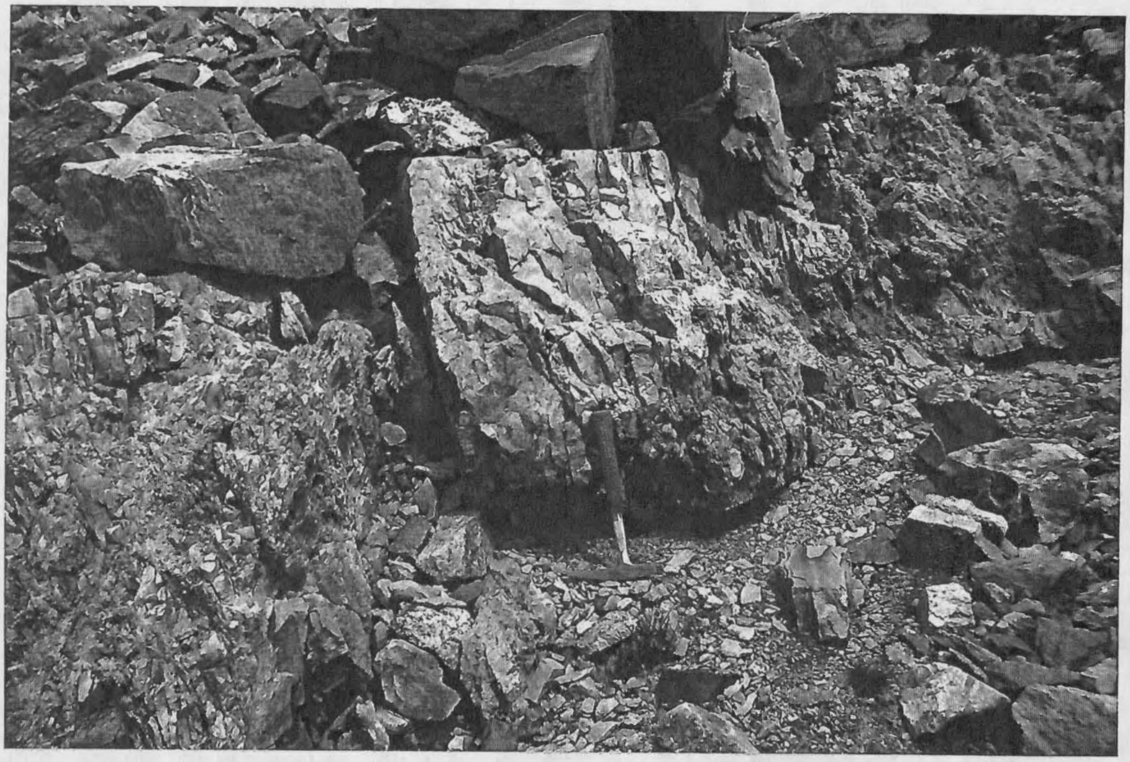

Figure 31 - Close-spaced fractures in the quartz monzonite and pegmatite of Buck Mountain. Rocks directly adjacent to the fault exhibit extreme brittle deformation.

kinematic epidote veins cross-cut multiple grain boundaries (Figure 28A).

Breccia and Gouge Zone

The zone of maximum deformation on the Buck Mountain and Stewart faults is identified by extreme brecciation, cataclasis and gouge formation. Comminution results in grain-size reduction forming cataclasites. In thin section, these are observed as veins (micron to centimeter scale) of minute, angular grains and polycrystalline fragments between larger grains of less deformed, but fragmented minerals (Mitra, 1984; Groshong, 1988) (Figure 32A). In the most

A

1mm

B

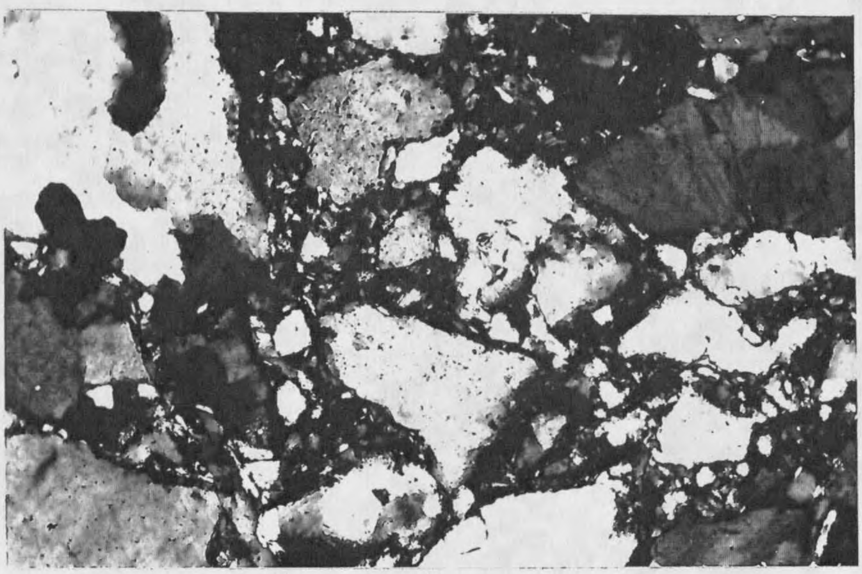

0.5mm

Figure 32 - A: Grain-size reduction has resulted in formation of cataclasites. Note the angular nature of the debris and the wide range of grain sizes. B: Matrix supported cataclasite. No grain rotation, pressure shadows or tails are observed.

highly deformed areas, angular fragments are supported in a matrix of comminuted grain debris and gouge. No obvious foliation or grain rotation is observed in these cataclasites (Figure 32B).

The assemblage chlorite + epidote + calcite + sericite is superimposed over the pulverized cataclasite material. Chlorite (chlorite-3) has grown in undeformed laths within cataclasite veins and is interpreted to be post-kinematic. Subhedral muscovite is observed in random orientations in the cataclasite veins and along grain boundaries suggesting post-kinematic formation. Calcite annealing also occurs within cataclasite veins and along grain boundaries (Figure 33). The calcite is generally undeformed and, when overgrowing cataclasite veins, stops sharply at vein boundaries. Because of this habit, the calcite is interpreted to be post-kinematic. The hydrous nature of these alteration minerals and the presence of late-stage epidote vein-filling (Bradley, 1956) suggest that thermal fluids were present in the fault zones during and after maximum deformation (Frost, 1971). The source of the fluid will be discussed later.

Quartz-filled, transgranular fractures cross-cut cataclasite veins at approximately 90^0. The cross-cutting relationship indicates that the quartz veins formed after the time of maximum deformation. The following evidence suggests that the quartz veins are extension or dilation

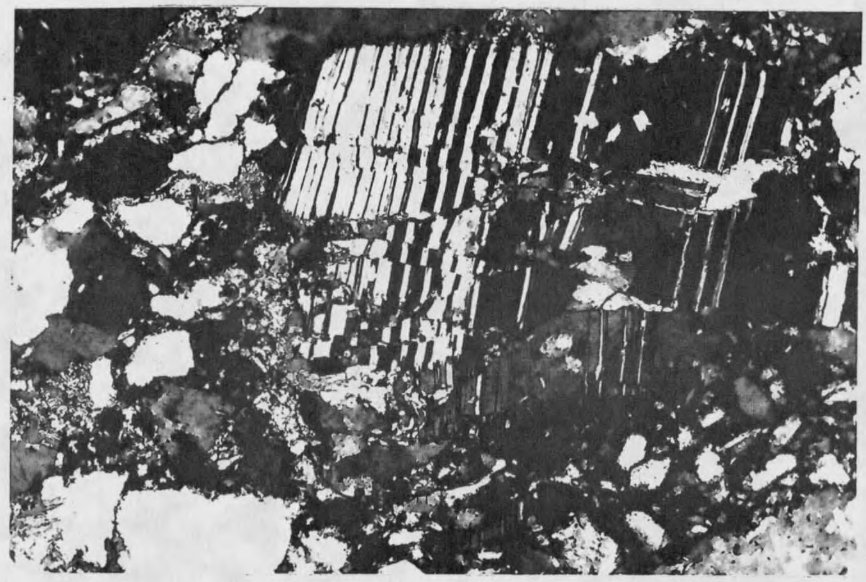

0.5mm

Figure 33 - Cataclasite from Buck Mountain - Static Peak divide. Calcite anneals the cataclasite debris to the left of the brittley fractured plagioclase crystal. Note brittley offset albite twins; no ductile bending is observed.

fractures exploited by late-stage thermal fluids in the fault zone: 1) no rotation is observed in the cataclasite veins, suggesting in-situ granulation caused by a principle stress direction perpendicular to the cataclasite veins; 2) the quartz veins cross-cut the cataclasite veins at approximately 90^0, subparallel to the least principle stress direction (equivalent to the maximum extension direction); and 3) most of these quartz veins exhibit homogeneous, undeformed vein-filling with sharp vein wall boundaries.

Several samples from the breccia zone of the Buck Mountain fault show possible evidence of pressure solution in fine-grained, quartz-filled cataclasites. Irregular suture boundaries in these samples may indicate proximity to the brittle-ductile transition (Mitra, 1984). Extremely fine-grained quartz within the gouge matrix of cataclasite veins may also exhibit pressure solution, however, at the microscopic scale it is difficult to verify. Evidence for ductile deformation such as pressure shadows of quartz recrystallization, grain rotations, and incipient foliation within fault zone material was not observed (Figure 32A and 32B).

The evidence presented above indicates that deformation on the Buck Mountain and Stewart faults was predominantly brittle, but may have been close to the brittle-ductile transition (Mitra, 1984). Thermal fluids must have been present to account for the post-kinematic hydration mineralogy described earlier (Turner, 1968). The following section discusses the X-ray diffraction analyses of gouge samples and what these results may indicate for the fluid flux.

X-Ray Diffraction

X-ray diffraction analyses were conducted on clay-sized gouge samples from the most highly deformed areas in the Buck Mountain and Stewart fault zones. Relative peak intensities derived from (two theta) copper radiation revealed a prevalence of chlorite alteration in all gouge samples tested. Montmorillonite was detected in only one location, on the highly deformed Buck Mountain - Static Peak divide. No kaolinite was observed in any of the fault gouges. The intense deformation zone at the intersection of Buck Mountain and Static faults juxtaposes hornblende-biotite gneiss and amphibolite of Static Peak against quartz monzonite and pegmatite of the Cathedral Group block (Figure 13A). The presence of montmorillonite indicates weathering of basic rocks with relatively low fluid flux (Deer and others, 1983). However, a sufficient fluid flux could result in kaolinite weathering from the acidic Cathedral Group block rocks by the reaction:

$$\underset{\text{muscovite}}{2KAl_3Si_3O_{10}(OH)_2} + 2H^+ + 3H_2O \quad = \quad \underset{\text{kaolinite}}{3Al_2Si_2O_5(OH)_4} + 2K^+$$

(Ehlers and Blatt, 1980).

Though late-stage muscovite and sericite was observed in the Buck Mountain fault zone at the microscopic level, the lack of kaolinite could indicate a relatively low fluid flux in the fault zone (Mitra and Frost, 1981). However, the presence of greenschist alteration assemblages in Phanerozoic, as well as Proterozoic fault zones suggests that some fluid was present.

Therefore, the X-ray analysis of clay alteration products in fault zones in the central Teton Range was inconclusive. A more thorough X-ray or SEM (scanning electron microscope) study, examining samples from a broader spectrum, is needed to clarify the clay mineralogy in the study area.

MESOSCOPIC STRUCTURES

Geometry

Foliation

Horberg and Fryxell (1942) reported that Precambrian gneissic foliation in the Teton Range has a generally steep eastward dip. Later workers also have recorded a prominent eastward dip of foliation along the Teton Range front (Figure 34) (Bradley, 1956; Love and Reed, 1971; Reed, 1973; Lageson, 1987; Smith and Lageson, 1989).

Bradley's (1956) structure map of the Phelps Lake-Buck Mountain area (Figure 7) shows north-striking, east-dipping foliation just west of the Buck Mountain fault in Alaska Basin. These measurements were taken from basement rocks, including banded gneiss, schist and mylonites, on the glacially scoured floor of Alaska Basin. Reed (1973) also indicates north-striking, east-dipping foliation in Alaska Basin and in the hanging wall of the Buck Mountain fault directly adjacent to the Teton Normal fault. However, Reed (1973) reports a variety of foliation orientations from the central Cathedral Group, with strikes ranging from east-west to north-south.

To help determine whether Archean foliation acted as a control on the Buck Mountain fault, this author measured

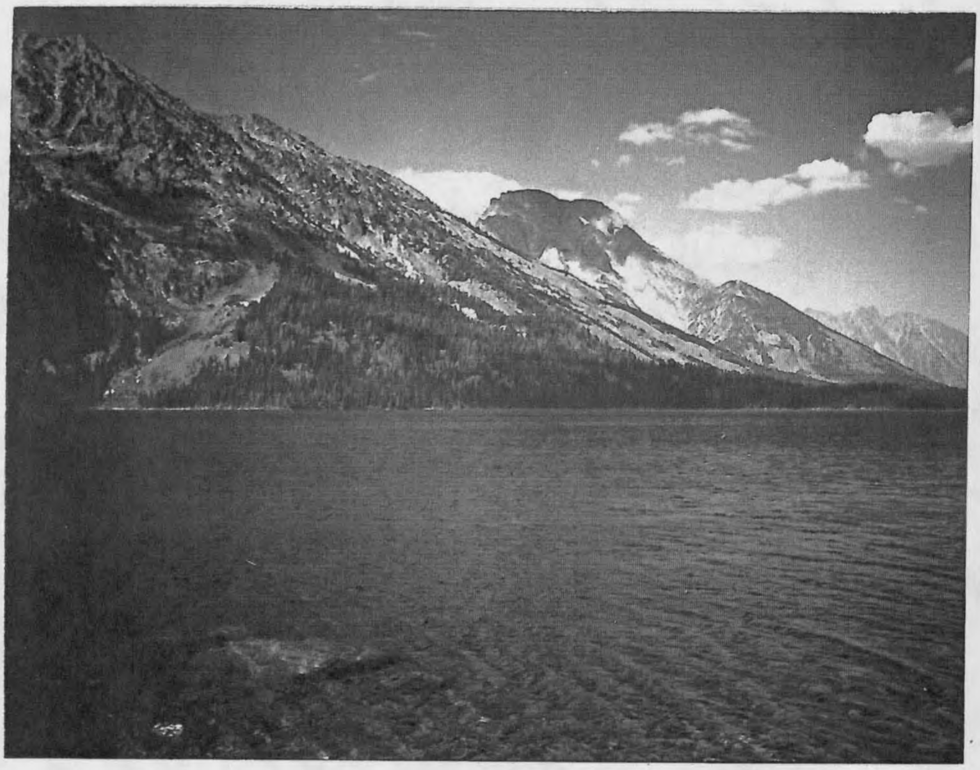

Figure 34 - Photo of the Teton range-front looking north. Jenny Lake in foreground; peak in center of photograph is Mount Moran. A north-striking, east-dipping fabric is evident and may have controlled the orientation of the Teton normal fault.

foliation in three widely separated areas: Alaska Basin, west of and in the footwall of the Buck Mountain fault; Static fault area, south of Buck Mountain; and the central Cathedral Group, in the vicinity of the Middle and South Tetons in the hanging wall of the Buck Mountain fault (Figure 9).

__Alaska Basin__. Archean foliation in Alaska Basin, adjacent to the Buck Mountain fault, strikes generally north-south and dips 30^0 to 50^0 east (Figure 35).

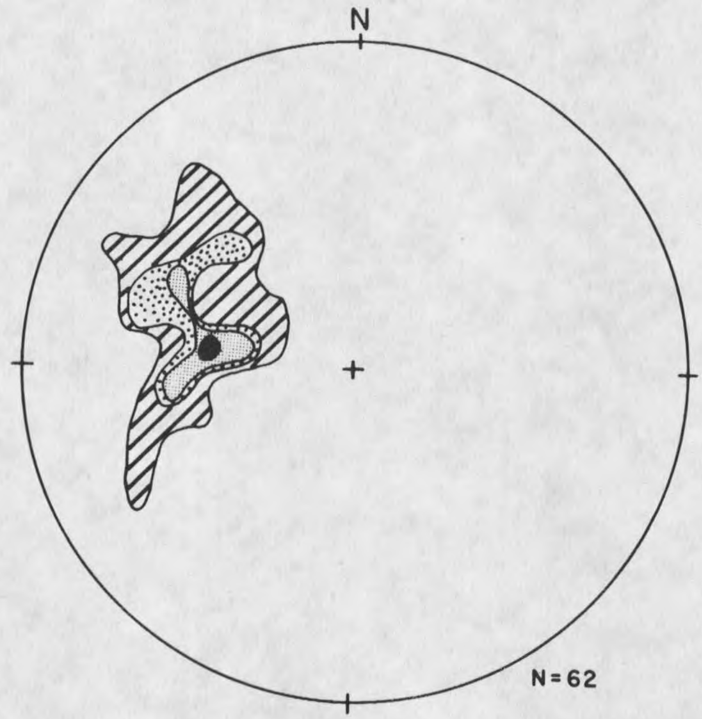

Figure 35 - Poles to S_2 and S_3 foliation in Alaska Basin, west of the trace of the Buck Mountain fault. Contours represent densities of 1.6, 4.8, and 8% / 1% area.

Measurements were taken from surfaces of compositional layering, schistosity, gneissic banding and Proterozoic deformation zones. Reed also recorded north-striking, east-dipping foliation along the Teton range front (Reed, 1973). These foliations reflect the preexisting S_2 and S_3 Archean fabric of the layered gneiss, schist and mylonite described in Chapter 3.

Static Fault Area. Along Static fault, in the footwall of the Buck Mountain fault, foliation strikes generally N 50 E to N 75 E and dips north to north-northwest and south

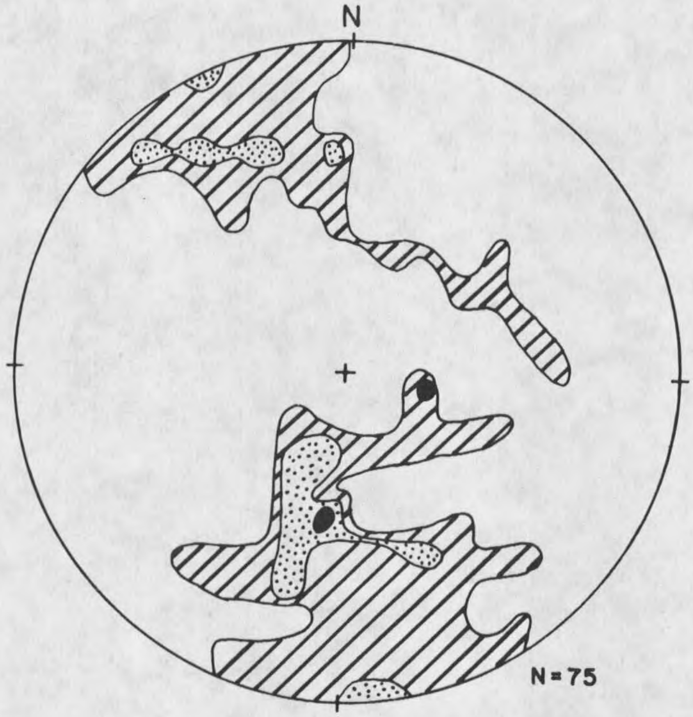

Figure 36 - Poles to axial-planar foliation in the Static fault area south of Buck Mountain. Contours represent densities of 1.3, 2.6, and 4% / 1% area. B = beta point.

to southeast (Figure 36). Foliation from this area is mostly axial-planar and reflects (F_3) fold trends in the area (Figure 39). A beta-point determination indicates that the overall antiformal axis trends N 75 E and plunges 16^0 (Figure 36). It is interesting to note that north-striking foliation along the Teton range-front bends sharply to the southwest in the vicinity of Stewart and Static faults striking subparallel to the faults (Horberg and Fryxell, 1942; Bradley, 1956; Reed, 1973). In the same area, the north-striking Teton normal fault also makes a dogleg to the southwest, becoming subparallel to the Stewart and Static

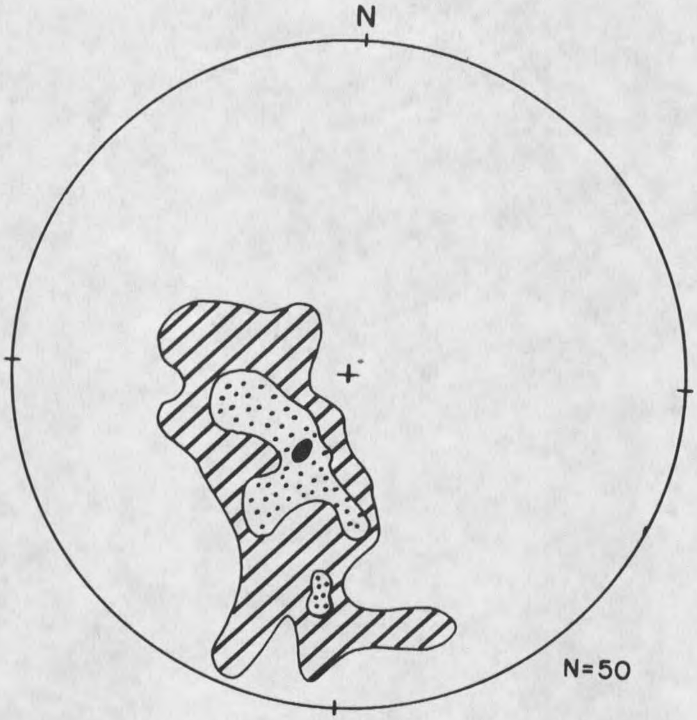

Figure 37 - Poles to foliation in the central Cathedral Group, mostly from the vicinity of the Middle and South Tetons. Contours represent densities of 2, 4, and 8% / 1% area.

faults and the dominant strike of axial-planar foliation in that area (Figures 9 and 36) (Bradley, 1956; Reed, 1973).

Central Cathedral Group. Foliation near the Middle and South Tetons in the hanging wall of the Buck Mountain fault strikes on average N 60 W, nearly perpendicular to both the Buck Mountain and Teton faults, and dips around 22^0 northeast (Figure 37). Measurements from the central Cathedral Group differ from the predominantly north strike and east dip of foliation on the margins of the Cathedral Group. This indicates that a fabric discontinuity exists

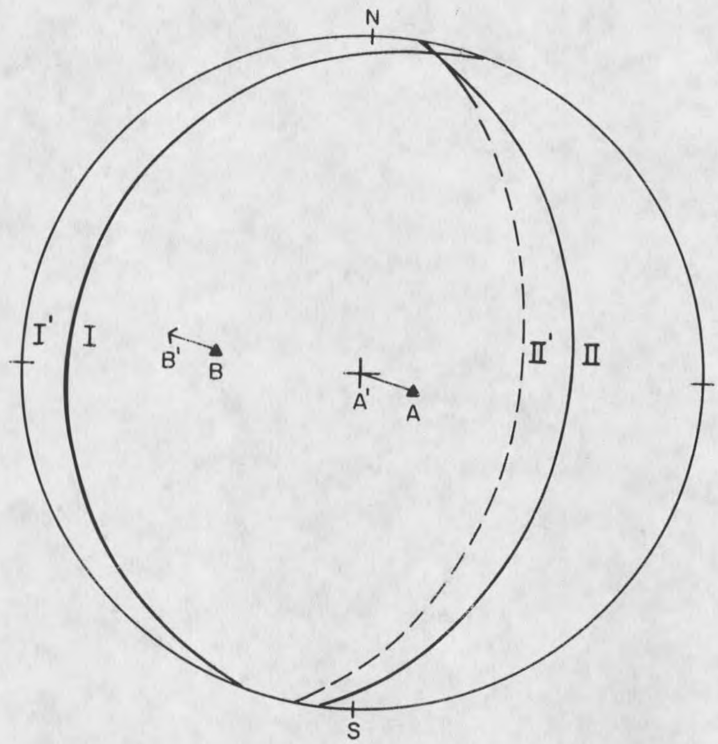

Figure 38 - A = average pole to great circle I (Paleozoic bedding) (25 data points from Reed, 1973); B = average pole to II (basement foliation in Alaska Basin). Rotation of bedding to horizontal provides the strike and dip of foliation prior to Phanerozoic deformation.

between the Buck Mountain fault and the Teton normal fault, and could suggest the rotation of foliated xenoliths within the Cathedral Group intrusive rocks. In addition, this heterogeneity could have structural significance to the overall geometry of the central Teton Range.

<u>Foliation Rotation</u>. Paleozoic bedding that overlies the Precambrian basement west of the Cathedral Group block strikes approximately N 20 E and dips 12^0 west (Figure 38). Using an average 40^0 dip for foliation in Alaska Basin

(Figure 35), rotation of Paleozoic strata to a horizontal attitude indicates that pre-deformation basement foliation had a strike of N 10^0 E and dipped around 50^0 E (Figure 38). Thus, the angular discordance between basement foliation and overlying bedding was approximately 50^0.

Fold Geometry

Most folds within the Archean basement are isoclinal to disharmonic, (F_1) passive-flow folds (Figure 18). In the hanging wall of the Buck mountain fault, F_1 folds are incorporated in large xenoliths (meters to tens of meters) of metamorphic basement rock suspended in the intrusive rocks of the Cathedral Group block. These early folds are gently deformed by a later (F_2) event (Chapter 3).

F_3 folds (Figure 20) that refold F_1 and F_2 folds in high-grade gneiss and schist are common in the vicinity of Static fault (Figure 21). These are tight to open, flexural-flow folds exhibiting pseudo-similar fold geometry (Chapter 3). The F_3 folds exhibit a range of axial trends, from N 55 E with a plunge of approximately 16 degrees, to N 90 E and doubly plunging 5-10 degrees (Figure 39). Of 116 measurements recorded, the highest concentration of axial trends is only 5.2% / 1% area. Thus there is a large amount of scatter between N 55 E and N 90 E. Additionally, similarities in geometry, style, and localization of the

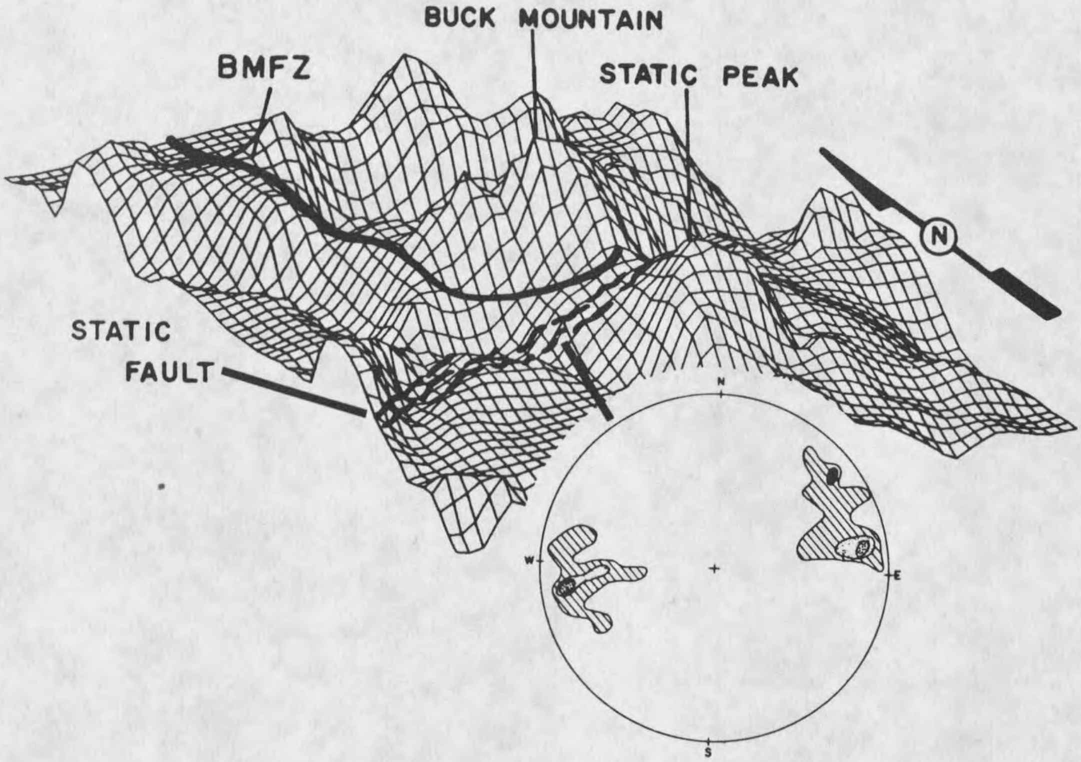

Figure 39 - Trend and plunge of F_3 fold axes in the area of Static fault. Contours represent 2, 2.6, 4.3, 5.2% / 1% area, of 116 measurements. BMFZ = Buck Mountain fault zone.

N 55 E to N 90 E trending folds around Static fault suggest they were formed during the same deformation event.

Folding of the Paleozoic cover is observed in the footwall of the Buck Mountain fault (Figure 40A). About 600 meters west-northwest of Veiled Peak, a steeply west-dipping, indurated outcrop of basal Cambrian Flathead Sandstone is gently folded concave-up (Love and Reed, 1971) (Figures 40 A and B). This cylindrical fold exhibits curved parallel geometry (Suppe, 1985) and maintains uniform layer thickness, indicating it formed through flexural-slip

(Donath and Parker, 1964). Layer thickness is on the order of 1-3 meters and the radius of curvature is very low (Figure 41); if this curvature were to continue, wavelength would be on the order of kilometers (Figure 41). Cylindrical, curved-parallel folds in Phanerozoic sedimentary rocks, formed through predominantly flexural-slip in the Teton Range, are here designated F_4 folds. The folded Cambrian Flathead Sandstone may be a remnant of the broad ancestral Teton-Gros Ventre uplift which occurred early in the Laramide orogeny (Love and Reed, 1971), or a remnant of the regional anticline which appears above the Buck Mountain fault in the retro-deformed cross-sections in the next chapter (Figures 41 and 45). F_4 drag folds in the Paleozoic cover are described below.

Kinematics

Kinematic Fold Indicators

Fault-related frictional forces diminish rapidly away from a fault; only folds closely localized near a fault surface may be considered drag folds (Suppe, 1985). In the vicinity of Kit Lake, just southwest of the South Teton, upturned beds of Paleozoic sedimentary rocks are observed in the footwall adjacent to the Buck Mountain fault and are juxtaposed against Precambrian quartz monzonite of the hanging wall (Figure 42). These folds have characteristics of F_4 folding as described above. Because of the upturned

A

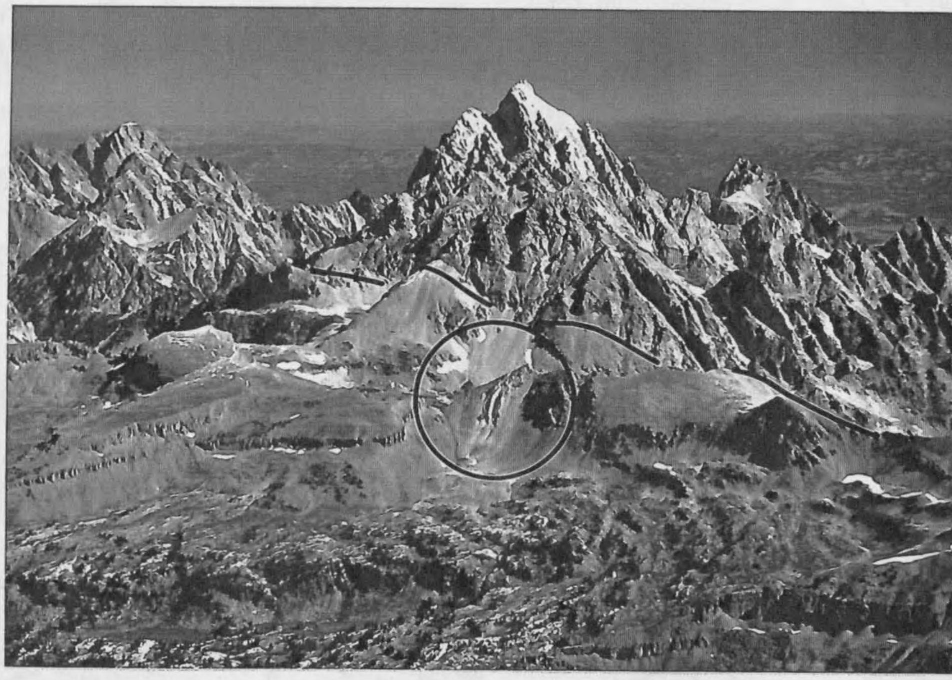

B

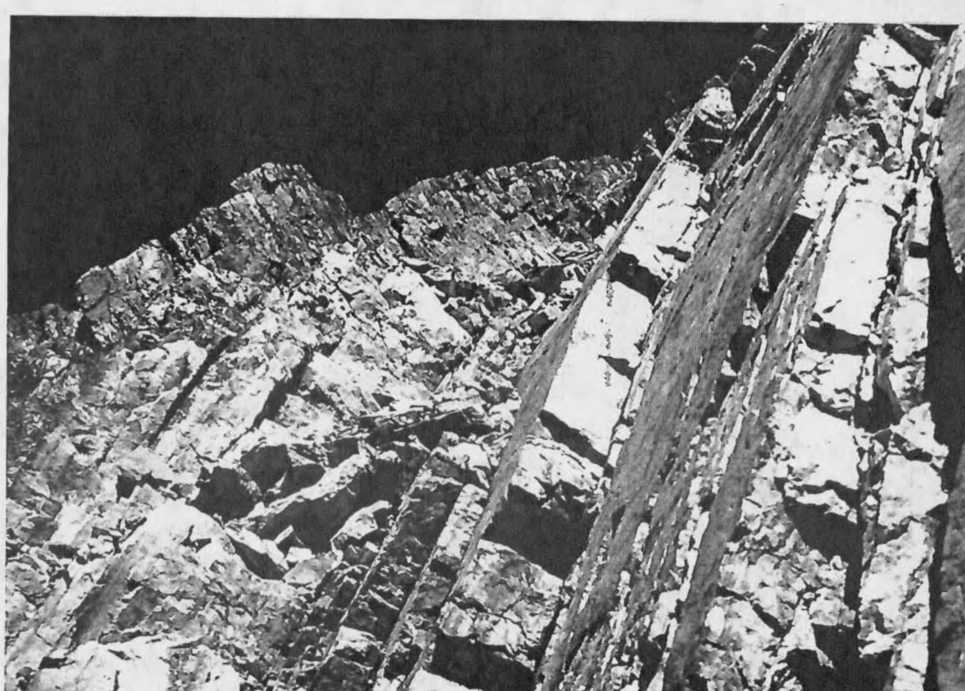

Figure 40 - A: Folded Cambrian Flathead Sandstone (in circle) west of the Buck Mountain fault. B: Steeply dipping beds of Cambrian Flathead Sandstone exhibit F_4 fold characteristics. Layers are 1-3 meters thick.

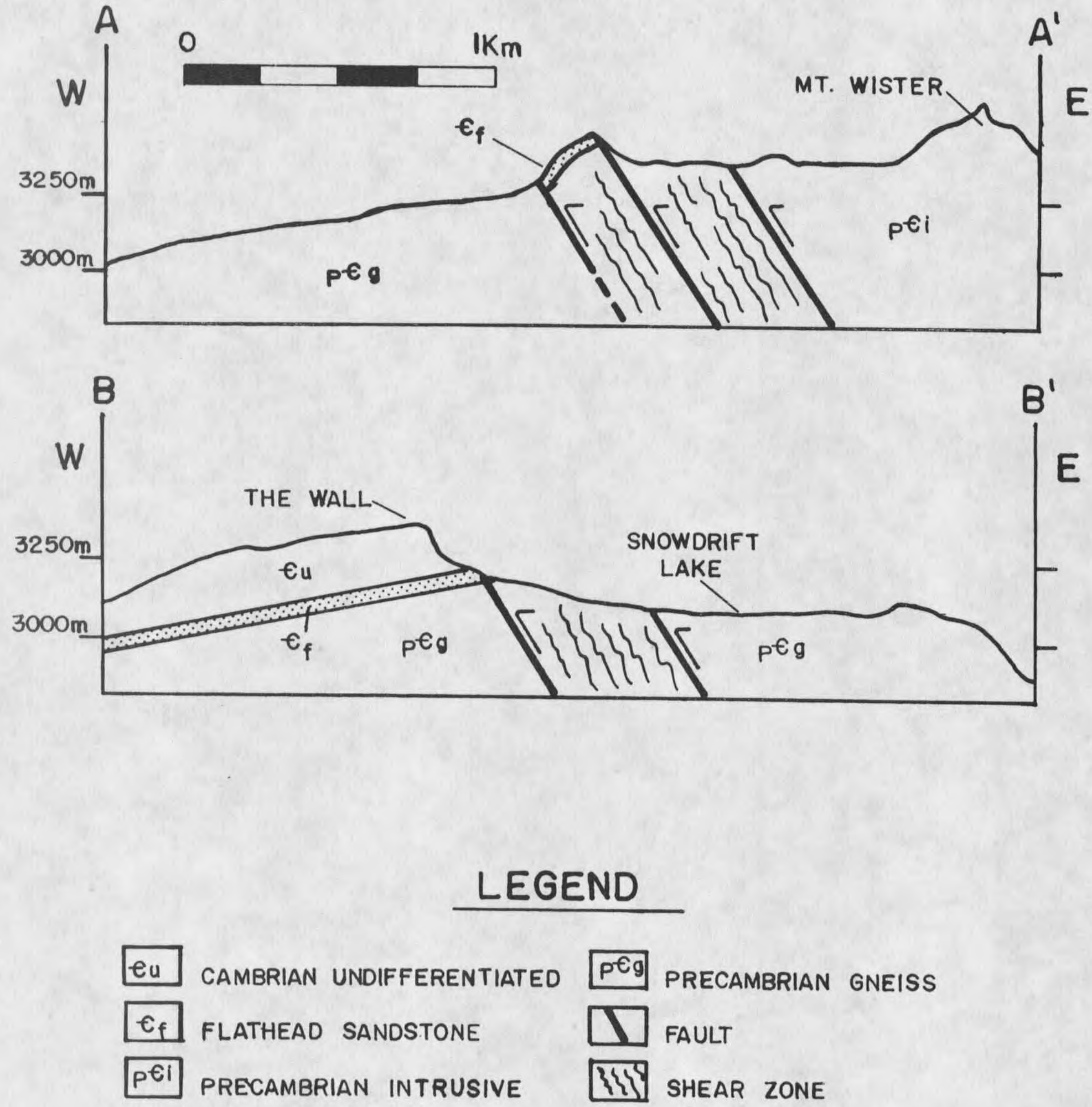

Figure 41 - Cross-section lines A-A' and B-B' can be found on Figures 2 and 9. Cross-section A-A' provides evidence for broad F_4 folding of the Paleozoic overburden as a result of uplift of the Cathedral Group block.

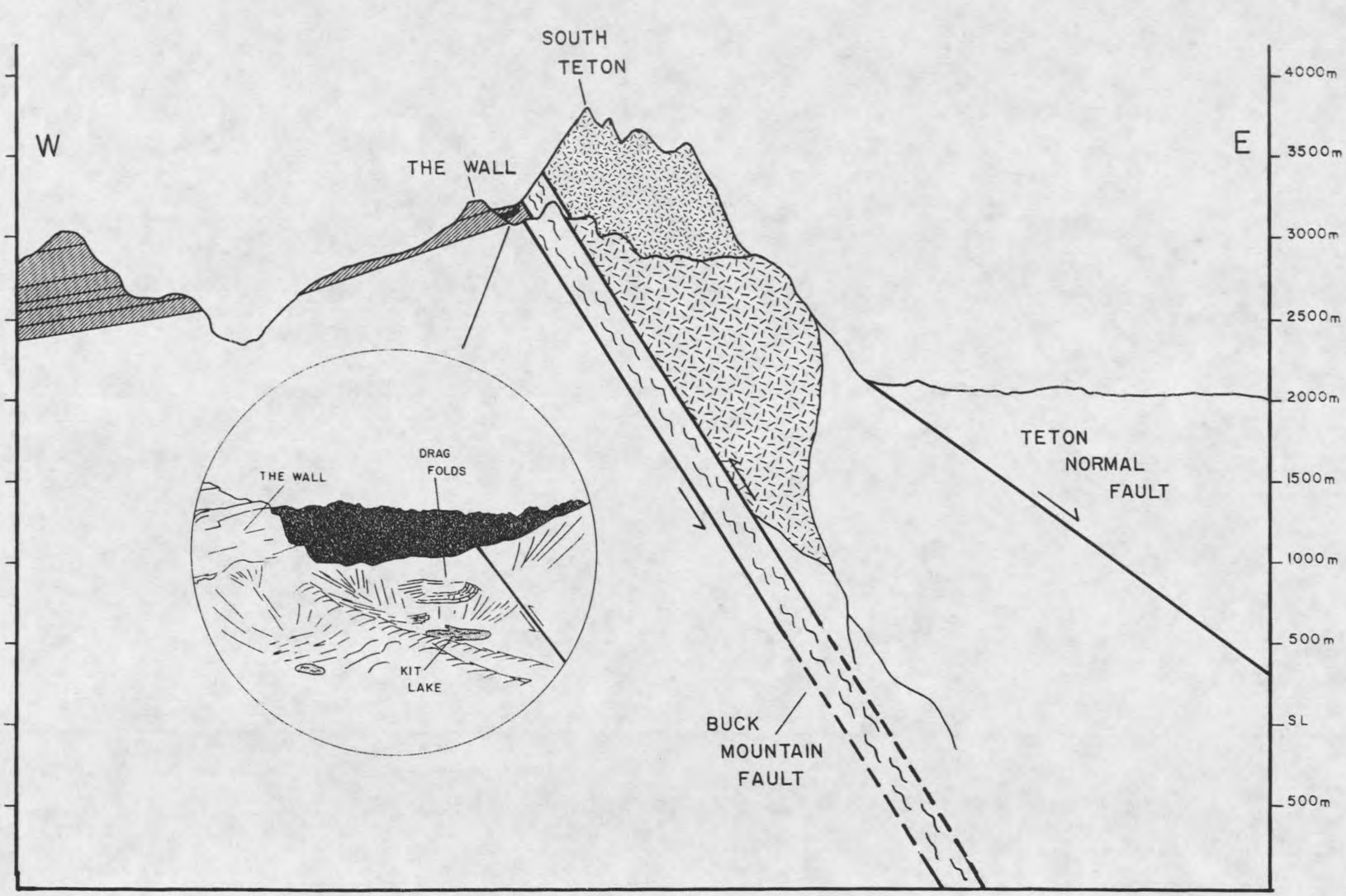

Figure 42 - Drag folds in the Cambrian rocks of the footwall of the Buck Mountain fault. The enlargement of the Kit Lake area shows drag folds in middle Cambrian rocks indicating reverse movement on the Buck Mountain fault.

geometry of the folds near Kit Lake and their close proximity to the Buck Mountain fault, they are interpreted as drag folds, and support Love and Reed's (1971) interpretation of reverse movement on the fault.

Drag folding is also evident on the east face of Static Peak in the hanging wall of the Static fault (Chapter 2) (Bradley, 1956). Competent layers in the hanging wall of Static Peak have been dragged down toward the fault zone indicating reverse movement (Figures 12 and 13) (Bradley, 1956).

<u>Slickenlines</u>

Slickenlines were not easy to locate within the Buck Mountain fault zone, as the highly cataclastic nature of the zone has obliterated most small-scale kinematic indicators. However, slickenlines on fracture surfaces and foliation planes adjacent to the fault were recorded from several locations (Figure 43). The average rake for all slickenlines measured is approximately 90 degrees, indicating dip-slip movement. Therefore, considering the drag fold evidence discussed above, the Buck Mountain fault may be interpreted to be a high-angle reverse fault which experienced west-directed movement perpendicular to the trace of the fault.

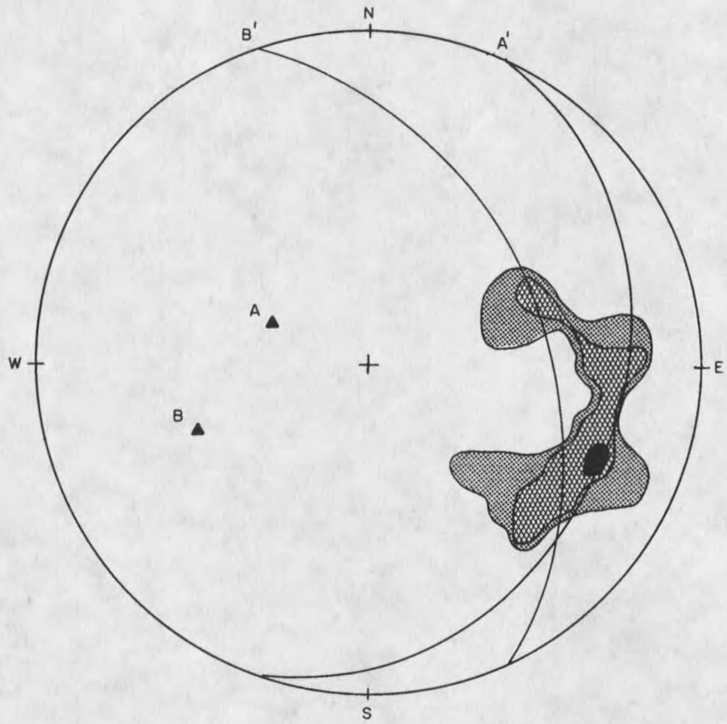

Figure 43 - Rake of slickenside lineations along the Buck Mountain fault recorded on a Schmidt net. Triangles A and B are average pole positions to fault zone fractures represented by great circles A' and B'. Contours show rake (trend and plunge) of slickenside lineations measured on the fracture and foliation surfaces. Pole and great circle A represent north-northeast striking, east-southeast dipping fracture and foliation planes. Pole and great circle B represent north-northwest striking, east-northeast dipping fracture and foliation planes. Contour intervals represent 10, 15, 20% per 1% area; of 20 measurements taken.

RETRODEFORMED CROSS-SECTIONS

An east-west cross-section perpendicular to the Buck Mountain fault, bisecting the Grand Teton, was prepared using data from Love (1968), Behrendt and others (1968), Reed, (1973), Smith and others, (1990), and this study (Figure 44). Retrodeformation of the Buck Mountain fault and the Teton normal fault by the method of Erslev (1986) (Figure 45) shows the geometry during the Laramide orogeny at the time of the ancestral Teton-Gros Ventre uplift (Love and Reed, 1971). Retrodeformation of the Cache Creek fault is beyond the scope of this thesis. The dashed upper contact of the Mesozoic section on the retrodeformed cross-section represents the unknown thickness of sediments that may have existed as overburden at the time of the Laramide orogeny. East of the study area, the extremely thick Late Cretaceous Harebell (up to 3,000 meters thick) and latest Cretaceous-Paleocene Pinyon (up to 1,500 meters thick) conglomerates are preserved in Jackson Hole (Love, 1977). However, several lines of evidence suggest there was much less overburden in the study area during late Cretaceous time:

1) The area of the Cathedral Group block is centrally located with respect to the ancestral Teton-Gros ventre uplift (Love, 1973) which rose during late Cretaceous time

(middle Campanian and Maestrichtian) on the Cache Creek thrust (Dorr, Spearing and Steidtmann, 1977; Wiltschko and Dorr, 1983). Evidence for the ancestral Teton Gros Ventre uplift includes the following: a) the lack of Precambrian metaquartzite clasts in the Hoback Formation indicates that an upland separated the Jackson Hole Basin from the Hoback Basin in Late Cretaceous to early Paleocene time, blocking the southward movement of the metaquartzite conglomerates (Dorr and others, 1977; Wiltschko and Dorr, 1983); b) the retrodeformed cross-section in this chapter indicates a highland in the area of the central Teton Range early in the Laramide orogeny (Figure 45); and c) Roberts and Burbank (1988), using fission-track dating of apatite, indicate there was a major pulse of uplift on the Teton Range (including the study area) in the Late Cretaceous (Chapter 3).

2) The latest Cretaceous to Paleocene Pinyon Conglomerate (150m-1500m) was never severely deformed in the Jackson Hole area (Love, 1973). Undeformed Pinyon Conglomerate rests on highly deformed rocks ranging in age from Mississippian to Late Cretaceous (Love, 1973). Because of this, Love (1973) places the last pulse of Laramide compression in this area at "latest" Cretaceous, after deposition of the Harebell and before deposition of the Pinyon Conglomerate. The Pinyon Conglomerate, therefore, was

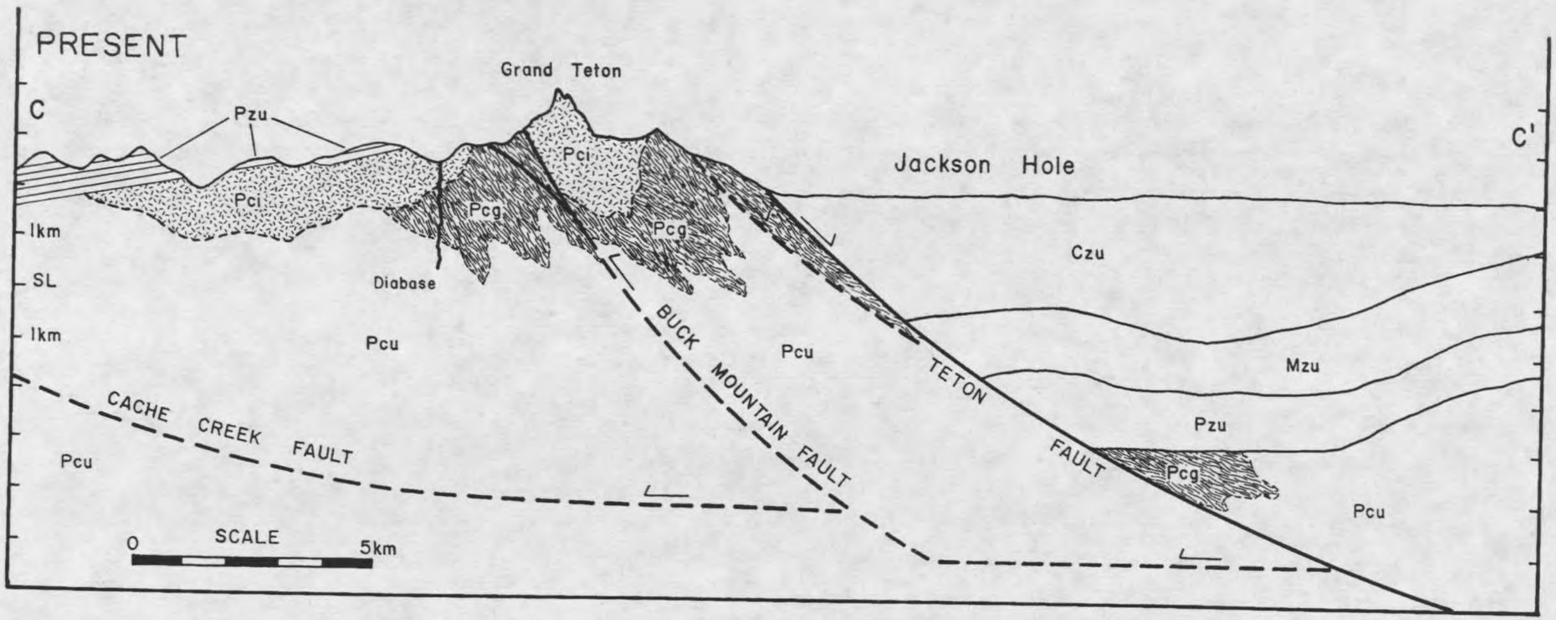

Figure 44 - East-west cross-section C-C' through the Grand Teton. Cross-section line on Figures 2 and 9. Czu = Cenozoic undifferentiated; Mzu = Mesozoic undifferentiated; Pzu = Paleozoic undifferentiated; Pci = Precambrian intrusive; Pcg = Precambrian gneiss and schist; Pcu = Precambrian undifferentiated. Structural data from Love, 1968; Behrendt and others, 1968; Reed, 1973; Smith and others, 1990; and mapping conducted in this study.

probably not deposited on the upland to the west of Jackson Hole.

3) The "latest" Cretaceous-Paleocene Pinyon Conglomerate lies unconformably against Mississippian Madison Limestone on the northwest side of the Teton Range (Love, 1973; p.A39), suggesting that erosion to the Paleozoic level had occurred on the ancestral Teton-Gros Ventre uplift before Pinyon deposition.

4) Further evidence for erosion of the upland in the Teton region in the Late Cretaceous includes: a) erosion of the Red Hills anticline, 20 kilometers east of the study area, to the Lower Cretaceous level before deposition of the Pinyon conglomerate (Love, 1973); b) uplift of the Washakie Range, 50 kilometers northeast of the study area, as a northwest-trending arch that was eroded to the Paleozoic level within latest Cretaceous time (Love, 1977); and c) formation of the Ramshorn and Spread Creek anticlines, east of the study area, during early Paleocene time and subsequent thrusting westward; these structures were stripped of 3,000m to 4,500m of sediment before being buried by the "latest" Cretaceous-Paleocene Pinyon Conglomerate (Love, 1973).

5) Love (1956 and 1973) makes reference to several lines of evidence that indicate a basement-cored uplift existed to the west of Jackson Hole before deposition of the latest Cretaceous-Paleocene Pinyon Conglomerate, and

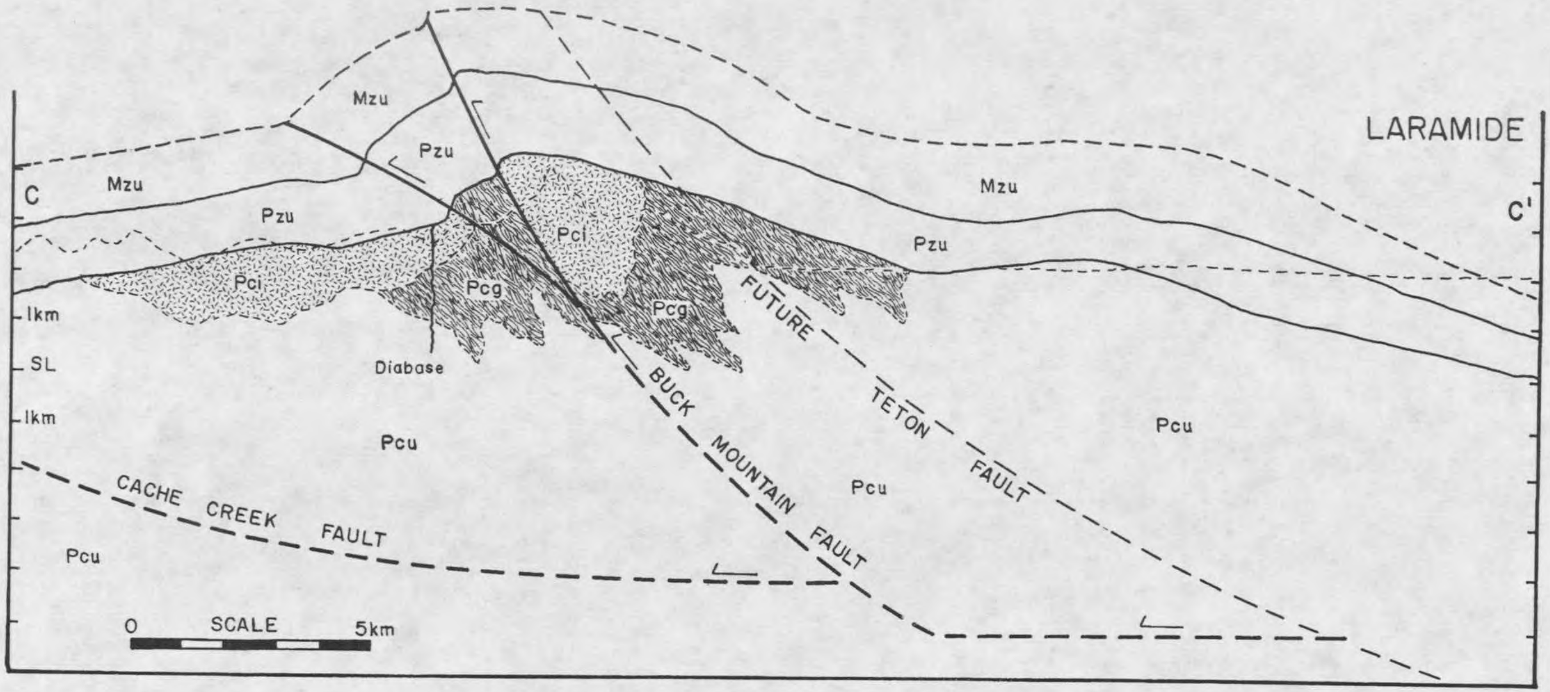

Figure 45 - East-west cross-section C-C' through the Grand Teton retrodeformed to the Laramide orogeny. Cross-section line on Figures 2 and 9. The present-day erosional surface is dashed through the center of the cross-section. Dashed upper contact of Mesozoic section represents unknown thickness. Mzu = Mesozoic undifferentiated; Pzu = Paleozoic undifferentiated; Pci = Precambrian intrusive; Pcg = Precambrian gneiss and schist; Pcu = Precambrian undifferentiated. Structural data from Love, 1968; Behrendt and others, 1968; Reed, 1973; Smith and others, 1990; and mapping conducted in this study.

possibly before deposition of the Late Cretaceous Harebell Conglomerate. The Harebell Conglomerate consists primarily of Upper Precambrian, Cambrian and Ordovician quartzite cobbles and boulders derived from the Cordilleran miogeocline (Schmitt, 1987). However, the southern-most exposure of the Harebell Conglomerate, located on the north fork of Fish Creek about 50 kilometers east-southeast of the Cathedral Group, contains roundstones of predominantly Paleozoic and Mesozoic rocks with sparse granite and quartzites (Love, 1956). Regional paleocurrent data (Lindsey, 1972) indicates a provenance to the west or northwest that is different from that which supplied the massive Precambrian and Lower Paleozoic metaquartzite roundstones.

The principle reference section of the Pinyon Conglomerate is located on Pinyon Peak, approximately 45 kilometers northeast of the Cathedral Group (Love, 1973). At that location, approximately 600 to 650 meters below the summit, Love (1973) recognized cobbles (to 15cm in diameter) of gray, coarsely crystalline granite exhibiting muscovite books. Some meters below he recognized a 20cm boulder of "black granite gneiss" containing garnet and abundant biotite; several meters below that, he observed several granite roundstones and pegmatite containing muscovite and large quartz and feldspar crystals (Love, 1973, p.A35). Again, these roundstones suggest the possibility of a crystalline basement provenance to the west or northwest, as indicated by regional paleocurrent data (Lindsey, 1972). In addition, the relatively detailed descriptions of the crystalline metamorphic roundstones indicate they are similar to lithologies found in the Teton Range, suggesting that a portion of the ancestral Teton-Gros Ventre uplift could have been eroded to its Precambrian basement core by early Tertiary time.

Taken together, this evidence indicates that a basement-cored uplift (the ancestral Teton-Gros Ventre uplift) may have existed to the west of Jackson Hole in the late Cretaceous. It also suggests that none of the thick sequence of Late Cretaceous-Paleocene metaquartzite conglomerates found in Jackson Hole were deposited on the uplands of the ancestral Teton-Gros Ventre uplift. Instead, erosion to lower Mesozoic and possibly to the Paleozoic level occurred during early stages of uplift.

Therefore, it is estimated that no more than 2-4 kilometers of sedimentary rocks nonconformably overlaid the Precambrian basement in the study area prior to uplift of the Buck Mountain fault during the Laramide orogeny in late Cretaceous time. The location of the anticlinal structure just above the Buck Mountain fault (Figure 45) indicates it may have been caused by movement on that fault. However, the general anticlinal nature of the overlying sedimentary rocks is likely a result of uplift of the ancestral Teton-Gros

Ventre Range on the Cache Creek thrust (Love, 1973; Dorr and others, 1977).

The retrodeformed cross-section (Figure 45) indicates that the Buck Mountain fault has a throw of approximately 1 kilometer and a heave of about 0.75 kilometers. Furthermore, the Teton normal fault has a throw of 6.9 kilometers (6,900m) and a heave of 8.5 kilometers (8,500m) (Figure 45).

DISCUSSION

Geometry

The orientations of Phanerozoic structures in the central Teton Range coincide strongly with preexisting Precambrian fabrics and deformation zones. Furthermore, Proterozoic structures appear to conform to Archean foliations. In addition, the Cathedral Group peaks in the hanging wall of the Buck Mountain fault are the erosional remnants of a coherent, resistent block that may have controlled the three-dimensional geometry of the Cathedral Group block.

Blackstone (1990) recognized a new phase in the study of Laramide deformation, that of understanding basement anisotropy at the mesoscopic and microscopic scales. A substantial body of detailed work conducted mostly in the Rocky Mountain foreland indicates that Precambrian rocks with well-developed anisotropies provide surfaces of weakness often exploited by Laramide deformation. For example, Wagner (1957) recognized flexural slip along compositional layering in quartzo-feldspathic gneiss and amphibolite in the Madison Range of southwestern Montana. Schmidt and Garihan (1983) and Garihan and others (1983) recognized folding of foliation surfaces in Archean basement rocks concordant with overlying Paleozoic folds in at least eight localities in southwestern Montana. Angle of discordance between foliation and overlying Paleozoic strata was low (5^0 to 30^0). Furthermore, they recognized chlorite growth on the slickensided foliation surfaces where slippage occurred during folding of the basement. Miller (1987) and Miller and Lageson (1990), as a result of field studies of Laramide faults conducted in south-central Montana, demonstrated that the angle of discordance between Phanerozoic strata and basement foliation surfaces "exerted fundamental control over the basement response." In areas where angle of discordance was low (10^0 to 24^0), folding of the basement occurred predominantly through oblique flexural slip along preexisting foliation surfaces; in areas where angle of discordance was high (70^0 to 80^0), deformation was accomplished by rigid body movements, though these faults were foliation parallel suggesting they may have exploited basement anisotropies. Harlan and others (1990), working in the west-central Madison Range of Montana, presented evidence for slip planes and folding within well-foliated quartzo-feldspathic gneiss where foliation is at a low angle of discordance (about 20^0) to bedding in the Phanerozoic cover folds. Dubois and Evans (1989, 1990) recognized a Laramide overprint on a Precambrian shear zone in the northern Wind River Range as evidenced by chlorite-rich, foliated cataclasite along the trace of the Laramide fault;

also, deformation was intense near the intersection of the Jakey's Fork fault and another Laramide fault as evidenced by "mylonite, breccia and veined clasts." Huntoon (1990) studied Laramide monoclines in the Grand Canyon region and found that "anisotropy, induced by preexisting Precambrian faults [in the basement], was of fundamental importance in localizing deformation." Bohn and Snoke (1990) recognized reactivation of "Precambrian, greenschist-facies plastic shear zones" by "brittle Laramide reverse faults and later Neogene normal faults" in the Seminoe and Shirley Mountains of southeastern Wyoming. Brown (1984 and 1990) theorized that reactivated Precambrian shear zones in the Wyoming foreland controlled east and northeast-striking compartmental faults "which intersect and segment other trends." Genovese and others (1990) cited "orientation and type of basement anisotropy," and "the degree of strain softening attendant on fluid/rock interaction" as two major factors influencing Laramide deformation in the Rocky Mountain foreland. In addition, Lageson (1987) suggested that north-striking basement shear zones, like those in the northwestern Wind River Range, may have controlled the orientation of the Teton normal fault (Figure 46).

The following evidence supports the contention that Precambrian textural and lithological anisotropies played a large role in controlling the structural geometry of the central Teton Range.

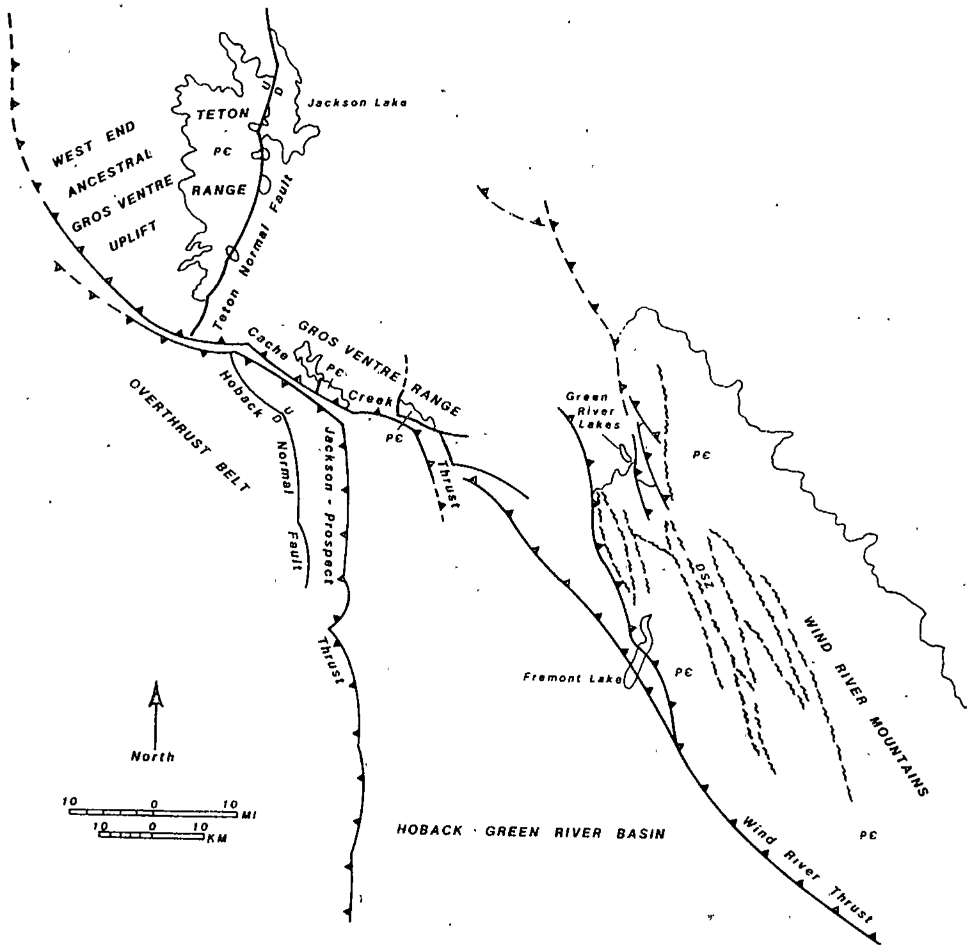

Figure 46 - Structure index map of western Wyoming. Note the north-striking basement shear zones in the north-western Wind River Range. From Lageson (1987).

1) The Cathedral Group block is mapped as a network of late Archean to early Proterozoic quartz monzonite stocks, dikes and pegmatites encasing large xenoliths of older Archean country rock (Chapter 2). In contrast, layered gneiss and schist occurs in the footwall of the Buck Mountain fault just west of the Cathedral Group block and along the trace of the Teton normal fault east of the Cathedral Group block (Figure 9) (Bradley, 1956; Reed, 1973). This lithologic contrast apparently was caused by

intrusion of Proterozoic quartz monzonite and pegmatite into the north-striking Archean fabric (Chapter 3), resulting in breakup and rotation of the Archean country rock. As described in Chapter 2, quartz monzonite bodies and pegmatite dikes are spatially related and occurred at approximately the same time. At the time of intrusion, pegmatite dikes extended into the layered gneiss and schist on the margins of the larger intrusives, but in relatively lower concentration. Thus, they did not compromise the overall north-striking foliation on the margins of the Cathedral Group block as they did within the block.

2) Well-developed planar anisotropies, including compositional layering, schistosity, gneissic banding and proto-mylonitic foliation, adjacent to the Buck Mountain fault in the footwall and along the Teton range-front (Reed, 1973), strike predominantly north-south and dip 30^0 - 50^0 east (Figure 47). Angular discordance of Precambrian foliation to Paleozoic bedding prior to Laramide deformation was about 50^0 (Chapter 5). In the study area the Buck Mountain fault and the Teton normal fault also strike north-south, oblique to the predominant northwest trend of structures in the Wyoming foreland (Figure 46), and exhibit dips similar to the average dip of foliation. Conversely, foliation measurements from within the Cathedral Group block represent inconsistent strikes averaging from east-west to northwest, and exhibit shallower dips (Figure 47). Thus,

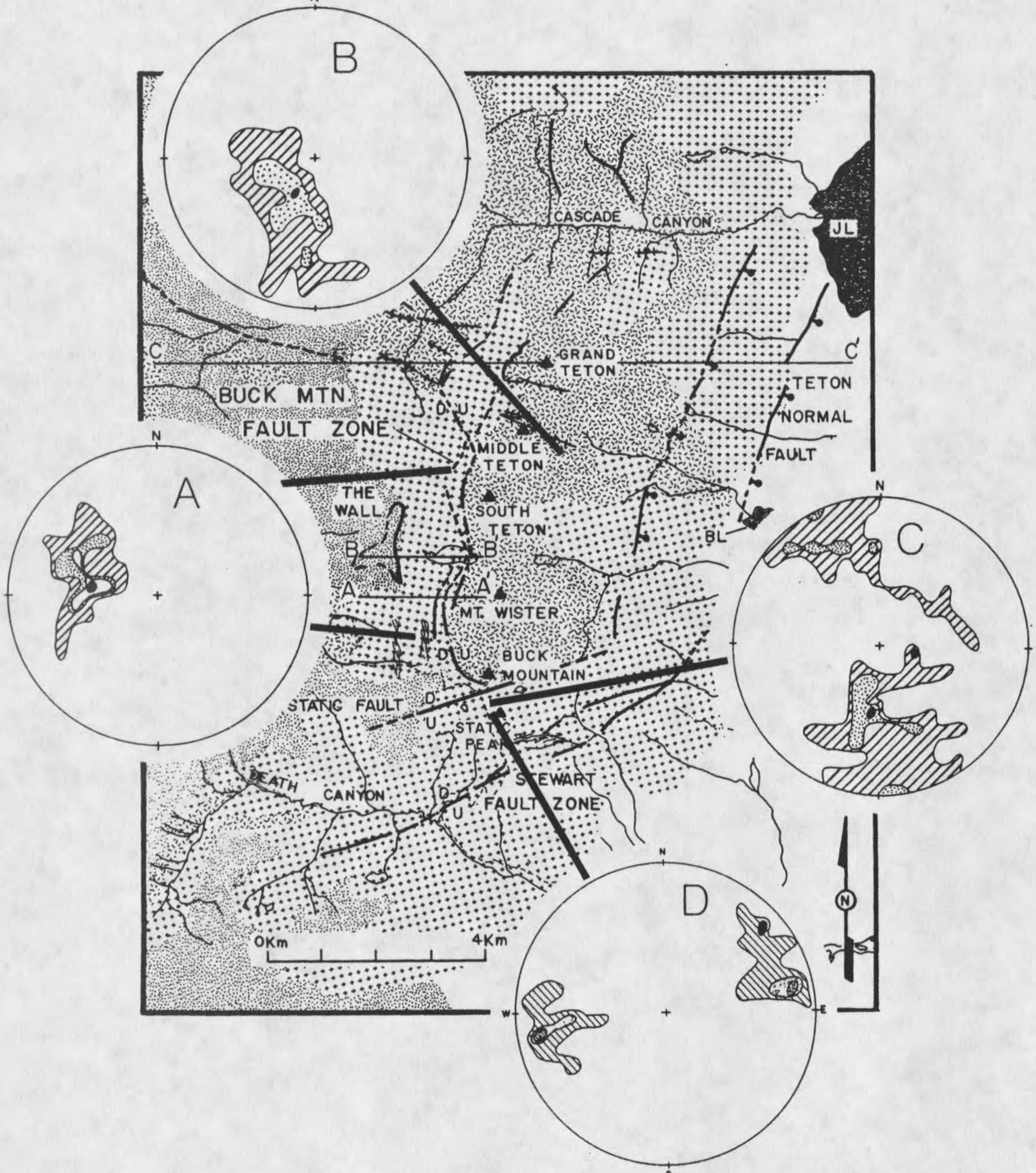

Figure 47 - Foliation orientations and fold trends in the central Teton Range. A = poles to foliation in the footwall block. B = poles to foliation in the Cathedral Group block. C = poles to axial-planar foliation near Static Peak. D = trend and plunge of fold axes in the Static fault area.

foliation within the Cathedral Group block is oblique to north-striking foliation on the margins of the Cathedral Group and to the strike of the Buck Mountain and Teton Normal faults.

3) The southern termination of the Buck Mountain fault coincides with three structural and/or lithological changes: a) the coherent, Cathedral Group block terminates at Buck Mountain, whereas, hornblende gneiss and amphibolites predominate south of there (Figure 9); b) the Proterozoic Static fault strikes N 75 E directly south of Buck Mountain and is reactivated by the Buck Mountain fault at that location (Figure 39); and c) Precambrian foliation changes strike from N-S to an axial-planar foliation striking NE-SW (Figure 47) corresponding to the northeast-trending F_3 folds of Static Peak (chapter 5) (Horberg and Fryxell, 1942; Bradley, 1956; Reed, 1973).

Horberg and Fryxell (1942) first noted a distinct change in Archean foliation orientation in the vicinity of Death Canyon. Bradley (1956) also mapped a Precambrian fabric discontinuity south of Buck Mountain (Figure 7). Reed (1973) mapped an abrupt change in strike of foliation in the layered gneiss and schist from N-S to NE-SW east of Static Peak on the Teton range-front. This can be traced as far south as Open Canyon where the Precambrian lithology changes to a nearly non-foliated metagabbro (Reed, 1973). Additional data provided in this work support the notion of Archean fabric transition in the vicinity of Static Peak (Chapter 5). The Static Peak area is herein named the "Static Peak discontinuity," where anisotropic Archean fabric orientation in the central Teton Range changes strike from N-S to NE-SW, possibly controlling later structural orientations in the area.

The brittley developed Stewart fault strikes NE-SW near the southern termination of, and oblique to, the Buck Mountain fault. In the same vicinity, the Teton normal fault abruptly changes strike from N 15 E to N 30 E (Figure 9). These Phanerozoic structures appear to conform to the distinct change in orientation of Precambrian fabrics at the Static Peak discontinuity.

The change in Archean foliation orientation, location of the southern boundary of the Cathedral Group block, and the orientation and location of the Proterozoic Static fault coincide strongly with the southern termination of the Buck Mountain fault and indicate control on that later structure. The concordance of Phanerozoic structures with Precambrian textural and lithological anisotropies provides strong evidence that Archean and Proterozoic basement fabrics controlled later structural geometries in the study area.

The average dip of the Buck Mountain fault along its length is 57 degrees-east as determined by three point problems (Chapter 2). Thus, the fault exhibits a high-angle attitude, in general agreement with east-dipping Precambrian foliation surfaces, at least in its upper reaches. Recent seismic reflection data and drill core samples have shown that many foreland (basement involved) faults exhibit listric geometry, shallowing with depth (Brown, 1981; Berg, 1981; Brown, 1984; Stone, 1990). The Buck Mountain fault may also be a downward-flattening listric fault, although this interpretation is speculative at present (Figure 6).

Kinematics

Folds in lower Paleozoic strata directly adjacent to the Buck Mountain fault in the footwall are interpreted as drag folds (Figure 42). These folds indicate reverse movement on the fault because they are folded up against the Precambrian granitoid intrusives of the hanging wall block. As described in Chapter 2, the east face of Static Peak (Figures 10 and 11) also displays drag folds indicative of reverse movement on the Static fault. No direct evidence was observed on the Stewart fault to demonstrate the sense of movement; however Bradley (1956) cites drag folds on the eastern front of the Teton Range that indicate reverse movement on the Stewart fault.

As mentioned earlier, some workers have suggested that the Teton normal fault and the Buck Mountain fault could be splays off the northwest-trending, northeast-dipping Cache Creek thrust ramp (Figure 32) (Sales, 1983; Lageson, 1987; Smith and Lageson, 1989; Lageson, 1990, in press). Lageson

(1987) provides evidence that the eastern Gros Ventre Range was uplifted through west-directed shortening, rather than dip-slip, on the Cache Creek thrust (Figure 5). Slickenline measurements indicate oblique-slip on the Cache Creek thrust and the Shoal Creek fault in the Gros Ventre Range, contradicting the common notion that foreland thrust faults experienced purely dip-slip displacement normal to strike (Lageson, 1987). Schmidt and Garihan (1983) also recognize oblique slip in Laramide structures of southwestern Montana. Slickenline measurements taken on the leading edge of the Buck Mountain fault and within the hanging wall block indicate dip-slip movement on the Buck Mountain fault (Figure 43), supporting the contention that movement on the Laramide Cache Creek fault was west-directed (Lageson, 1987).

Timing of Deformation

The following discussion will, first, outline the criteria developed by Mitra and Frost (1981) for distinguishing Laramide from Precambrian deformation zones and, second, compare the basement deformation zones of Mitra and Frost (1981) to deformation zones in the central Teton Range.

Deformation Zones in the Wind River Range

Mitra and Frost (1981) recognized three generations of basement deformation zones in the Torey Creek and Dinwoody

Lakes areas of the northeastern Wind River Range: 1) "Early Precambrian deformation zones characterized by the development of recrystallized banded mylonitic rocks," (p.163); 2) "Late Precambrian deformation zones characterized by the growth of retrograde assemblages containing chlorite and actinolite," (p.163); and 3) "Laramide deformation zones characterized by intense brittle deformation and little or no recrystallization," (p.163). Descriptions of the main characteristics of these zones are as follows:

Early Precambrian Deformation Zones. Early Precambrian Deformation Zones exhibit intense recrystallization. The zones show evidence of grain size reduction and severe stretching of grains, deforming original textures beyond recognition. Pinstripe mylonites represent the extreme extent of this deformation. Post-kinematic recrystallization has resulted in annealed textures which are not usually preferentially weathered (Mitra and Frost, 1981).

Late Precambrian Deformation Zones. Late Precambrian deformation zones cut all Precambrian rocks, but are not observed penetrating Phanerozoic strata. They range in width from microscopic to kilometers in scale and form conjugate sets recognized on aerial photos because of their susceptibility to weathering. The "retrograde" assemblages chlorite + actinolite + K-feldspar + albite + quartz, or chlorite + albite + quartz are common in these zones (Mitra and Frost, 1981). Chlorite and actinolite exhibit strong preferred orientation. Small veins (up to 1 centimeter) and tensional fractures are filled with epidote and quartz, with minor actinolite, chlorite and calcite. The veins exhibit little or no deformation. A large fluid flux is indicated by decalcification of the deformation zones and formation of epidote in tensional fractures. According to Mitra and Frost (1981), the assemblage chlorite + actinolite + epidote indicates that deformation occurred at temperatures in excess of 250°C in the greenschist facies. This environment, they concluded, is too hot for Laramide deformation and supports a pre-Laramide age for the zones.

Laramide Deformation Zones. Laramide deformation zones in the northern Wind River Range may or may not follow earlier deformation zones. Laramide deformation is characterized by non-penetrative, intense fracturing of a homogeneous granitic basement, leaving relatively undeformed blocks between unstable fractures both on a microscopic and mesoscopic scale (Mitra and Frost, 1981). During Laramide deformation in the northeastern Wind River Range,

> "the sedimentary overburden was about 3000 meters thick. This would give rise to a lithostatic pressure of 1 kilobar and temperatures of about 150°C (assuming a fairly high geothermal gradient of over 40°C/km" (Mitra and Frost, 1981; p.167).

Mitra and Frost (1981) are apparently using a geothermal gradient of 50°C/km to achieve the 150°C with 3,000 meters of overburden, as indicated above. They estimate that features of Laramide deformation formed under brittle conditions, typical of zeolite facies metamorphism. Minor secondary mineral growth was detected with the scanning electron microscope in the form of phengitic muscovite along fractures in K-feldspar grains, indicating a fluid phase during deformation. However, a lack of kaolinite in the fault zones suggested that fluid flux was small (Mitra and Frost, 1981).

A different style of Laramide deformation was observed by Mitra (1984) on the White Rock thrust in the north-central Wind River Range. There, basement rocks had an overburden of 10-12 kilometers during Laramide deformation indicating that,

> "pressures were about 4 kilobars and temperatures were less than 250°C, assuming a geothermal gradient of 20°C/km" (Mitra, 1984; p.54)

Mitra (1984) assumes a geothermal gradient of 20°C/km in the north-central Wind River Range, whereas Mitra and Frost (1981) use a geothermal gradient of 50°C/km for the north-eastern Wind River Range. These two locations are no more than 10 kilometers apart; a difference in geothermal gradient of 30°C/km over a 10 kilometer distance seems unlikely. No explanation for this extreme variation in modelling is provided.

Mitra (1984) recognized a range of deformation mechanisms from unstable fracturing on the margins of the fault zone to pressure-solution in the center of the White Rock thrust, indicating a brittle to ductile transition. This transition is attributed to large strains in the center of the fault zone. Evidence for ductile deformation includes formation of "tails" of recrystallized quartz in pressure shadows behind larger rotated brittle grains, and alignment of opaque minerals as a result of pressure solution creating an incipient foliation. Retrograde alteration of feldspars was almost non-existent, indicating there was "very little if any" fluid present during most of the deformation. However, thick calcite veins and breccias with calcite in the matrix are present in the fault. Mitra (1984) attributes the calcite annealing to a large amount of fluid flux, most likely post-kinematic, as indicated by non-deformed coarse-grained calcite vein-filling.

Deformation Zones in the Central Teton Range

Buck Mountain Fault. Several lines of evidence indicate that the Buck Mountain fault is a Laramide fault:

1) The Buck Mountain fault is a high-angle reverse fault, as indicated by drag folds in Paleozoic strata in the footwall (Chapter 5), and juxtaposition of Proterozoic granitoids against Phanerozoic sedimentary rocks (Figure 9).

Thus, the Buck Mountain fault can be described as a contractional fault.

2) It is also a basement-involved fault that exhibits extensive non-penetrative brittle deformation in the form of close-spaced fractures, breccia, gouge and cataclasites (Chapter 4), similar to the Laramide deformation zones of Mitra and Frost (1981) and Mitra (1984).

3) Retrodeformation (Chapter 6) of the Buck Mountain fault, assuming the fold-thrust model of Laramide deformation (Berg, 1962), indicate the area was a broad anticlinal highland before the fault breached the overlying strata. That highland is interpreted to be the ancestral Teton-Gros Ventre uplift which rose on the Laramide Cache Creek thrust in middle Campanian to Maestrichtian time (Love, 1973; Wiltschko and Dorr, 1983). Sedimentary evidence for existence of the uplift is detailed in Chapter six.

The restored cross-section through the Buck Mountain fault (Figure 45) indicates that during the Laramide orogeny the Precambrian basement, exposed today along the fault, had an overburden of approximately 3-4 kilometers (Chapter 6). Assuming the earth's average crustal geothermal gradient of (30°C/km) (Strahler, 1981), pressures would have been about 1 kilobar and temperatures 90° - 120°C. Thus, the ambient physical conditions in the Buck Mountain fault zone appear similar to the "zeolite-facies" conditions of Laramide deformation in the northern Wind River Range described by

Mitra and Frost, (1981) and Mitra (1984). Laramide deformation zones in the northern Wind River Range show evidence of only minor amounts of fluid flux. Mitra and Frost (1981) attributed minor phengitic muscovite growth to the presence of a small fluid phase during deformation. Mitra (1984) found almost no syn-kinematic fluid flux in the White Rock thrust and attributed brittle to ductile transition in the fault zone to large strains.

Several differences distinguish the Laramide Buck Mountain fault from Laramide deformation zones in the northern Wind River Range. Extensive greenschist-grade mineralization overprints cataclasites in the Buck Mountain fault zone, where the alteration assemblage chlorite + epidote + sericite + calcite is pervasive. Mitra and Frost (1981) suggest that temperatures needed for greenschist mineralization (temperatures in excess of 250°C) are "too high" for Laramide deformation. The following discussion suggests an explanation for the observed alteration assemblage found in the Laramide Buck Mountain fault zone.

In general, the Buck Mountain fault displays evidence for brittle granulation, under low-temperature and low-pressure conditions, similar to the Laramide deformation zones of Mitra and Frost (1981). The presence of the greenschist-grade mineral assemblage which overprints the Buck Mountain fault requires a mechanism for initiating the regressive metamorphism. Accessibility of an aqueous or CO_2-

rich fluid is essential for retrograde alteration in order to facilitate either hydration and/or carbonation reactions (Turner, 1968). Furthermore, the water would have to be hotter than the estimated ambient temperature of the Buck Mountain fault (90° - 120°C) (see Chapter 6) at the time of the Laramide orogeny (Mitra and Frost, 1981). Adiabatic expansion of water as it travels upward in a deformation zone will increase temperatures above the existing geothermal gradient (Beach, 1976). Post-kinematic, convective thermal fluids exploiting the Laramide fault zones from depth could have increased the ambient temperature of the Buck Mountain fault zone to greenschist facies conditions, causing retrograde mineral alteration and incipient pressure solution in a zone that otherwise shows evidence of brittle granulation.

Evidence for post-kinematic convective thermal fluid flux in the Buck Mountain fault includes the presence of undeformed calcite and non-oriented chlorite in cataclasites, cross-cutting quartz and epidote veins, and indications of brittle-ductile transition: 1) calcite annealing, resulting from decalcification of plagioclase (Reed and Zartman, 1973) occurs in cataclasites, but the coarse, euhedral calcite grains show little evidence of deformation, suggesting that crystallization occurred post-kinematically; 2) chlorite within the Buck Mountain fault zone grows either in randomly oriented laths within cataclasite veins, or as mimetic chlorite replacing biotite. The chlorite is not strongly oriented in the Buck Mountain fault as it is in the Proterozoic Static fault and is interpreted to be post-kinematic; 3) Transgranular epidote and quartz-filled dilation fractures are common in the fault zone. They are generally undeformed and cross-cut all deformation features, indicating a post-kinematic, silica-rich fluid flux (Frost, 1971); and 4) Suturing of fine grained quartz, indicating pressure solution, was observed in some cataclasite veins. However, the other textural features which usually accompany pressure solution in cataclasites at the brittle-ductile transition (Mitra, 1984), including incipient foliation, rotation of grain fragments and recrystallization in pressure shadows, were not evident. Introduction of hot, late-stage or post-kinematic fluids could have thermally enhanced deformation of the fine-grained quartz without formation of the kinematic textures that usually accompany deformation (Turner, 1968; Genovese and others, 1990).

Other workers in the Rocky Mountain foreland have reported alteration of Laramide deformation zones by greenschist mineral assemblages (Hoppin, 1979; Schmidt and Garihan, 1983; Miller, 1987; Miller and Lageson, 1990). In particular, Miller (1987) recognized Laramide brittle and brittle-ductile deformation, "in a near surface (< 2km), sub-greenschist environment where hydrothermal played a critical role," (Miller, 1987; p.41) in the Bridger and Gallatin Ranges of south-central Montana. In addition, Miller (1987) found chlorite to be the most common Laramide alteration mineral phase in those ranges.

Stewart Fault. The Stewart fault strikes approximately N 55 E and is located approximately 1 kilometer southeast of the Static fault (Figure 9). Rocks in the Stewart fault are highly cataclastic and show alteration mineralization similar to that found in the Buck Mountain fault (Chapter 4). Unstable fracturing and granulation, as well as sericitization of plagioclase, calcite annealing, unoriented chlorite laths, and late-stage epidote veins were observed in the Stewart fault zone. Because of the structural and mineralogical similarities to the Buck Mountain fault, Stewart fault is also interpreted to be a Laramide fault.

Static Fault. Mitra and Frost (1981) recognized retrograde metamorphic chlorite-actinolite assemblages with strong preferred orientation in their late Precambrian deformation zones. These zones were not observed in the Phanerozoic section of the Wind River Range (Mitra and Frost (1981). The following evidence suggests the Static fault is a Proterozoic deformation zone, the northeast segment of which was reactivated during the Laramide orogeny.

The Static fault exhibits variable geometry and lithology along its trace. On the northeast segment, where the Static and Buck Mountain faults converge, cataclasites consist of angular fragments of K-feldspar suspended in a groundmass of consolidated, unoriented, chloritic gouge. The dominantly brittle nature of the northeast segment is suggestive of Laramide reactivation (Mitra and Frost, 1981). Chlorite grows in random orientations, and is interpreted to be post-kinematic. Calcite also exhibits post-kinematic annealing and plagioclase is highly sericitized.

The southwest segment of the Static fault cuts the Archean basement, but does not cut overlying Phanerozoic strata, thus broadly constraining its age to the Proterozoic (Chapter 3). Static fault rocks from the southwest segment exhibit extensive alteration mineralogy. Chlorite replaces biotite and, to a lesser degree, hornblende. Also, hornblende hosts epidote rims. The chlorite exhibits moderate to strong preferred orientation parallel to preexisting north-striking foliation. Rocks in this section of the fault have been identified as syn-kinematic phyllonites (Chapter 3), and reflect the extreme retrograde deformation of earlier amphibolite-grade rocks (see Chapters 3 and 4). Calcite is noticeably absent from the chlorite-rich phyllonites of the southwest segment of Static fault. However, several maroon-orange colored, iron and quartz-rich zones (several meters long and one-to-two meters wide) (Chapter 4) exhibit brecciated opaque minerals, recrystallization of quartz, and late-stage calcite overgrowths. Reprecipitation of calcite and obvious recrystallization of quartz indicates these zones could have resulted from decalcification and heterogeneous fluid flux in the Proterozoic deformation zones, or possibly from a convective Laramide fluid phase (Frost, 1971).

The difference in texture of the unoriented cataclasites from the Buck - Static divide and the phyllonites collected from the southwest segment of the Static fault indicates that the fault records two generations of movement; the earliest movement occurring in the Proterozoic, and latest coinciding with Laramide reactivation of the northeast segment. Timing of alteration is more difficult to sort out. The metamorphic alteration mineralogies of both segments indicate hydration reactions that require convective thermal fluid flux through the zones (Beach, 1976). The northeast segment of Static fault was reactivated by the Laramide Buck Mountain fault; whereas, the southwest segment shows little evidence of brittle deformation. Because of this relationship, the deformation event that formed the syn-kinematic chlorite of the southwest segment was probably pre-Laramide. However, evidence for this is not conclusive.

Early and Late Precambrian Deformation Zones. Several ductile deformation zones, including phyllonites and proto-mylonites, cut Archean gneiss in Alaska Basin and south of Buck Mountain (Chapter 3), and are interpreted to be

Proterozoic. The zones are chlorite-rich, like the Static fault, but exhibit variable chlorite habits ranging from oriented to plumose. The N 75° E striking southwest segment of the Static fault (described in the previous section) is a phyllonite, exhibiting strong preferred orientation of chlorite and biotite.

At the mesoscopic scale, the north-striking Alaska Basin deformation zones have a phyllitic sheen with foliation parallel to regional foliation surfaces. However, at the microscopic scale, the zones exhibit radiating (plumose) void-filling chlorite, and feldspars hosting chlorite platelets. The relationship of chlorite habits, with respect to these samples only, indicates the plumose chlorite is chlorite-1 and the platelets altering remnant feldspars are chlorite-2. The relative relationship of these chlorites can be postulated from textural evidence. However, microprobe mineral analysis of these chlorites is necessary to untangle the complex temporal relationships and to begin to correlate different stages of alteration with the thermal history of the Teton Range.

The proto-mylonites of Alaska Basin (Chapter 3) are not as highly recrystallized as the early Precambrian deformation zones of Mitra and Frost (1981). Also, they penetrate the Archean gneiss and could be Proterozoic in age (Miller and others, 1986). In Alaska Basin, the proto-mylonites are associated with amphibolites, whereas the phyllonites are associated with quartzo-feldspathic and biotite gneisses.

Furthermore, early Precambrian deformation zones are recognized in the central Teton Range. However, they are highly recrystallized and were not observed to be reactivated by later structures.

Conclusions

1) The Buck Mountain fault is a high-angle, Laramide reverse fault that strikes N-S and dips approximately 57° east in the hanging wall of the Cache Creek thrust. The fault has a throw of approximately 1 kilometer and a heave of about 0.75 kilometers. Drag folds in the footwall of the Buck Mountain fault and juxtaposition of Precambrian granitic rocks against Paleozoic sedimentary rocks indicate reverse movement on the fault. In addition, slickenline measurements in the field area indicate dip-slip movement on the Buck Mountain fault, supporting the notion of west-directed movement on the Laramide Cache Creek thrust.

2) The Stewart fault exhibits characteristics of deformation similar to those in the Buck Mountain fault and is also interpreted as a Laramide fault. The Stewart fault strikes N 55° E and dips steeply to the southeast.

3) The Static fault is a high-angle Proterozoic fault that strikes N 75° E and dips 70° to 80° to the southeast. Drag folds on the east face of Static Peak indicate reverse

movement on the Static fault. The northeast segment of the Static fault was reactivated by the southern termination of the Buck Mountain fault during the Laramide orogeny.

4) The Cathedral Group block consists of late Archean to early Proterozoic quartz monzonite and pegmatite intrusives localized in the hanging wall of the Buck Mountain fault. The coherent, non-directional nature of the block may have acted to control the three-dimensional geometry of the hanging wall, and location of the Buck Mountain fault trace.

5) The Precambrian basement of the Teton Range is highly anisotropic. Proterozoic and later deformation zones coincide strongly with Archean foliation orientations and may be controlled by them. North-striking basement fabrics east and west of the Cathedral Group block may have controlled the Buck Mountain and Teton normal faults. In the area of Static Peak, Archean and Proterozoic fabric orientations change abruptly. Later deformation reflects the preexisting orientations. For this reason, the Static Peak area is designated the "Static Peak discontinuity." Substantial evidence indicates the southern termination of the Buck Mountain fault was partially controlled by basement structure at the Static Peak discontinuity.

6) Three generations of deformation zones are recognized in the central Teton Range, similar to those

studied in the northern Wind River Range by Mitra and Frost (1981):

a) Early Precambrian deformation zones are frozen in the Archean gneisses. They display evidence of intense deformation, but are highly recrystallized and show no evidence of reactivation. Close study of these zones was not undertaken in this study.

b) Proterozoic deformation zones penetrate the earlier Archean compositional layering and foliation. They are characterized by phyllonitic or proto-mylonitic textures. The phyllonites exhibit strongly oriented chlorite and biotite, and have a phyllitic sheen. The proto-mylonites exhibit rotation of porphyroblasts, recrystallization and incipient foliation from reworking.

c) Laramide deformation is represented by the Buck Mountain, Stewart, and northeast segment of Static faults. Deformation occurred under low-temperature, low-pressure, brittle conditions. Ambient temperatures in the fault zone, determined by palinspastic restoration, were 90° to 120°C and pressure around 1 kilobar. The faults are characterized by unstable, close-spaced fractures, brittle granulation, and non-oriented gouge formation. Post-kinematic greenschist-facies alteration mineralogies in the cataclasites indicate a late convective thermal flux of fluid in the fault zones.

REFERENCES

Allmendinger, R.W., Brewer, J.A., Brown, L.D., Kaufman, S., Oliver, J.E., and Houston, R.S., 1982, COCORP profiling across the Rocky Mountain front in southern Wyoming, part 2: Precambrian basement structure and its influence on Laramide deformation: Geological Society of America Bulletin, v.93, p.1253-1263.

Allmendinger, R.W., Sharp, J.W., Tish, D. Von, Serpa, L., Brown, L., Kaufman, S., and Oliver, J., 1983, Cenozoic and Mesozoic structure of the eastern Basin and Range province, Utah, from Cocorp seismic reflection data: Geology, v.11, p.532-536.

Anders, M.H., Geissman, J. WM., Piety, L.A., and Sullivan, T., 1989, Parabolic distribution of circumeastern Snake River Plain seismicity and latest Quaternary faulting: migratory pattern and association with the Yellowstone hotspot: Journal of Geophysical Research, v.94, n.B2, p.1589-1621.

Armstrong, F.C., and Oriel, S.S., 1965, Tectonic development of Idaho-Wyoming thrust belt: American Association of Petroleum Geologists Bulletin, v.49, n.11, p.1847-1865.

Beach, A., 1976, The interrelations of fluid transport, deformation, geochemistry and heat flow in early proterozoic shear zones in the Lewisian complex: Philosophical Transactions of the Royal Society of London, A280: p.569-604.

Behrendt, J.C., Tibbets, B.L., Bonini, W.E., Lavin, P.M., Love, J.D., and Reed, J.C., 1968, A geophysical study in Grand Teton National Park and vicinity, Teton County, Wyoming: U.S. Geological Survey Professional Paper 516-E, 23p.

Behrmann, J.H., and Mainprice, D., 1987, Deformation mechanisms in a high-temperature quartz-feldspar mylonite: evidence for superplastic flow in the lower continental crust: Tectonophysics, 140, p.297-305.

Bell, T.H., and Ethridge, M.A., 1973, Microstructure of mylonites and their descriptive terminology: Lithos 6, p.337-348.

Berg, R.R., 1962, Mountain flank thrusting in Rocky Mountain Foreland, Wyoming and Colorado: American Association of Petroleum Geologists Bulletin, v.46, n.11, p.2019-2032.

Berg, R.R., 1981, Review of thrusting in the Wyoming foreland: Contributions to Geology, University of Wyoming, v.19, n.2, p.93-104.

Berg, R.R., 1983, Geometry of the Wind River thrust, Wyoming: in Lowell, J.D., ed., Rocky Mountain foreland basins and uplifts: Rocky Mountain Association of Geologists, p.257-262.

Beutner, E.C., 1977, Causes and consequences of curvature in the Sevier orogenic belt, Utah to Montana, Wyoming Geological Association Guidebook, Twenty-Ninth Annual Field Conference, p.353-365.

Blackstone, D.L., 1977, The overthrust belt salient of the Cordilleran fold belt, western Wyoming - southeastern Idaho - northeastern Utah, in Rocky Mountain thrust belt geology and resources, Wyoming Geological Association Guidebook 29th Annual Field Conference, p.367-384.

Blackstone, D.L., and Verploeg, A.J., 1981, Tectonic map of the overthrust belt, western Wyoming, southeastern Idaho and northeastern Utah: Geological Survey of Wyoming.

Blackstone, D.L., 1990, Concepts concerning Rocky Mountain foreland structural geology: Geological Society of America Abstracts with Programs, v.22, n.6, p.3.

Bohn, D., and Snoke, A.W., 1990, Laramide shortening and Neogene extension superimposed on Precambrian shear zones, Seminoe and Shirley Mountains, Wyoming: Geological Society of America Abstracts with Programs, v.22, n.6, p.3.

Boyer, S.E., and Elliott, D., 1982, Thrust systems: American Association of Petroleum Geologists Bulletin, v.66, n.9, p.1196-1230.

Bradley, F.H., 1873, Geological report of the Snake River division: Sixth Annual Report of the U.S. Geological Survey of the Territories, p.216-217.

Bradley, C.C., 1956, The Precambrian complex of Grand Teton National Park, Wyoming: in, Jackson Hole field conference guidebook: Wyoming Geological Association 11th Annual Field Conference Guidebook, p.34-42.

Brewer, J.A., and Turcotte, D.L., 1980, On the stress system that formed the Laramide Wind River Mountains, Wyoming: Geophysical Research Letters, v.7, n.6, p.449-452.

Brewer, J.A., Allmendinger, R.W., Brown, L.D., Oliver, J.E., and Kaufman, S., 1982, COCORP profiles across the Rocky Mountain front in southern Wyoming, part 1: Laramide structure: Geological Society of America Bulletin, v.93, p.1242-1252.

Brown, W.G., 1981, Surface and subsurface examples from the Wyoming foreland as evidences of a regional compressional origin for the Laramide orogeny: Contributions to Geology, University of Wyoming, v.19, n.2, p.175-177.

Brown, W.G., 1983, Sequential development of the fold-thrust model of Foreland deformation, in Lowell, J.D., ed., Rocky Mountain foreland basins and uplifts: Rocky Mountain Association of Geologists, p.57-64.

Brown, W.G., 1984, Basement involved tectonics of Foreland areas: Continuing Education Course Note Series #26, American Association of Petroleum Geologists Bookstore, Tulsa OK.

Brown, W.G., 1984, A reverse fault interpretation of Rattlesnake Mountain anticline, Big Horn Basin, Wyoming: The Mountain Geologist, v.21, n.2, p.31-35.

Brown, W.G., 1990, Structural style of the Wyoming foreland: Geological Society of America Abstracts with Programs, v.22, n.6, p.4.

Burchfiel, C., 1981, Structural evolution of western North America and tectonics of marginal fold and thrust belts: Syllabus to accompany AAPG Continuing Education Course: Montana Geological Society, 48p. and figures.

Choukroune, P., Gapais, D., and Merle, O., 1987, Shear criteria and structural symmetry: Journal of Structural Geology, v.9, n.5/6, p.525-530.

Condie, K.C., Leech, A.P., and Baadsgaard, H., 1969, Potassium-argon ages of Precambrian mafic dikes in Wyoming: Geological Society of America Bulletin, v.80, p.899-906.

Dahlstrom, C.D.A., 1970, Structural geology in the eastern margin of the Canadian Rocky Mountains: Bulletin of Canadian Petroleum Geology, v.10, p.332-406.

Davis, G.A., 1979, Problems of intraplate extensional tectonics, western United States, with special emphasis on the Great Basin: Rocky Mountain Association of Geologists, p.41-54.

Deer, W.A., Howie, R.A., and Zussman, J., 1983, An introduction to the rock forming minerals: Longman Group Limited, England, 528p.

Dixon, J.S., 1982, Regional structural synthesis, Wyoming Salient of Western Overthrust Belt: American Association of Petroleum Geologists Bulletin, v.66, n.10, p.1560-1580, 20 Figs.

Donath, F.A., and Parker, R.B., 1964, Folds and Folding: Geological Society of America Bulletin, v.75, p.45-62.

Dorr, J.A. Jr., Spearing, D.R., and Steidtmann, J.R., 1977, Deformation and deposition between a Foreland uplift and an impinging thrust belt: Hoback Basin, Wyoming: Geological Society of America Special Paper 177, 82p.

Doser, D.I., and Smith, R.B., 1983, Seismicity of the Teton-southern Yellowstone region, Wyoming: Bulletin of the Seismological Society of America, v.73, n.5, p.1369-1394.

Dubois, M.A., and Evans, J.P., 1989, Laramide deformation in Precambrian granitic rocks, northeastern Wind River Range, Wyoming: Geological Society of America Abstracts with Programs, v.21, n.5, p.74.

Dubois, M.A., and Evans, J.P., 1990, Internal deformation of the Wind River thrust sheet along Laramide and Precambrian zones: detailed structural analyses and scales of brittle deformation, NE Wind River Range, Wyoming: Geological Society of America Abstracts with Programs, v.22, n.6, p.8.

Dunn, S.L.D., 1983, Timing of foreland and thrust-belt deformation in an overlap area, Teton Pass, Idaho and Wyoming: Rocky Mountain Association of Geologists; Rocky Mountain foreland basins and uplifts, J.D. Lowell, Ed., p.263-269.

Ecklemann, F.D., 1963, Zircon paragenesis in Precambrian crystalline rocks of the Teton Range, Wyoming: Geological Society of America Special Paper 73, p.143.

Edmund, R.W., 1956, Resume of structures and physiography in the northern Teton Mountains, Wyoming, in, Jackson Hole field conference guidebook: Wyoming Geological Association, 11th Annual Field Conference Guidebook, p.151-157.

Ehlers, E.G., and Blatt, H., 1980, Petrology; igneous, sedimentary and metamorphic: W.H. Freeman and Company, San Francisco, 732p.

Elliot, D., 1973, Diffusion flow laws in metamorphic rocks: Geological Society of America Bulletin, v.84, p.2645-2664.

Engebretson, D.C., Cox, A., and Gordon, R.G., 1985, Relative motions between oceanic and continental plates in the Pacific Basin: U.S. Geological Survey Special Paper n.206, 59p.

Engel, A.E.J., 1963, Geologic evolution of North America: Science, v.140, n.3563, p.143-152.

Erslev, E.A., 1986, Basement balancing of Rocky Mountain foreland uplifts: Geology, v.14, p.259-262.

Erslev, E.A., and Sutter, J.F., 1990, Evidence for Proterozoic mylonitization in the northwestern Wyoming Province: Geological Society of America Bulletin, v.102, p.1681-1694.

Frost, B.R., 1971, Geology of the Double Lake area, Wind River Mountains, Fremont County, Wyoming: Masters Thesis, University of Washington, 53p.

Fryxell, F.M., Horberg, L., and Edmund, R., 1941, Geomorphology of the Teton Range and adjacent basins, Wyoming-Idaho: Geological Society of America Bulletin, v.52, pt.2, p.1903.

Gast, P.W., Kulp, J.L., and Long, L.E., 1958, Absolute age of early Precambrian rocks in the Bighorn Basin of Wyoming and Montana, and southeastern Manitoba: American Geophysical Union Transactions 39, p.322-334.

Genovese, P.W., Schmidt, C.J., and Chase, R.B., 1990, Role of basement and cover rock behavior in kinematics of Rocky Mountain foreland folds: Geological Society of America Abstracts with Programs, v.22, n.6, p.12.

Giletti, B.J., and Gast, P.W., 1961, Absolute age of Precambrian crystalline rocks in Wyoming and Montana: New York Academy of Science Annals, v.91, p.454-458.

Gries, R., 1983, Oil and gas prospecting beneath Precambrian of Foreland thrust plates in Rocky Mountains: American Association of Petroleum Geologists Bulletin, v.67, n.1, p.1-28.

Groshong, R.H., Jr., 1988, Low-temperature deformation mechanisms and their interpretation: Geological Society of America Bulletin, v.100, p.1329-1360.

Grubbs, K.L., and Vander Voo, R., 1976, Structural deformation of the Idaho-Wyoming overthrust belt (U.S.A.) as determined by Triassic paleomagnetism: Tectonophysics, v.33, p.321-336.

Hamilton, W., 1981, Plate-tectonic mechanism of Laramide deformation: Contributions to geology, University of Wyoming, v.19, n.2, p.87-92

Harlan, S., Batatian, D., Evans, J., Derr, D., Malizzi, L., McDowell, R., Nelson, G., Parke, M., Schmidt, C., and Weberg, E., 1990, Mechanical behavior of footwall basement rocks, Scarface thrust, central Madison Range, Montana: Geological Society of America Abstracts with Programs, v.22, n.6, p.13.

Higgins, M.W., 1971, Cataclastic rocks: U.S.Geological Survey Professional Paper 687, 97p.

Hoppin, R.A., 1970, Structural development of Five Springs Creek area, Bighorn Mountains, Wyoming: Geological Society of America Bulletin, v.81, p.2403-2416.

Horberg, L., and Fryxell, F., 1942, Precambrian metasediments in Grand Teton National Park, Wyoming: American Journal of Science, v.240, n.6, p.385-393.

Horberg, L., Nelson, V., and Church, V., 1949, Structural trends in central western Wyoming: Geological Society of America Bulletin, v.60, p.183-216.

Horberg, L., Edmund, R.W., and Fryxell, F.M., 1955, Geomorphic and structural relations of Tertiary volcanics in the northern Teton Range and Jackson Hole, Wyoming: Journal of Geology, v.63, n.6, p.501-511.

Houston, R.S., 1990, A review of the Precambrian geology of Wyoming: Geological Society of America Abstracts with Programs, v.22, n.6, p.15.

Huntoon, P.W., 1990, Variable influence of basement anisotropies on Laramide monoclinal folding, Grand Canyon, Arizona: Geological Society of America Abstracts with Programs, v.22, n.6, p.15.

Hyndman, D.W., 1985, Petrology of igneous and metamorphic rocks: McGraw-Hill, New York, 786p.

Kanter, L.R., Dyer, R., and Dohmen, T.E., 1981, Laramide crustal shortening in the northern Wyoming Province: Contributions to Geology, University of Wyoming, v.19, n.2, p.135-142.

Kerrich, R., Allison, I., Barnett, R.L., Moss, S., and Starkey, J., 1980, Microstructural and chemical transformations accompanying deformation of granite in a shear zone at Mieville, Switzerland; with implications for stress corrosion cracking and super-plastic flow: Contributions to Mineralogy and Petrology, v.73, p.221-242.

Lageson, D.R., and Zim, J.C., 1985, Uplifted basement wedges in the northern Rocky Mountain foreland: Geological Society of America, Rocky Mountain Section, 38th Annual Meeting (abs.), Boise, Idaho, p.250-251.

Lageson, D.R., 1986, Structural controls on the origin of the Teton Range, Western Wyoming: Unpublished funding proposal, 13p.

Lageson, D.R., 1987, Laramide uplift of the Gros Ventre Range and implications for the origin of the Teton fault, Wyoming: in Wyoming Geological Association, Thirty-Eighth Field Conference Guidebook, p.79-89.

Lageson, D.R., 1990, Possible Laramide influence on the Teton normal fault, western Wyoming: Geological Society of America Special Paper, in press.

Laubscher, H.P., 1977, Fold development in the Jura: Tectonophysics, v.37, p.337-362.

Lindsey, D.A., 1972, Sedimentary petrology and paleocurrents of the Harebell Formation, Pinyon Conglomerate, and associated coarse clastic deposits, northwest Wyoming: United States Geological Survey Professional Paper 734-B, 68p.

Love, J.D., 1956, Geologic map of Teton County, Wyoming: United States Geological Survey.

Love, J.D., and de la Montagne, J., 1956, Pleistocene and recent tilting of Jackson Hole, Teton County, Wyoming: in Jackson Hole field conference guidebook: Wyoming Geological Association 11th Annual Field Conference Guidebook, p.169-178.

Love, J.D., 1956, Summary of geologic history of Teton County, Wyoming, during late Cretaceous, Tertiary, and Quaternary times: in, Jackson Hole field conference guidebook: Wyoming Geological Association, 11th Annual Field Conference Guidebook, p.140-150.

Love, J.D., 1956, Cretaceous and Tertiary stratigraphy of the Jackson Hole area, northwestern Wyoming: Wyoming Geological Association, 11th Annual Field Conference Guidebook, p.140-150.

Love, J.D., 1968, Geologic cross section of the Teton Range: U.S. Geological Survey topographic map of Grand Teton National Park, Teton County, Wyoming: Scale 1:62,500.

Love, J.D., and Reed, J.C. Jr., 1971, Creation of the Teton landscape: Grand Teton Natural History Association, Moose, Wyoming, 120p.

Love, J.D., Reed, J.C. Jr., Christiansen, R.L., and Stacy, J.R., 1973, Geologic block diagram and tectonic history of the Teton region, Wyoming-Idaho: Grand Teton Natural History Assoc., Moose, Wyoming.

Love, J.D., 1973, Harebell Formation (upper Cretaceous) and Pinyon Conglomerate (uppermost Cretaceous and Paleocene), northwestern Wyoming: U.S. Geological Survey Professional Paper 734-A, 54p.

Love, J.D., 1977, Summary of upper Cretaceous and Cenozoic stratigraphy, and of tectonic and glacial events in Jackson Hole, northwestern Wyoming: Wyoming Geological Association Guidebook, Twenty-Ninth Annual Field Conference, p.585-593.

Love, J.D., 1978, Eocene rocks, fossils, and geologic history, Teton Range, northwestern Wyoming: United States Geological Survey Professional Paper 932-B, 40p.

Love, J.D., and Christiansen, A.C., 1985, Geologic map of Wyoming: U.S. Geological Survey, Scale 1:500,000.

Love, J.D., 1989, Yellowstone and Grand Teton National Parks and the middle Rocky Mountains: 28th International Geological Congress Guidebook, 93p.

Lowell, J.D., 1983, Foreland deformation: in Lowell, J.D., ed., Rocky Mountain foreland basins and uplifts: Rocky Mountain Association of Geologists, p.1-8.

Macleod, M.K., 1981, The Pacific Creek Anticline: buckling above a basement thrust fault: Contributions to Geology, University of Wyoming, v.19, n.2, p.143-160.

Matthews, V. III, 1986, A case for brittle deformation of the basement during the Laramide revolution in the Rocky Mountain Foreland Province: The Mountain Geologist, v.23, n.1, p.1-5.

McBride, B.C., Schmidt, C.J., Guthrie, G.E., and Sheedlo, M.K., 1989, Multiple reactivation of a collisional boundary: an example from southwestern Montana: 8th International Conference on Basement Tectonics, in press.

Miller, E.W.B., 1987, Laramide basement deformation in the northern Gallatin Range and southern Bridger Range, southwest Montana: Unpublished master's thesis, Montana State University, 78p.

Miller, E.W.B., and Lageson, D.R., 1990, Laramide basement deformation in the northern Gallatin Range and southern Bridger Range, southwest Montana: Geological Society of America Abstracts with Programs, v.22, n.6, p.39.

Miller, S.H., Hildebrandt, P.K., Erslev, E.A., and Reed, J.C., 1986, Metamorphic and deformation history of the gneiss complex in the northern Teton Range, Wyoming: 1986 Montana Geological Society - Yellowstone-Bighorn Research Association Field Conference, p.91-109.

Mitra, G., 1978, Ductile deformation zones and mylonites: the mechanical processes involved in the deformation of crystalline basement rocks: American Journal of Science, v.278, p.1057-1084.

Mitra, G., and Frost, B.R., 1981, Mechanisms of deformation within Laramide and Precambrian deformation zones in basement rocks of the Wind River Mountains: Contributions to Geology, University of Wyoming, v.19, n.2, p.161-173.

Mitra, G., 1984, Brittle to ductile transition due to large strains along the White Rock thrust, Wind River mountains, Wyoming: Journal of Structural Geology, v.6, n.1/2, p.51-61.

Mitra, G., 1990, Deformation processes in brittle deformation zones in granitic basement rocks: a case study from the Torey Creek area, Wind River Mountains: Geological Society of America Abstracts with Programs, v.22, n.6, p.39.

Morel, John A., 1977, Gravity modeling of the Wyoming thrust belt at 43° N. latitude, Wyoming Geological Association Guidebook, 29th Annual Field Conference, p.595-601.

Mueller, P.A., Wooden, J.L., Henry, D.J., and Bowes, D.R., 1985, Archean crustal evolution of the eastern Beartooth mountains, Montana and Wyoming: Montana Bureau of Mines and Geology Special Publication 92, p.9-20.

Narr, W., and Suppe, J., 1990, Deformational behavior of basement in low-temperature, basement-involved, compressive structures: Geological Society of America Abstracts with Programs, v.22, n.6, p.40.

Nelson, G.C., and Chase, R.B., 1990, Basement deformation in the core of the North Twin anticline, south-central Colorado: Geological Society of America Abstracts with Programs, v.22, n.6, p.40.

Olson, T.J., and Schmitt, J.G., 1987, Sedimentary evolution of the Miocene-Pliocene Camp Davis Basin, northwestern Wyoming: in Miller, W.R., ed., Wyoming Geological Association Guidebook, Thirty-Eighth Field Conference, p.225-243.

Paterson, M.S., 1978, Experimental rock deformation-the brittle field: Springer-Verlag, 254p.

Petersen, F.A., 1983, Foreland detachment structures: in Lowell, J.D., ed., Rocky Mountain foreland basins and uplifts: Rocky Mountain Association of Geologists, p.65-78.

Prucha, J.J., Graham, J.A., and Nickelsen, Richard P., 1965, Basement-controlled deformation in Wyoming Province of Rocky Mountains Foreland: American Association of Petroleum Geologists Bulletin, v.49, n.7, p.966-992.

Ramsay, J.G., 1980, Shear zone geometry: a review: Journal of Structural Geology, v.2, n.1/2, p.83-99.

Ramsay, J.G., 1987, The techniques of modern structural geology; volume 2: folds and fractures: Academic Press, 700p.

Reed, J.C., 1963, Structure of precambrian crystalline rocks in the northern part of Grand Teton National Park, Wyoming: U.S.Geological Survey Professional Paper 475-C, p.C1-C6.

Reed, J.C. Jr., 1973, Geologic map of the Precambrian rocks of the Teton Range, Wyoming: U.S. Geological Survey Open File Report.

Reed, J.C., and Zartman, R.E., 1973, Geochronology of Precambrian rocks of the Teton Range, Wyoming: Geological Society of America Bulletin, v.84, p.561-582.

Reese, D.L., 1974, Unpublished cross-sections of the Teton Range.

Roberts, S.M., and Burbank, D.W., 1988, Late Cretaceous to recent differential uplift in the Teton Range, N.W. WY, by apatite fission-track dating: Geological Society of America Abstracts with Programs, v.20, n.6, p.465.

Rogers, J., 1990, Limits to basement folding in small Laramide uplifts: Geological Society of America Abstracts with Programs, v.22, n.6, p.43.

Rowland, S.M., 1986, Structural analysis and synthesis: Blackwell Scientific Publications, Inc., Palo Alto, CA, 208p.

Royse, F. Jr., Warner, M.A., and Reese, D.L., 1975, Thrust belt structural geometry and related stratigraphic problems, Wyoming-Idaho-northern Utah, in, Bolyard, Dudley W., Symposium on deep drilling frontiers in the central Rocky Mountains: Rocky Mountain Association of geologists, p.41-54.

Royse, F., 1983, Extensional faults and folds in the foreland thrust belt, Utah, Wyoming, Idaho: Geological Society of America Abstracts with Programs, v.15, n.5, p.295.

Sales, J.K., 1968, Crustal mechanics of cordilleran foreland deformation: a regional and scale-model approach: American Association of Petroleum Geologists Bulletin, v.52, n.10, p.2016-2044.

Sales, J.K., 1983, Collapse of Rocky Mountain basement uplifts, in Lowell, J.D., ed., Rocky Mountain foreland basins and uplifts: Rocky Mountain Association of Geologists, p.79-97.

Schmidt, C.J., and Chase, R.B., 1989, Behavior of foliated basement in Rocky Mountain foreland folds, southwestern Montana: Geological Society of America Abstracts with Programs, v.21, n.5, p.140.

Schmidt, C.J., and Garihan, J.M., 1983, Laramide tectonic development in the Rocky Mountain foreland of southwestern Montana, in Lowell, J.D., (ed.), Conference on Rocky Mountain Foreland Basins and Uplifts: Rocky Mountain Association of Geologists Guidebook, p.271-279.

Schmitt, J.G., 1987, Origin of late Cretaceous to early Tertiary quartzite conglomerates in northeastern Wyoming, in Miller, W.R., ed., The thrust belt revisited, 38th Field Conference Guidebook: Wyoming Geological Association, p.217-224.

Simpson, C., and Schmid, S.M., 1983, An evaluation of criteria to deduce the sense of movement in sheared rocks: Geological Society of America Bulletin, v.94, p.1281-1288.

Skinner, B.J., and Porter, S.C., 1987, Physical Geology: John Wiley and Sons, New York, 750p.

Smith, D.J., and Lageson, D.R., 1989, Structural geology and history of the Buck Mountain fault, Teton Range, western Wyoming: Geological Society of America Abstracts with Programs, v.21, n.5, p.144.

Smith, R.B., Pelton, J.R., and Love, J.D., 1977, Seismicity and the possibility of earthquake related landslides in the Teton-Gros Ventre-Jackson Hole area, Wyoming, Wyoming Geological Association Guidebook, Twenty-Ninth Annual Field Conference, p.603-610.

Smith, R.B., and Bruhn, R.L., 1984, Intraplate extensional tectonics of the western U.S. Cordillera: inferences on structural style from seismic reflection data, regional tectonics and thermal-mechanical models of brittle-ductile deformation: Journal of Geophysical Research, v.89, n.B7, p.5733-5762.

Smith, R.B., 1990, Evolution and kinematics of the Yellowstone hotspot: Geological Society of America Abstracts with Programs, v.22, n.6, p.45.

Smith, R.B., Byrd, J.O.D., and Susong, D.D., 1990, Neotectonics and structural evolution of the Teton fault, in Roberts, S., ed., Geological field tours of western Wyoming: Geological Survey of Wyoming, Public Information Circular No.29, p.127-138.

Smithson, S.B., 1979, Structure of the Laramide Wind River uplift, Wyoming, from COCORP Deep Reflection Data and from Gravity Data: Journal of Geophysical Research. v.84, n.B11, p.5955-5972.

Spang, J.H., Evans, J.P., and Berg, R.R., 1985, Balanced cross sections of small fold-thrust structures: The Mountain Geologist, v.22, p.41-46.

Stearns, D.W., 1978, Faulting and forced folding in the Rocky Mountain foreland, in Matthews, V., III, ed., Laramide folding associated with basement block faulting in the western United States: Geological Society of America Memoirs 151, p.1-37.

Steidtmann, J.R., McGee, L.C., and Middleton, L.T., 1983, Laramide sedimentation, folding, and faulting in the southern Wind River Range, Wyoming, in Lowell, J.D., ed., Rocky Mountain foreland basins and uplifts: Rocky Mountain Association of Geologists, p.161-167.

Steidtmann, J.R., 1990, Uplift history of the southern Wind River Range: implications for Laramide deformation: Geological Society of America Abstracts with Programs, v.22, n.6, p.46.

St. John, O., 1879, Geological Report of the Teton Division: Eleventh Annual Report of the U.S. Geological Survey of the Territories, p.474-475.

Stone, D.S., 1975, A dynamic analysis of subsurface structure in Northwestern Colorado: Rocky Mountain Association of Geologists, p.33-40.

Stone, D.S., 1984, The Rattlesnake Mountain, Wyoming, Debate: a review and critique of models: The Mountain Geologist, v.21, n.2, p.37-46.

Stone, D.S., 1990, Seismic verification of the basement-involved thrust-generated fold model: Geological Society of America Abstracts with Programs, v.22, n.6, p.47.

Strahler, A.N., 1981, Physical geology: Harper and Row Publishers, New York, 612p.

Suppe, J., 1985, Principles of structural geology: Prentice-Hall, Englewood Cliffs, New Jersey, 537p.

Susong, D.D., Smith, R.B., and Bruhn, R.L., 1987, Quaternary faulting and segmentation of the Teton fault zone, Grand Teton National Park, Wyoming: EOS, Transactions of the American Geophysical Union, v.68, p.1452.

Tullis, J., Schmid, S., and Ethridge, M., 1982, Short course on ductile deformation mechanisms and microstructures: Structural Geology Division, Geological Society of America, 28p.

Turner, F.J., 1968, Metamorphic Petrology: McGraw-Hill Book Company, New York, 403p.

Vasko, A.M., 1982, Structural setting of Teton Pass with emphasis on fault breccia associated with the Jackson thrust fault, Wyoming: Montana State University, unpublished Masters thesis, 64p.

Vernon, R.H., and Flood, R.H., 1988, Contrasting deformation of S and I-type granitoids in the Lachlan Fold Belt, eastern Australia: Tectonophysics, 147, p.127-143.

Wagner, S.W., 1957, Effect of Laramide folding on previously folded Precambrian metamorphic rocks, Madison County, Montana: unpublished master's thesis, Indiana University, Bloomingdale, Indiana, 26p.

Weinberg, D.M., and Stearns, D.W., 1978, Kinematic analyses of drape folds in the Rocky Mountain Foreland-some geologic implications: Wyoming Geological Association, Thirtieth Annual Field Conference Guidebook, p.199-234.

Wernicke, B., and Burchfiel, B.C., 1982, Modes of extensional tectonics: Journal of Structural Geology, v.4, n.2, p.105-115.

White, S., 1975, Tectonic deformation and recrystallization of oligoclase: Contributions to Mineralogy and Petrology, v.50, p.287-304.

White, S., 1979, Grain and sub-grain size variations across a mylonite zone: Contributions to Mineralogy and Petrology, v.70, p.193-202.

Wiltschko, D.V., and Dorr, J.A. Jr., 1983, Timing of deformation in Overthrust belt and foreland of Idaho, Wyoming,and Utah: American Association of Petroleum Geologists Bulletin, v.67, n.8, p.1304-1322.

Winkler, H.F.G., 1965, Petrogenesis of metamorphic rocks: Springer-Verlag, New York, 220p.

Woodward, L.A., 1986, A case for brittle deformation of the basement during the Laramide Revolution in the Rocky Mountain foreland province: discussion: The Mountain Geologist, v.23, n.3, p.90-94.

Zeller, C.G., 1982, Structural geology along Teton Pass, Wyoming: in Geologic studies of the Cordilleran thrust belt, Powers, R.B., ed., Rocky Mountain Association of Geologists, v.2, p.831-843.

Zim, J.C., and Lageson, D.R., 1985, Neotectonics and seismicity of the eastern Three Forks Basin, Montana: Geological Society of America Abstracts with Programs, v.17, n.4, p.273 (Boise).

Zoback, M.L., and Zoback, M., 1980, State of stress in the conterminous United States: Journal of Geophysical Research, v.85, n.B11, p.6113-6156.